1991

Muscle strain injury : an in vitro study of stretch rate dependence in elongation to failure

Richard Evan Gellman
Yale University

MUSCLE STRAIN INJURY:
An In Vitro Study of Stretch Rate Dependence in Elongation to Failure

Richard Evan Gellman

Yale University

1991

Muscle Strain Injury:
An In Vitro Study of Stretch Rate Dependence in Elongation to Failure

A Thesis Submitted to the Yale University
School of Medicine in Partial Fulfillment
of the Requirements for the Degree of
Doctor of Medicine

by

Richard Evan Gellman

1991

ABSTRACT

Muscle Strain Injury:
An In Vitro Study of Stretch Rate Dependence in Elongation to Failure

Richard Evan Gellman

1991

Muscle strains or tears occur frequently in the workplace, in athletics and in the performing arts. The mechanism of strain injuries is not presently known but the stress producing failure is thought to be generated by elongation. Since muscle is a viscoelastic material, the stress in the muscle is dependent upon the rate at which it is stretched. In an *in vitro* passively stretched muscle model, we sought to determine the influence of stretch rate. When stretch rate was increased from 0.1 mm/sec to 1 m/sec, the failure stress increased significantly from an average of 0.3 $\pm$ 0.09 MPa to 0.7 $\pm$ 0.2 MPa. Similarly, the elastic modulus increased from 1.8 $\pm$ 0.7 N/mm^2 to 4.1 N/mm^2 $\pm$ 1.5 N/mm^2. Energy absorbed to failure increased on average from 94.7 $\pm$ 27.1 N*mm to 245.87 $\pm$ 101.5 N*mm. There was, however, no significant difference in the failure strain with the 10,000 fold increase in stretch rate. Failure strain at each rate was approximately 19% $\pm$ 4%. We found no difference between the material characteristics of tibialis anterior and medial gastrocnemius muscles. The site of failure was consistently at the distal myotendinous junction in TA and at either the proximal or distal myotendinous junction in the MG specimens. Morphology at the site of failure was studied using histology and scanning electron microscopy.

Our results suggest that muscle exhibits stretch rate dependence when continuously elongated to failure and that the site of injury is most likely to occur at the myotendinous junction.

Acknowledgments

I would like to thank Drs. Trey Crisco and Manohar Panjabi for your instruction and guidance over the last year. I would also like to thank Tom Oxland and Mike Morin for your willing assistance and friendship that has made the biomechanics lab such a pleasant learning environment.

Thank you Cathy Nelson for your help in getting things done; Nancy Troiano and Rick Darnell for preparing the histology slides; and Bruce Wolanin for the SEM photographs.

And my deepest gratitude to my family and Michelle for your constant and continuing support in all aspects of my life which has helped me tremendously.

Richard Evan Gellman
April, 1991

Table Of Contents

Introduction

Muscle strains or tears occur frequently in the workplace, in athletics, and in the performing arts. "Epidemiologically, soft-tissue strains, or pulls, are still the most common injuries seen by sports medicine physicians" [81]. In fact, about 90% of all sports-related injuries are contusions and minor muscle pulls [9, 14, 22]. Time lost before pre-injury performance levels are reached is often months and a recurrence or progression to a more serious injury is likely.

It is impossible to give an accurate estimate to the medical costs and loss of employment days from muscle strains due to the great variation in the types and extent of these injuries [22]. However, the frequency and number of cases that require care by physicians make that cost extremely high. After considering these facts, it is remarkable that there is little research into the mechanisms and treatment of muscle strain injuries.

Muscle strains are classified into three types. A mild, or first degree strain, commonly called a "pulled muscle," is an over-stretching of the muscle or tendon resulting in approximately 5% or less disruption of the musculotendinous unit. A moderate, or second degree tear is disruption of a greater portion of the muscle but not complete rupture. And a severe or third degree tear is complete rupture of the muscle or tendon. Severity and location of injury to the musculoskeletal system is influenced by age in humans. The growth plate is the weakest point in the young, making avulsion fractures through the apophysis or epiphysis common. In middle and old age, blood supply decreases to the tendon, making it more susceptible to strain injury. Muscle is susceptible to tears at all ages [99].

Clinically, a muscle strain is an injury to the musculotendinous unit from excess tension which occurs from a force overload during an eccentric (lengthening) contraction [17]. The mechanism of injury lies in the summation of forces within and external to the muscle-tendon unit that exceeds the tensile strength of one of the components. Higher intrinsic forces result from eccentric contractions [12]. External forces are a combined effect of the muscle-tendon unit being at or near its maximum length, then having overload thrust upon it, exceeding the passive range of motion. One example of such an injury is a tear of the medial head of the gastrocnemius muscle, which is common in tennis players [24, 68, 80]. During a serve, the foot is dorsiflexed causing the gastrocnemius muscle to approach its physiologic maximum length. From this position, there is a sudden application of a powerful tensile force when the quadriceps muscle contracts to extend the knee.

Muscles most frequently strained, particularly those in the lower limb, share anatomical features. The muscle activates or crosses two joints, which predisposes it to excessive ranges of motion and high stresses generated by the antagonistic muscle groups [29]. These muscles also have a high percentage of type II, fast-twitch muscle fibers which generate more forceful, rapid contractions and so cause higher tension development [31, 57, 83]. In humans, commonly strained muscles are the hamstrings, adductor magnus, rectus femoris, triceps and gastrocnemius.

Therapy for most strain injuries usually involves the application of ice and compression. The time and frequency of these treatments is conducted without understanding healing processes at the injury site [66]. Numerous factors contribute to the physiology of repair at the tear site, most notably formation of scar tissue. Decreased flexibility and strength of the muscle due

to the pattern of scar formation at the injury site is the primary etiology of re-injury. The amount, alignment and degree of cross-linking of the collagen laid down by fibroblasts at the tear site determines the strength and elasticity of the healed tissues. Studies are beginning to quantitate optimum methods of immobilization, positioning, rehabilitation and the use of anti-inflammatory medications [3, 6, 44, 45, 46, 48, 58, 60, 61].

Orthopaedic research in musculoskeletal injury has focused primarily on bone, tendon and ligament. With the exception of compartment syndromes, these tissues are more frequently in need of surgical intervention. However, it is now evident that trauma to muscle and the myotendinous junction are important causes of long-term disability if not properly treated. The choice of surgical versus conservative treatment is an area of controversy [68].

Another consideration is the high incidence of soft tissue contracture that develops following post-operative immobilization [36, 58, 87]. Long term morbidity from shortened, atrophied muscles and tendons can be more challenging and expensive to manage then a presenting fracture or ligament tear.

Athletes that are properly warmed before intense muscle activity are more flexible and tend to have less lower extremity muscle strains [85, 96]. Preventative measures that increase flexibility have been developed in the last decades based on neuronal circuits that mediate the stretch reflex, golgi tendon organs and the gamma efferent motor neurons [82]. Following work by Kabat in his study of proprioceptive neuromuscular facilitation (PNF), Holt developed a stretching method for athletes called the 3-S system (scientific stretching for sport), which offers the benefit of increasing range of motion, retention of flexibility and muscle strengthening [53, 81]. This

method is superior to passive stretching because it develops muscle while enhancing flexibility. Ballistic or bounce stretching is now accepted as ineffective in promoting flexibility and is associated with a stretch reflex that actually shortens the muscle [4, 23, 67, 81].

Studies comparing different groups of athletes show that flexibility is sport specific. Dancers and gymnasts attain their ability to reach extremes in range of motion primarily through training exercises that incorporate lengthening the muscles during contraction [82, 92]. Increased flexibility, a deterrent to muscle strain injuries, is thus possible in all populations if properly conducted and continued.

This study will provide insight into the biomechanical nature of muscle, which may help prevent muscle strain injuries and lead to better methods of increasing soft tissue flexibility.

Why Biomechanics?

Understanding the mechanical forces that overload muscle is the basis of muscle strain injury. Biomechanics applies mechanical laws to living structures, such as the locomotor system of the human body.

Most biologic tissues respond viscoelastically when subjected to tensile loading forces. Materials are viscoelastic if their response varies with the rate of loading. To date there have been only a few studies of simple elongation in whole muscle, and no rigorous studies of muscle's viscoelastic failure properties.

Questions that needed to be addressed were: what is the peak stress required for a muscle to tear? What is the length muscle deforms before it starts to fail? How does the stretch rate affect these parameters? And where anatomically does muscle fail?

Goal

The goal of this project was to determine stretch rate dependence (viscoelastic response) in muscle passively pulled to failure at a low (0.1 millimeter/second) and a high (1,000 millimeter/second) rate using an *in vitro* model. Failure loads and displacements of rabbit muscle-tendon units were accurately measured and the stiffness, energy absorbed to failure, stress, strain and elastic modulus were calculated. The site of failure was also studied and histology and scanning electron microscopy were performed to describe the tear site.

Review of the Literature

A. Biomechanics

This section will cover biomechanical concepts important to the interpretation of the results. Stress-strain and load-deformation curves will be described first, followed by a discussion of viscoelasticity and a three-element model.

Stress-Strain Relationships

A stress-strain curve represents the deformation (change in length or shape) of a material as a force is applied to it. Such curves are instrumental in describing the behavior of a material, such as muscle, as it is pulled to failure **(See Figure 1)**.

Stress equals tensile force in newtons divided by the area over which the load is applied. Area of muscle is difficult to measure due to its non-uniform shape, so calculation of the physiologic cross-sectional area is determined by dividing volume by length.

Strain is a measure of deformation of a material. Strain is measured in % and can be calculated by dividing the displacement (deformation) by the initial length.

The term strain is also used clinically, as above, to describe an injury to musculotendinous or ligamentous tissues. It is not normally used to describe a specific injury, but rather a loading and deforming of some part of the body that results in pain and often swelling.

Stress-strain values for muscle are derived from load-deformation curves for the structure of the muscle-tendon-bone unit. Thus stress-strain

curves measure material properties whereas load-deformation curves measure structural properties.

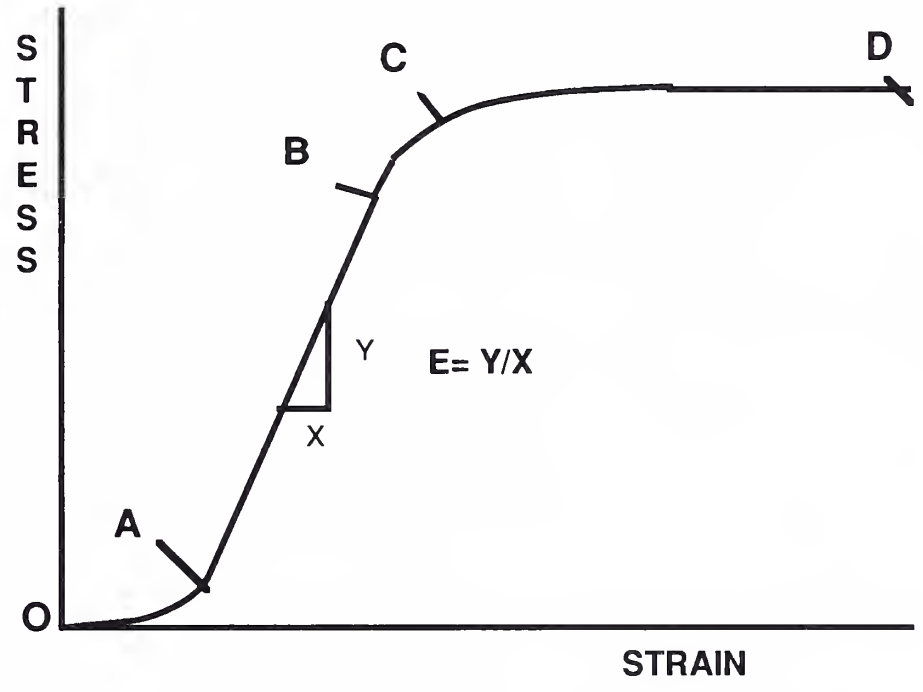

Stress-strain curve: OA= toe region, AB= linear elastic range, BC= nonlinear elastic range, CD= plastic range, D= yield point; E= elastic modulus.

Figure 1

Segment **OA**. represents the toe region where force is small compared to the displacement. At low stretches, connective tissue has a high degree of overlap in the wavy collagen fibers, as in a piece of yarn [64].

AB represents the linear elastic range. It is the range of stresses where original length or shape is maintained after removal of the deforming stress. The slope of the curve in the linear elastic range, **E**, determines the elastic modulus, a measure of a material's resistance to deformation. It is measured

in N/mm^2 or MPa. Cortical bone has a high elastic modulus, whereas muscle has a low elastic modulus.

BC is the nonlinear elastic range. The unique feature of this part of the curve is that the relationship of stress to strain is exponential or constantly changing. Most biologic materials, especially soft tissues, exhibit significant nonlinear elasticity [26]. A material will return to its original length if the stress is removed in this range.

CD is the plastic range. Plasticity is permanent deformation in a material when loaded beyond its elastic range. An example of plastic deformation is a metal spring that is stretched to a point where it will no longer return to its original length. In this range, deformation occurs with only small increases in stress as the slope (elastic modulus) approaches zero.

Point **D** is the yield or failure point. It is the stress at which a material breaks or ruptures.

Stiffness (the linear elastic slope of load-deformation curves) is similar to the elastic modulus, except that it describes structural behavior. For example, as a material, steel has a higher elastic modulus than cortical bone. However, as a structure, the neck of the femur has greater stiffness than a steel hip nail. This is explained by the three-dimensional shape of the two structures, where the femur has greater mass located at a distance from its center, making it more resistant to bending [73] **(See Figure 2)**.

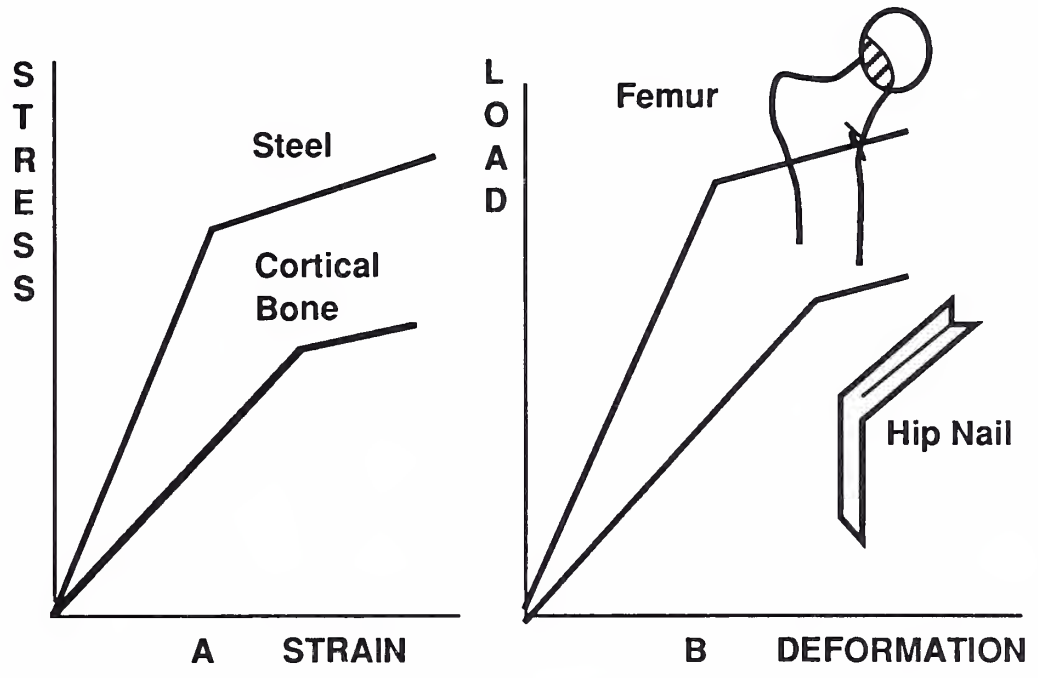

Stiffness and Elastic Modulus (A) Steel is a stiff material as compared to bone. It has a higher modulus of elasticity. (B) The femoral neck is stiffer than any hip nail. This is due to the advantageous distribution of material in the femoral neck. (Adapted from Panjabi, et. al., 1990)

Figure 2

Viscoelasticity

Most biologic tissues behave viscoelastically. Viscoelasticity describes the time-dependent response of a material to loading. As the word implies, there are two components: viscosity and elasticity.

Elasticity is the property of a material to return to its original shape after removal of a deforming load. It implies that length changes, x, or deformations, are directly proportional to applied forces, F. Thus, **F=kx**, where k is a constant defined by the material.

In biomechanics, elasticity is represented by Hooke's model of a spring **(See Figure.3)**. A perfect spring represents the reversible nature of elastic

materials where deformation remains only as long as there is an applied force. Thus, potential energy is stored during loading and kinetic energy is released completely during unloading. There is no energy lost in the process, and there is no permanent deformation.

Figure 3

Hookean Body: Force a Deformation

Viscosity is the property of a material to resist shear, a force parallel to its surface. It is time-dependent and rate change-dependent, where the rate of deformation is directly proportional to the applied forces.

In biomechanical models, viscous elements are represented by Newton's model of a hydraulic piston known as the dashpot **(See Figure 4)**. The plunger inside the piston will move through the fluid of the cylinder at a rate, v, proportional to the amount and duration of an applied force, F. Thus, $F=mv$, where m is a constant defined by the material. In other words, lengthening a viscous material rapidly requires the application of a greater force.

Figure 4

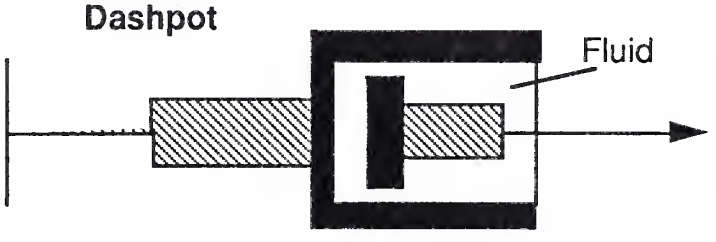

Newtonian Body: Force a Velocity

Picture a cliff-diver jumping into water from two heights. At the low height, say five feet, the loading rate, v, will be low so the force, F, absorbed by the water (and the diver) is low. If the diver jumps from fifty feet, the loading rate, v, is much higher, so the force absorbed by the water (and unfortunately the diver) will also be much greater.

There are four important phenomena characteristic of viscoelastic materials. The first, related to the description of viscosity, is strain rate dependency. The shape of the load-displacement curve is dependent on the rate of loading, with higher strain rates causing the slope of the curve to become steeper. A steeper slope will generate a higher failure load and energy absorbed to failure if displacements are similar **(See Figure 5)**.

All viscoelastic materials are sensitive to the rate of loading. Rapid loading rates require the material or structure to absorb more energy to resist failure (Remember the diver) [73].

Hysteresis, the loss of energy that occurs during loading and unloading cycles, is another viscoelastic property seen on load-deformation curves **(See Figure 6)**. Energy loss represents the conversion of potential or strain energy to kinetic energy or heat.and is measured as the area between the curves.

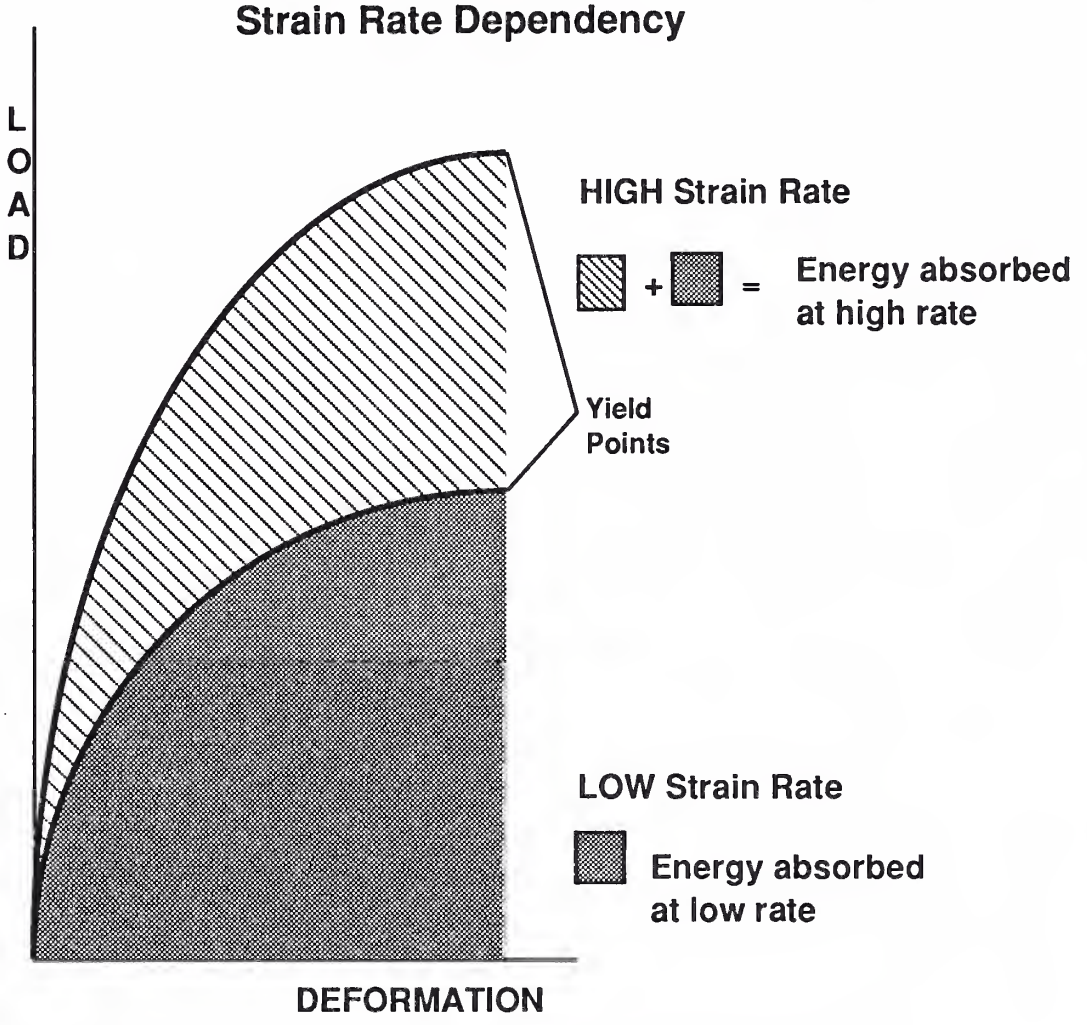

Strain Rate Dependency-Faster strain rates in viscoelastic structures such as muscle-tendon units cause higher failure loads and greater energy absorbed to failure (the area beneath the curve) than slower strain rates.

Figure 5

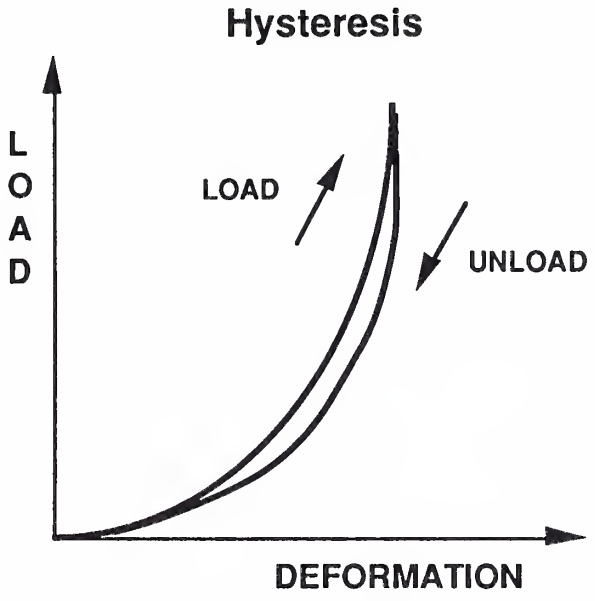

Hysteresis: The area between the curves is the energy loss in one load/unload cycle.

Figure 6

Creep and relaxation are the other two phenomena of viscoelastic materials. During creep, a load is suddenly applied and kept constant, while displacement is recorded against time. The change that occurs in the length usually approaches a steady-state value asymptotically **(See Figure 7)**.

Stress relaxation is the decrease in stress (load) of a deformed material with time when the deformation is held constant. The internal stresses decrease with time exponentially, reaching a lower value (zero at infinite time) **(See Figure 7)**.

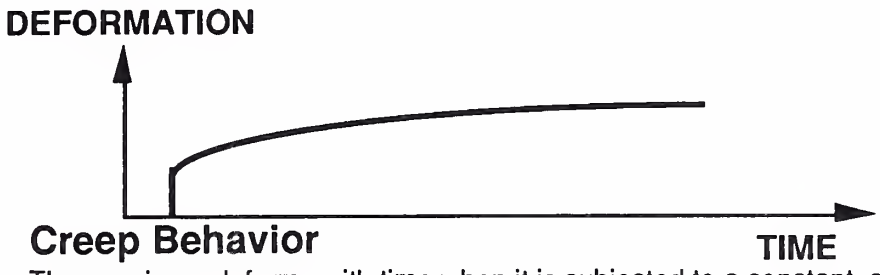

The specimen deforms with time when it is subjected to a constant, suddenly applied load.

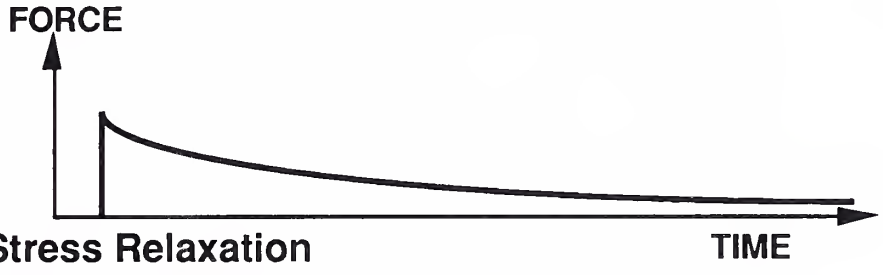

The tension in a specimen decreases with time after the application of a load.
(Adapted from Panjabi et. al., 1990)

Figure 7

Both creep and stress relaxation are demonstrated in the clinical situation of stretching, as practised in warm-up and flexibility training for athletics. If a person sits on the ground with both legs extended and reaches forward, grabbing the soles of the feet without pulling or letting go, then the tension in the muscles of the lower back and hamstring muscles will eventually decrease. This is an example of stress relaxation. If the same person pulls on the soles of the feet at a constant tension, the low back and hamstring muscles will lengthen (deform) with time, until their nose hits their knees, an example of creep. It is understood that there are also important neuronal reflexes governing flexibility training.

Viscoelastic properties can be simulated mathematically in a three-element model. The model consists of three symbols: a spring in parallel with a dashpot and then connected in series with another spring **(See figure 8)**. It has been experimentally determined that tendon, bone, ligament and passive muscle can be simulated using such a model [27].

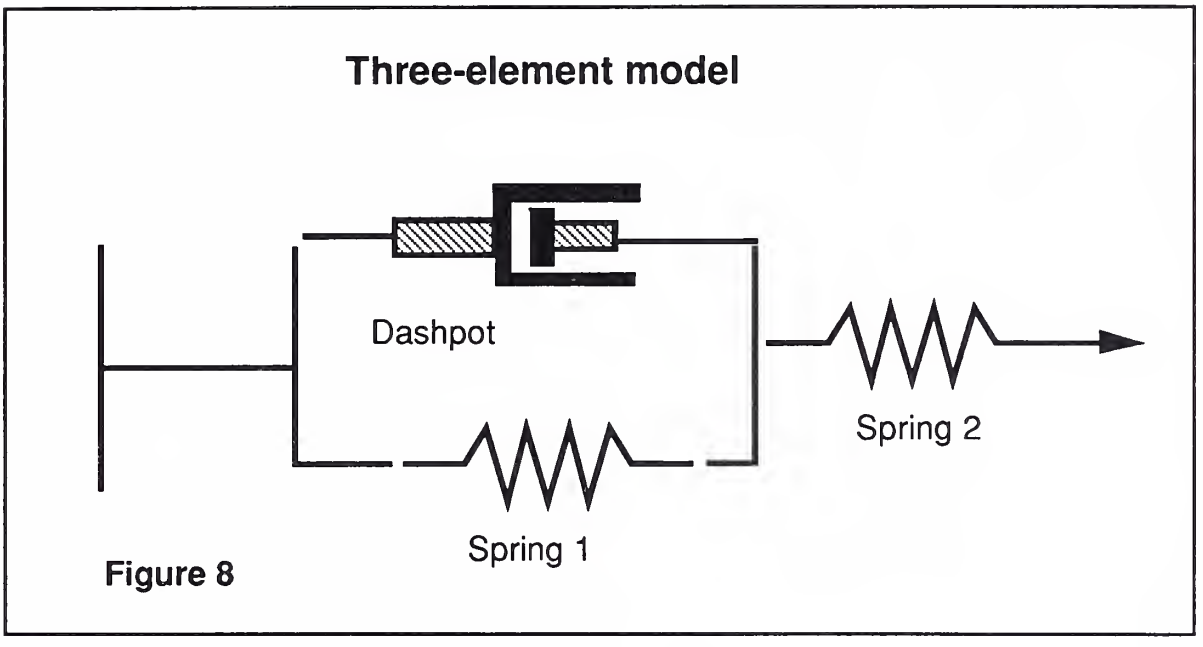

Figure 8

A look at the three-element model explains the creep phenomenon described above. Remember that creep begins with the sudden application of a constant force. When there is a sudden force at the arrow, the dashpot produces a resistance and locks in, but spring 2 elongates, producing an immediate displacement. Then, as time passes, the resistance of the dashpot decreases, allowing spring 1 to elongate proportional to the dashpot and its own stiffness properties. Thus, there is an immediate elastic deformation (displacement) followed by a slower additional deformation [73].

B. Physiology

This section contains two parts. The first reviews the composition and molecular behavior of muscle and the second covers types of muscle contraction.

I. Composition and Molecular Behavior

The musculotendinous unit studied in this project is comprised of the muscle belly surrounded by connective tissue and attached to tendon. Tendons attach muscle to either bone or other tendons. Striated muscle contains two principal components: contractile and connective tissue. Contractile tissue provides the change in length or tension while the connective tissue acts to support the contractile machinery and transfer the movement to the tendons and bones.

Each muscle fiber is surrounded by loose connective tissue called endomysium. Fibers are then organized into groups or fascicles enclosed in the denser connective tissue of the perimysium. Surrounding the entire muscle is fascia of fibrous connective tissue named the epimysium [76]. The predominant component of connective tissue, as well as tendons and ligaments, is collagen.

Collagen fibers of the perimysium and epimysium appear continuous with collagen in the tendon, however, detailed studies of this region, called the myotendinous junction (MTJ), show that the structure is more complex. It is a highly specialized region for transmitting force from the intracellular myofibril, across the plasma membrane, to the extracellular collagen fibers. Understanding mechanical forces at the myotendinous junction is important because *in vivo* and *in vitro* studies, as well as clinical observations,

frequently show muscle failure occurs near the muscle-tendon junction [16, 24, 30, 33, 65].

There are three types of muscle found in the human body: skeletal or striated, smooth, and cardiac muscle. This discussion will only address skeletal muscle, which comprises 40-45% of the total body weight. The structural unit of muscle is the fiber. Fibers are 10-100 μm in diameter and 1-30 cm in length [76]. Each fiber is a cell that contains hundreds of nuclei, making it a syncitium. Numerous myofibrils run the length of the fiber.

Myofibrils are 1 μm in diameter and are arranged in parallel so that the surface under the light microscope gives a characteristic banding pattern; hence the name striated muscle. Each repeat in this pattern represents a sarcomere, the functional unit of contraction in the muscle [76]. The sarcomeres comprise 90% of skeletal muscle and contain the contractile proteins or myofilaments [74].

The ultra structure of muscle has been studied quite extensively [35, 41, 43]. Contractile proteins are thin filaments of actin and thick filaments of myosin. Thick filaments are centrally located and form a dark region known as the "A" band. Thin filaments are attached to the borders of the sarcomere at the "Z" line. The thin filaments extend centrally to overlap with the thick myosin filaments.

Repeating sarcomeres are surrounded by a network of tubules known as the sarcoplasmic reticulum. This membrane invaginates each myofibril forming transverse sacs known as terminal cisternae, which enclose a system of smaller tubules called T tubules. This extracellular duct system serves as a reservoir for the exchange of fluids and ions, particularly calcium, into and out of the muscle cell [35, 76]. Calcium plays a key role in the mechanism of contraction.

Myosin molecules have a tail region and a globular head region that resembles a lollipop, with the head able to interdigitate into the actin filament [76]. Actin is a double helix of polymers that contains a polypeptide chain, tropomyosin, within the groove of the double helix. Troponin is a globular protein that lies at regular intervals along the tropomyosin. These two constituents regulate the formation and breaking of contacts between the actin and myosin filaments.

The sliding filament theory, proposed at the same time by A.F. Huxley and H.E. Huxley is now widely accepted as the mechanism of muscle contraction [43]. According to the theory, active shortening of the sarcomere results from the actin and myosin filaments sliding past one another. The force of contraction is developed by the interaction of the myosin heads with the actin filaments in the region of overlap, the "A" band. The globular heads of myosin swing past actin in an arc that resembles the stroke of an oar. During contraction of a sarcomere, this stroke-like process repeats itself 5-6 times "with an action similar to a man pulling on a rope hand over hand" [94].

Calcium primarily turns contractility on and off. When an action potential is fired at the motor neuron end plate, depolarization of muscle cell membrane occurs. The action potential is passed to the T tubules and the membranes of the terminal cisternae, making them permeable to calcium ions [35]. There follows a series of events in which calcium binds troponin, causing the tropomyosin-actin affinity to decrease. Once this occurs, tropomyosin moves deeper into the actin helix, uncovering binding sites for the myosin globular heads on the actin filament [41].

Interaction of myosin heads with actin filaments is an ATP-dependent process. Movement occurs when the Actin-myosin-ATP complex is

hydrolyzed to yield actin-myosin-ADP+Pi. Energy is also released as heat. The actin-myosin bond will not release until another ATP molecule binds to the myosin cross-bridge and displaces the ADP. This explains the phenomena of rigor mortis where the last movements of the muscle are maintained, 8-24 hours post-mortem, because there is no ATP to release the actin-myosin bonds.

II. Types of Contraction

The principal function of muscle is to provide locomotion and stability for the skeleton. Locomotion is dynamic work while maintenance of body posture is static work. Movement that is coordinated depends on the simultaneous action of both types of work. For example, an athlete kicking a ball must perform dynamic work with the kicking leg and an equal amount of postural work with the standing leg to efficiently transmit the greatest force into the ball.

There are several types of muscle contraction. When muscle develops enough tension to overcome external resistance, it shortens, causing joint movement. This is concentric contraction, an example is the action of the quadriceps when the knee is extended ascending stairs. When a muscle cannot develop sufficient tension to overcome an external load, lengthening of the muscle occurs, which is called eccentric contraction. Eccentric contraction of the biceps occurs when lowering from a pull-up.

Both concentric and eccentric contraction are described as dynamic since they involve movement. In an isometric contraction, muscle works statically to maintain posture or prevent movement. For example, by holding a book against gravity, muscles in the back and upper limb work without

apparent movement. Apparent, because there *is* stretch (movement) of the elastic components in the muscle-tendon unit as the muscle attempts to shorten. This produces a moment sufficient to support the load in a fixed position [76].

No mechanical work is performed in isometric contraction. Instead, the muscle work is physiologic with energy expended as heat [76]. Tension in muscle varies with the type of contraction. Eccentric contraction develops the most tension, followed by isometric and then concentric contraction. Eccentric loads may be as much as twice the maximum isometric load if applied rapidly [11, 55]. The difference is due to the longer contraction time, which allows more muscle fiber recruitment and greater transmission of tension to the series elastic component. As mentioned earlier, muscle strain injuries tend to occur during eccentric contractions.

Eccentric contraction is also associated with delayed-onset muscle soreness (DOMS) or muscle pain developing 24-48 hours following muscular work [5, 13, 52, 59, 79, 88]. This subjective soreness also correlates with elevation of serum creatine phosphokinase levels, which can remain elevated for many weeks following one bout of eccentric exercise [18]. Clinically, muscle ruptures in weight-lifters or sprinters are often associated with pre-existing muscle soreness. Safran has proposed that a continuum of muscle injury exists beginning with DOMS and progressing to first, second and third degree muscle strains [78].

C. Experimental

Experimental studies in muscle strain injury will cover work in muscle mechanics, viscoelasticity and site of rupture in the muscle-tendon unit.

A.V. Hill and others in the 1920's demonstrated that muscle has both contractile and non-contractile elements contributing to its viscoelastic behavior. Hill proposed that muscle is a contractile component arranged in parallel with an elastic component (PEC) and in series with a second elastic component. Tendon was thought to represent the series elastic component [37, 49]. He developed a three-element model for muscle that replaces the dashpot of the three-element model for viscoelastic materials with a contractile element **(See Figure 9)**. Hill's model assumes the contractile element is stress-free and distensible in the resting state. It also assumes the contractile component is time-dependent (viscous) under tension and the non-contractile connective tissue elements are purely elastic.

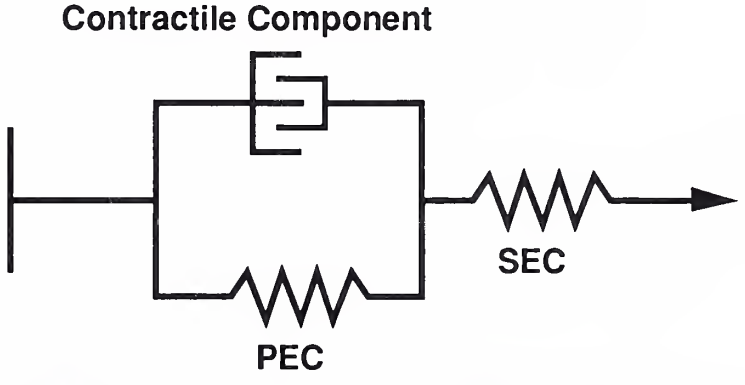

Hill's three-element model of a muscle-tendon unit.
PEC = parallel elastic component. SEC=series elastic component. (Adapted from Nordin and Frankel, 1989)

Figure 9

The source of elasticity is in the passive elastic structures such as the muscle sheath. Banus and Zetlin proposed that the connective tissue sheath (the epimysium, perimysium and sarcolemma) was the important site for the PEC [8]. Later evidence suggested some passive tension comes from the interaction of cross-bridges within myosin filaments that have a spring-like quality contributing to muscle elasticity [39, 43].

Fung described the basic problem of Hill's model. "The series element is functionally, but not necessarily structurally, separated from the contractile element" and "the division of forces between the parallel, contractile and series elements is arbitrary" [26, 27]. In other words, it is not possible to assign the tendon, connective tissue and sarcomeres into the three components of Hill's model. This is true because tendon, connective tissue and muscle each behave viscoelastically [93]. Hill's model serves only as a gross representation of muscle mechanics [64]. This is true for both *in vivo* and *in vitro* models. For example, this project uses *in vitro* muscle which has non-extensible sarcomeres and yet still behaves viscoelastically.

Early work in muscle elongation involved *in vitro* stimulation of individual muscle fibers to determine relationships in force-velocity, tension-length and properties of resting tension [38, 50]. Tension-length curves examine both passive and active properties of muscle **(See Figure 10)**. Passive properties of muscle are recorded as muscle is stretched to constant lengths without stimulation. The curve gets steeper at larger stretches (deformations) because the fibrous elements become tensed. The area in between the two curves is the developed tension. Pinto and Fung found that the derivative of stress with respect to strain provides a linearly increasing function that describes the behavior of many biologic tissues including skeletal muscle in passive extension [75].

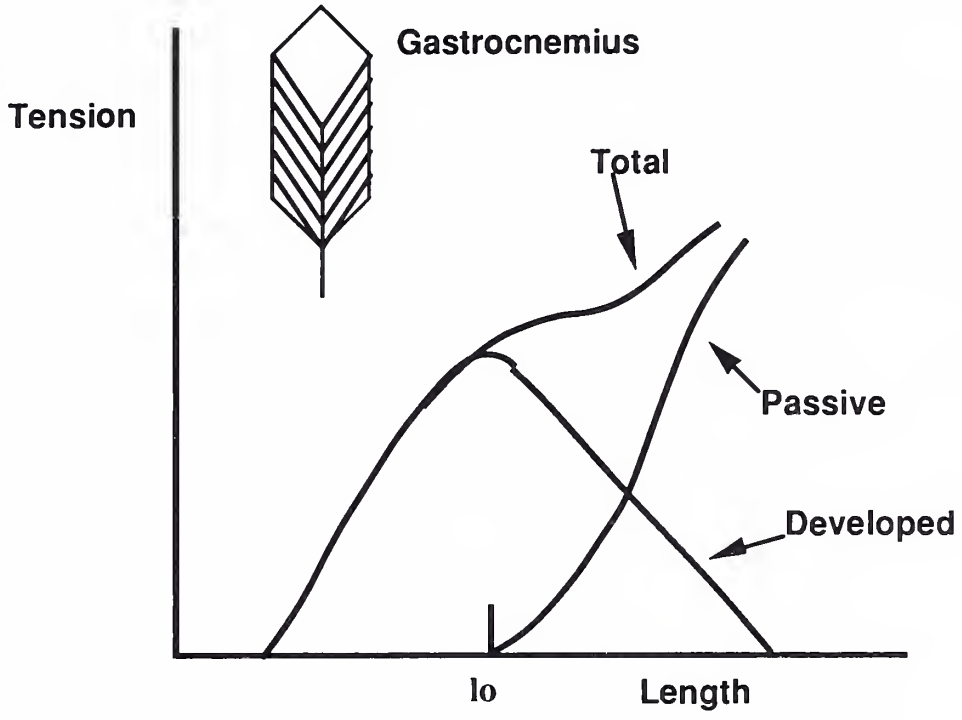

Tension-length curve for gastrocnemius muscle. The high content of connective tissue in the muscle shows a rapidly increasing slope in the passive curve. (Adapted from McMahon, 1984).

Figure 10

The shape of the passive curve is influenced by muscle architecture as well as rate of loading. Muscle-tendon units with a greater proportion of tendon (connective tissue) in their length, such as gastrocnemius, develop tension more quickly giving the curve a continuous, rapidly increasing slope. Faster loading rates also increase the slope of the curve.

Muscle was first demonstrated to behave as a viscoelastic material by Abbot and Lowy who examined stress relaxation in muscle stimulated to tetanus and stretched at constant rates to less than optimal contractile lengths [1]. Because of the active state of the muscle, a true engineering stress

relaxation test (where the length is fixed after an initial displacement) may not be applicable. In contrast to the present study, they examined non-failure properties of pre-shortened muscle at lengths where there was negligible resting tension; lengths below our initial lengths.

The length (tension) of a muscle fiber changes its mechanical characteristics. At rest, tension is attributed to the PEC [26]. During submaximal contraction, the tensile force is determined by the contractile component and the PEC is negligible [15]. It was hypothesized that when muscle is passively pulled to failure, the PEC is predominantly stressed.

Failure mechanics were not addressed by these early studies. Reference to the stress-strain curve in **Figure 1** confirms this short-coming. The experiments determine behavior only in the early linear elastic range. Failure mechanics of other biologic tissues such as ligament, tendon and bone demonstrate that biologic tissues in simple elongation do not fit classical linear elastic theory [26, 84, 91, 93]. For example, biologic tissues cannot be completely represented by Young's modulus. Thus, failure mechanics requires information past the linear elastic range. A second criticism is that these studies were conducted mostly on muscle fibers, which do not apply to stretch characteristics of whole muscle.

Experimental work in muscle strain injury of whole muscle began with *in vitro* studies of muscle-tendon units. In 1933 McMaster examined properties of tendon and muscle ruptures [65]. He was intrigued by clinical cases of late tendon rupture following direct and indirect trauma, such as spontaneous ruptures of the extensor and flexor tendons of the thumb following Colle's fracture. After accumulating numerous clinical cases, he pursued experimental work of failure sites in healthy and surgically-altered muscle-tendon units. Experiments consisted of loading avascular rabbit

gastrocnemius bone-muscle-bone specimens to failure. McMaster's methods of loading were too crude to assess viscoelastic properties, but his clinical and experimental observations found the following:

1) Normal tendon does not rupture when subjected to severe strain. Avulsion of tendon from bone, muscle rupture or separation near the musculotendinous junction occurs.

2) Disease processes in tendon are necessary for rupture at low strains and blood supply is more important in healing than an intact tendon sheath.

3) Rupture of muscle fibers occurs following direct and indirect trauma, leading to degenerative changes and disease processes that predispose to rupture. These muscle ruptures are often overlooked clinically.

These early conclusions suggest the frequency and importance of muscle injuries are underestimated. And since avulsions of tendon from bone are infrequent in strain injuries, it points to the muscle and muscle-tendon junction as important areas in understanding strain injuries.

After McMaster, research in muscle-tendon failure was not pursued until the 1970's. Welsh demonstrated viscoelastic properties in isolated rabbit tendon pulled to failure, reporting 50% increases in stiffness and failure load for strain rates from 0.2 mm/sec to 20 mm/sec [93]. He also found the muscle belly and muscle-tendon junction to be the weakest point.

Jarvinen studied the effect of mobilization and immobilization (up to 42 days after injury) on a contusion injury in a rat model [45, 47]. Tensile failure tests demonstrated a significant difference with the type of treatment. All muscles were tested at a stretch rate of 0.25 mm/sec. Force, length and energy to failure were reported in detail, but comparisons with the present study cannot be made as values of stress and strain were not reported.

In studying the ability of muscle to recover from laceration, Garrett passively pulled rabbit muscle to failure using *in vivo* models [34]. Garrett modified his techniques to study the biomechanics of muscle strain more closely [28]. Using an *in vivo* model of anesthetized rabbits, he found maximal isometric contraction by nerve stimulation could *not* produce muscle fiber disruption. For gross or microscopic failure to occur, an external or passive stretch of the muscle was needed. The forces necessary to cause failure proved to be several times the force of maximal isometric contraction [30]. Passive forces come from tension generated outside of the muscle that is strained.

Garrett investigated the effect of passive stretch on five muscles with varied architecture at three strain rates [30]. He found the site of failure to occur consistently within 1 mm of the muscle-tendon junction. Peak loads at the different strain rates were not reported, which precludes a measurement of viscoelasticity.

Kabo conducted one of the few studies on passive stretch in human cadaveric muscle preparations [54]. Previous work utilized either individual muscle fibers or bundles, instead of whole muscle. This work will be expanded on in the discussion.

Taylor demonstrated stress relaxation, stretch-rate dependency and hysteresis with passive stretch in anesthetized rabbits [86]. This study provides evidence that viscoelastic properties in muscle form the basis of flexibility and stretching techniques. However, by limiting measurements to the linear elastic range, the data does not directly address strain injuries.

Materials and Methods

Preparation:

Ten New Zealand white rabbits (weighing 5-6 lbs, approx. 3 months old) were sacrificed by an intravenous injection of 3 ml Sodium Pentobarbital (Conc. 65 mg/ml; Butler Pharmaceuticals, Columbus, Ohio). Organs were harvested by two other research facilities and we amputated the hind limbs at the hip, keeping right and left legs together. Specimens were immediately bagged in heavy plastic and frozen at -20^{o} C until required for preparation and testing.

After thawing the specimens in a 37°C water bath, bone-muscle-bone mounts were constructed using plaster mounts. For each hind limb, the tibialis anterior (TA) and the medial head of gastrocnemius (MG) were isolated by carefully dissecting away the skin, fascia and other lower limb musculature, leaving origins and insertions intact.

The gastrocnemius muscle, when combined with the soleus, forms the triceps surae, the powerful flexor of the ankle. These muscles share a common insertion at the Achilles' tendon [19]. The gastrocnemius muscle has a multipennate structure and a common central tendon that requires careful dissection to separate the medial and lateral muscle bellies. For the MG specimens, it was possible to identify and separate the respective halves of the tendon to a point approximately 2 cm above the calcaneus. A drill hole was made in the femur proximal to the origin and stainless steel suture wire was then passed through the hole, enabling solid fixation of the femur into the plaster cast. A similar procedure was carried out at the calcaneus.

TA is a fusiform muscle that has its origin on the lateral condyle and tuberosity of the tibia. The insertion is by a narrow tendon that passes under

the crural ligament near the distal leg and reaches the base of the second metatarsal bone [19]. TA specimens were fixed by placement of a screw into the tibial plateau. Suture wire was then wrapped around the screw and placed into the plaster. This allowed good fixation of the proximal muscle without contact of the muscle to plaster. It also kept tension in line with the normal stresses of the muscle. The distal insertion was fixed by a wire through the mid forefoot placed in plaster.

Muscle and tendons were wrapped in gauze and kept wet during the procedure with 0.9% normal saline.

Experimental Tensile Failure Apparatuses:

Each muscle specimen was stretched to failure at either a slow (0.1 millimeter per second) or a fast (1 meter per second) rate. Although the 10,000 factor difference in stretch rate necessitated using two different experimental machines, the load and displacement measurement equipment and protocol were similar. Load was measured with a specially constructed load cell mounted in series with the specimen, between the plaster casting and the fixed portion of experimental apparatus. The load cell was simply constructed of a section of aluminum tubing instrumented with four strain gages in a Wheatstone bridge. The load cell was calibrated with dead weights, and designed to maintain a linear response well above 150 N. Displacements were measured with a linear voltage displacement transducer (LVDT) placed in parallel with the specimen and attached to the traveling end of the specimen and experimental apparatus **(See Figure 12)**. Using an IBM PC compatible, specifically written software (Turbo PASCAL, Borland, Scottsdale, California) controlled the elongation, recorded the analog signal from the load cell and

LVDT, and then stored the data. The stored data was transferred to a Macintosh system for analysis and presentation.

Each specimen was adjusted in the apparatus so that there was no slack in the muscle belly or tendon prior to tearing. The following measurements were made at this point with Mitutoyo vernier calipers: muscle-tendon unit, muscle, muscle with a uniform width, width, thickness and tendon length.

Low Speed:

In the slow stretch apparatus the travelling end of all left hind limb specimens were attached to the threaded shaft of a stepping motor (Berglahr RDM 5913/50). This apparatus is very similar to the common material tester. The turning rate of the stepping motor, which in turn defined the rate of shaft displacement, was controlled by the IBM PC compatible. The rates available ranged from 0.1 mm/sec to 10 cm/sec. For this study we chose the slowest rate available, 0.1 mm/sec. These muscles were pulled until failure in a continuous manner and there was no accelerative component as in the high speed specimens.

Specimens were removed from the apparatus and the muscle and tendon were dissected from their insertions. The gross site of failure was carefully noted. Weight and volume (displacement in water, assuming the density of muscle equals 1 gram/cc) of each muscle were recorded and the tissue was placed in 3.7% formaldehyde for later histologic examination.

The load and displacement at failure were taken directly from the data points and plotted using Grapher software. (Grapher, Golden, CO.) Stiffness, stress, strain, elastic modulus and energy absorbed to failure were calculated from the load-deformation curves at a later time.

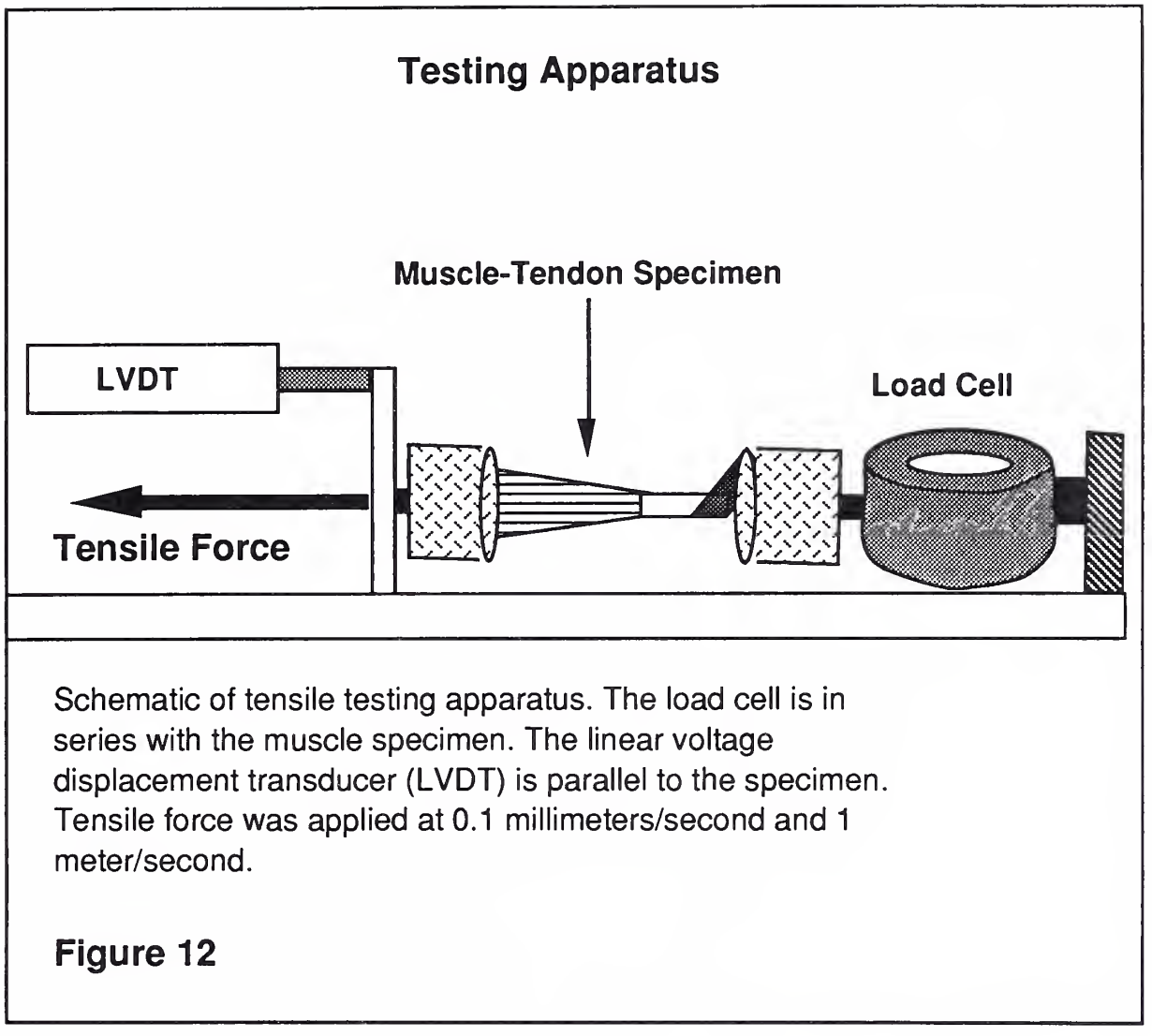

Schematic of tensile testing apparatus. The load cell is in series with the muscle specimen. The linear voltage displacement transducer (LVDT) is parallel to the specimen. Tensile force was applied at 0.1 millimeters/second and 1 meter/second.

Figure 12

High Speed:

In the high speed apparatus, the travelling end of each right hind limb specimen was attached to a piston driven by a reservoir of compressed air (80 psi). A solenoid valve, controlled by the IBM PC, was opened to begin each test. The rate at the which the muscle was stretched to failure depended upon many factors that included the initial storage pressure, the storage volume, the size of the solenoid valve, and the specimens resistance to stretch. Despite all of these factors we were consistently able to maintain a linear stretch rate of approximately 1 meter per second. The average stretch rate was 1.06 $\pm$ 0.13

meters/second for TA and 1.00 ± 0.16 meters/second for MG specimens. A graph of the velocity curve for tibialis anterior specimen 7 is shown.

Figure 13 High Speed Rate

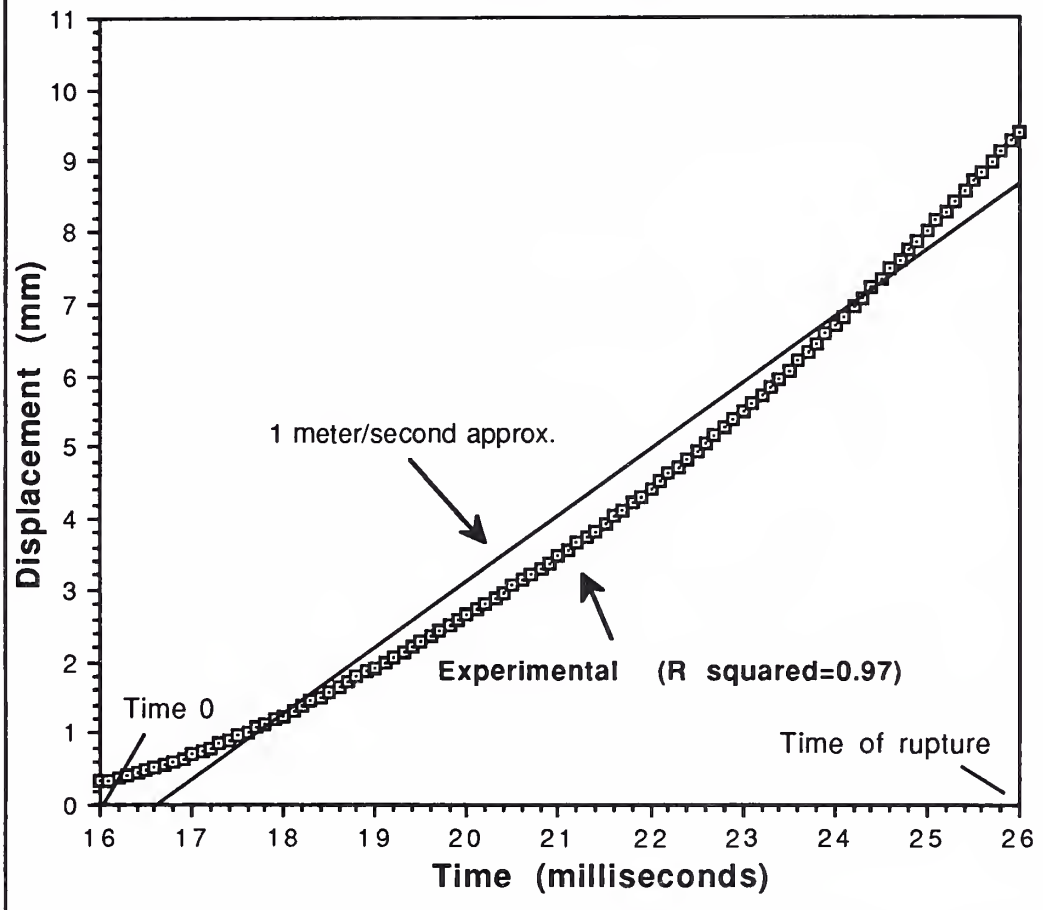

High Speed Rate: Specimen 7 gives a typical rate curve for the high speed tears. The straight line is the first polynomial of the rate curve. (R=0.97) Time zero is 16 msec, time of rupture is 26 msec.

Time zero was defined as the point where displacement began continuously increasing. There was a 16-20 msec delay in the computer circuitry **(See Figure 13)**.

Length measurements, weight and volume were recorded as in the low speed group. Specimens were also fixed in formaldehyde following rupture and the same biomechanical parameters were measured.

Histology:

After fixation of the specimens in serial changes of 3.7% formaldehyde over a three week period, the muscle and tendon surrounding the tear site was embedded in parafilm, sectioned and stained with Masson's Trichrome, hematoxylin and eosin.

This staining technique best visualizes the muscle fibers against collagen bundles of tendon [7]. The histology of the rupture site was studied. The normal anatomy of tibialis anterior and gastrocnemius muscles were also examined in transverse and longitudinal sections using the same techniques.

Scanning Electron Microscopy:

Scanning electron microscopy (SEM) was conducted for study of the myotendinous junction. (AUTOSCAN, ETEC Co.) Specimens were fixed immediately following rupture with 3% glutaraldehyde in 0.1 M cacodylate, dehydrated in graded concentrations of ethanol and plated with 200A of gold palladium (protocol of Alan Pooley; Peabody Museum, New Haven, CT). SEM allows extremely high resolution of the myotendinous junction because the wavelength of the x-ray beam is three orders of magnitude smaller than the wavelength of visible light [69].

Analysis:

Measurement of these seven parameters enabled comparison of the mechanical failure properties at low and high stretch rates:

Load
Displacement
Stiffness
Energy absorbed to Failure
Stress
Strain
Elastic Modulus

Failure load was defined as the peak on the load-displacement curve or in the case of a plateau region near the peak load, the point where the stiffness had decreased sharply, the beginning of the plastic region. Both groups were normalized with a 0.5 N preload, which is the approximate resting tension of the muscles.

Failure displacement was defined as the displacement recorded by the LVDT at the peak load (defined above). Initial length was calculated at the the 0.5 N preload.

Stiffness is the resistance of a material to a load. As shown on the load-displacement curves, the relationship between the load and displacement was linear prior to failure. A simple linear regression was applied to all of the load-displacement curves and the average R^2 value (a measure of linearity with a straight line having an R^2 value of 1) was 0.97. Based on the assumption of linearity, the stiffness was measured from the slope at the point of failure.

The energy absorbed to failure was determined by integrating the area under the load-displacement curves from a preload of 0.5 N to the failure load.

Failure stress was determined by dividing the peak load by the physiologic cross-sectional area (PCSA). PCSA was calculated by dividing the volume of the muscle, displacement in water (assuming density of 1 gram/cc), by the length.

Strain values were measured by dividing displacement by the initial length of muscle. Several methods of describing strain exist, as discussed by Fung [27]. We have chosen this representation for its simplicity and the small differences from the formula suggested by Fung, L^2-$Lo^2/2Lo^2$, (Lo=initial

length) for biologic tissues. Note the stretch ratio, $(\Delta L+Lo)/Lo$, is related to the strain reported here. For example a strain of 20% had a stretch ratio of approximately 1.20.

Finally, the elastic modulus was calculated by dividing stress by strain.

The stiffness, energy absorbed to failure, and R^2 values were calculated using Macintosh software (Passage II, Passage Software, Inc., 1989). Column graphs were made with Cricketgraph, version 1.3.2. The remaining calculations and tables were made in Microsoft Excel, version 2.2.

Statistical analysis was determined using the students t-test (Statview, Abacus Concepts, Inc., Berkeley California). When we compared the effect of stretch rate on failure properties, a paired t-test for each muscle type was used. An unpaired t-test was used to determine the significance of muscle type at each rate.

Results

Results are summarized in the following manner.

A column graph accompanies each property. Rates are plotted on the x-axis and the dependent variable (load, energy absorbed, etc.) including error bars, are plotted on the y-axis. The two columns on the left are TA. The two columns on the right are MG. The mean value for the specimens in each group (n= 10) and the standard deviations (STD) are contained in the graph. P values comparing the two rates are printed below the columns.

Table 1 contains the values of the 7 parameters for each specimen, including means and STDs. **Table 2** contains measurements of length, volume, weight, preload, area, high speed rates and R^2 values.

Load-displacement curves are given in Figure 21 and the appendix.

Load

The average failure load for TA was 28.42 N $\pm$ 6.32 N for the high stretch rate and 12.30 N $\pm$ 2.34 N for the low stretch rate (p=0.0001). The average failure load for MG was 42.99 N $\pm$ 10.31 N for the high stretch rate and 18.17 N $\pm$ 2.84 for the low stretch rate (p=0.0001). Failure load for both TA and MG muscles increased by the same amount, 230%, from low to high speeds **(See Figure 14, Table 1)**.

Figure 21 is a typical load-displacement curve for the TA 1 and MG 1 specimens. The appendix contains the load-displacement curves for specimens 2-10.

Displacement

Mean displacement for TA was 13.13 N $\pm$ 2.83 N for high speed and 13.83 N $\pm$ 2.68 N for low speed (p=0.41). The mean displacement for MG was

10.75 N ± 3.13 N for high speed and 12.33 N ± 2.74 N for low speed (p=0.21). There was a slight trend for the gastrocnemius to lengthen further before failure, but it was not statistically significant **(See Figure 15, Table 1)**.

Stiffness

The average stiffness for TA was 2.24 N/mm ± 0.53 N/mm for high speed and 0.96 N/mm ± 0.24 N/mm for low speed (p=0.0001). This is an increase of 233% in stiffness between the high and low speed TA groups. The average stiffness for MG was 4.05 N/mm ± 1.63 N/mm for high speed and 1.48 N/mm ± 0.59 N/mm for low speed (p=0.0003). The stiffness increased 274% between the high and low speed MG groups **(See Figure 16, Table 1)**.

Energy absorbed

The average energy for TA was 200.11 N*mm ± 74.48 N*mm for the high speed group and 83.31 N*mm ± 23.52 N*mm for the low speed group (p=0.0003). This is a 240% increase in the energy absorbed for TA. The average energy for MG was 291.63 N*mm ± 128.47 N*mm for the high speed and 109.02 N*mm ± 30.71 N*mm for the low speed group (p=0.0009). This is a 268% increase in the energy absorbed for MG **(See Figure 17, Table 1)**. The energy absorbed to failure is shown graphically in Figure 6.

Stress

Average failure stress for TA was 0.76 MPa ± 0.22 MPa in the high speed group and 0.35 MPa ± 0.09 MPa in the low speed group (p=0.0001). The mean failure stress for MG was 0.66 MPa ± 0.23 MPa for the high speed group and 0.31 MPa ± 0.09 MPa for the low speed group (p=0.0001). This is an increase of approximately 215% between the high and low speed groups for both TA and MG stress **(See Figure 18, Table 1)**.

TA experienced greater mean stresses than MG at both rates, but the difference was not significant (p=0.32 at the fast rate and p=0.31 at the slow rate).

Strain

The average strain to failure for TA was 19% $\pm$ 4% for the high speed group and 19% $\pm$ 3% for the low speed group (p=0.44). The average strain for MG was 18% $\pm$ 5% for the high speed group and 20% $\pm$ 5% for the low speed group (p=0.21). As in failure displacement, there was no statistically significant difference between high and low speed groups **(See Figure 19, Table 1)**.

There was also no statistical difference between MG and TA for strain at low or high stretch rates (p=0.88 for the low rate and p=0.57 for the high rate).

Modulus of elasticity

The average elastic modulus for TA was 4.23 MPa $\pm$ 1.53 MPa for the high speed group and 1.83 MPa $\pm$ 0.57 MPa for the low speed group (p=0.0001). This is an increase of 231% from the low to high speed loading rates. The average elastic modulus for MG was 3.99 MPa $\pm$ 1.57 MPa for the high speed group and 1.68 MPa $\pm$ 0.82 MPa for the low speed group (p=0.0001). This is an increase of 238% between the two groups **(See Figure 20, Table 1)**.

The elastic modulus was not different between muscle types for each rate (p=0.63 for the slow rate and p=0.73 for the fast rate).

Figure 14 Failure Load

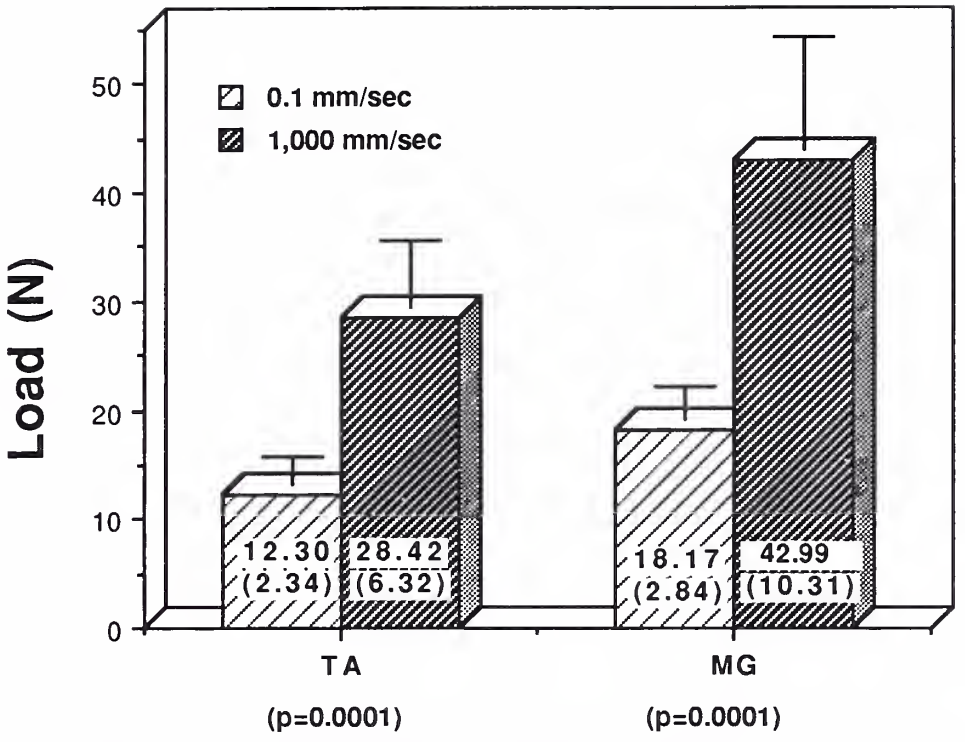

Failure Load: Low stretch rates on the left are significantly lower than high stretch rates on the right. Mean, standard deviations and p values are given.

Figure 15 Failure Displacement

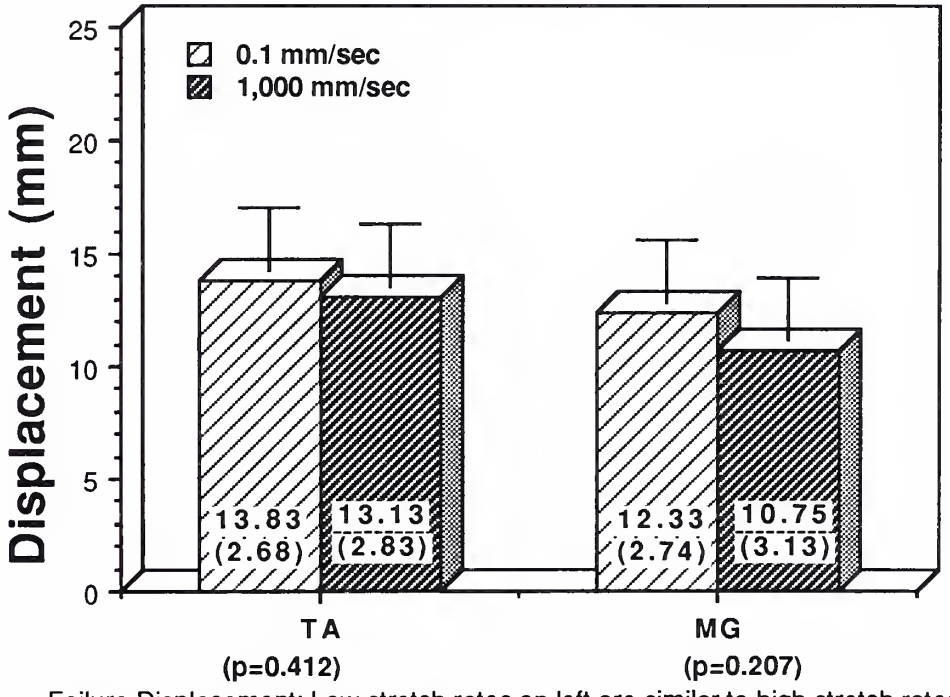

Failure Displacement: Low stretch rates on left are similar to high stretch rates. Mean, standard deviations and p values are given.

Figure 16 Failure Stiffness

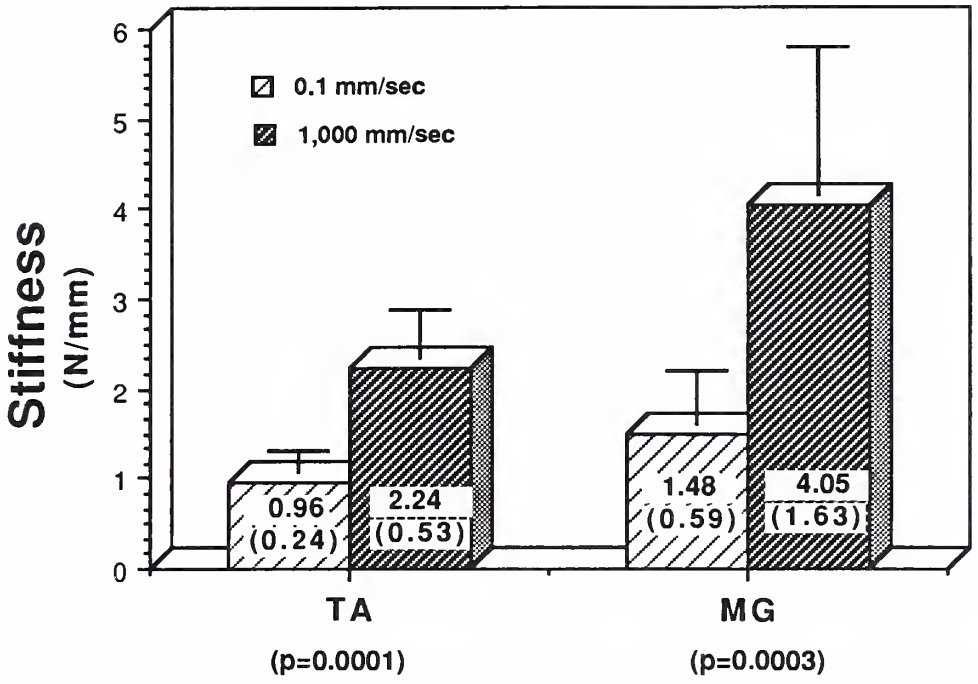

Failure Stiffness: Low stretch rates on the left are significantly less stiff than hgi stretch rates on right. Means, STDs and p values given.

Figure 17 Energy absorbed to Failure

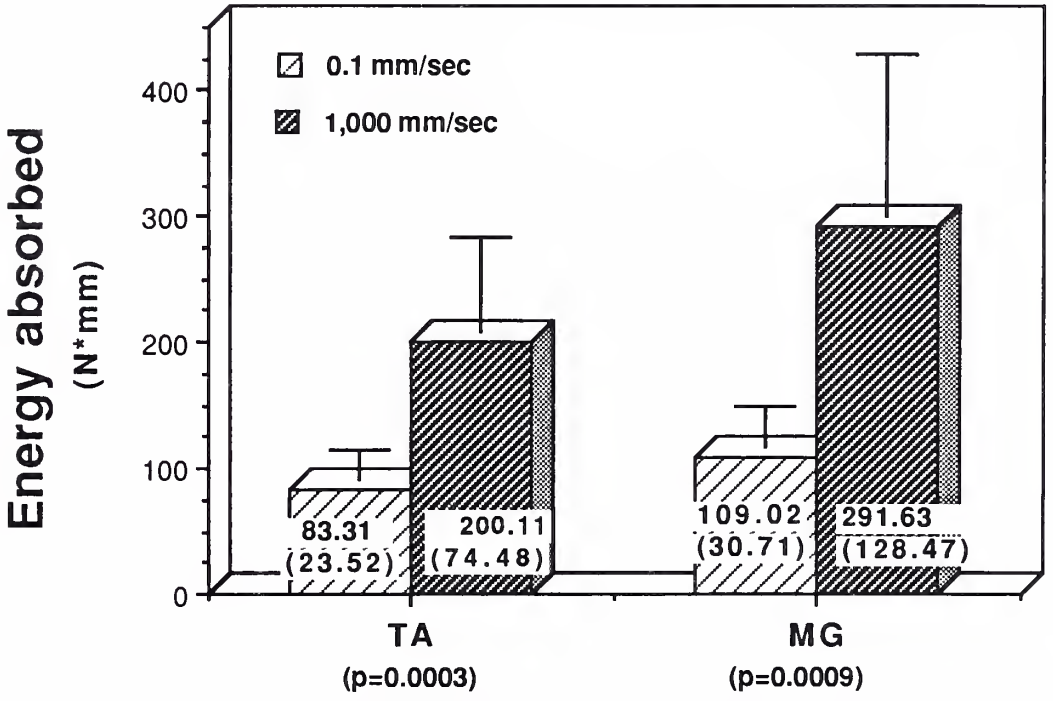

Energy Absorbed: Low stretch rates on the left absorbed significantly less than high stretch rates on the right. Means, STDs and p values are given.

Figure 18 Failure Stress

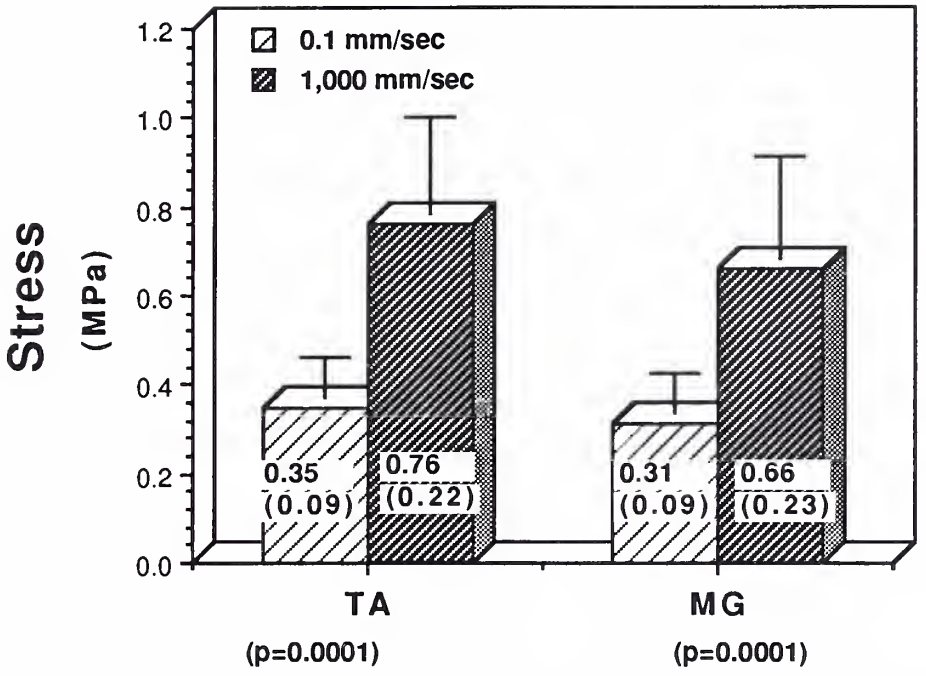

Failure Stress: Low stretch rates on left have significantly lower stresses than high stretch rates on the right. Means, STDs and p values are given.

Figure 19 Failure Strain

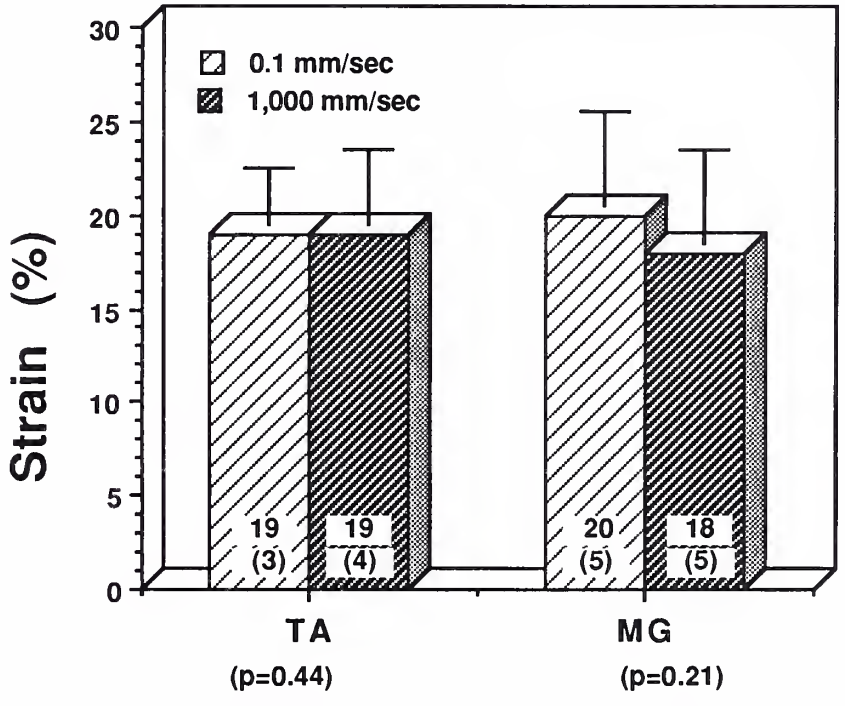

Failure strain: There was no difference between the high and low speed groups in strain to failure. Mean values, STDs and p values are given.

Figure 20 Modulus of Elasticity

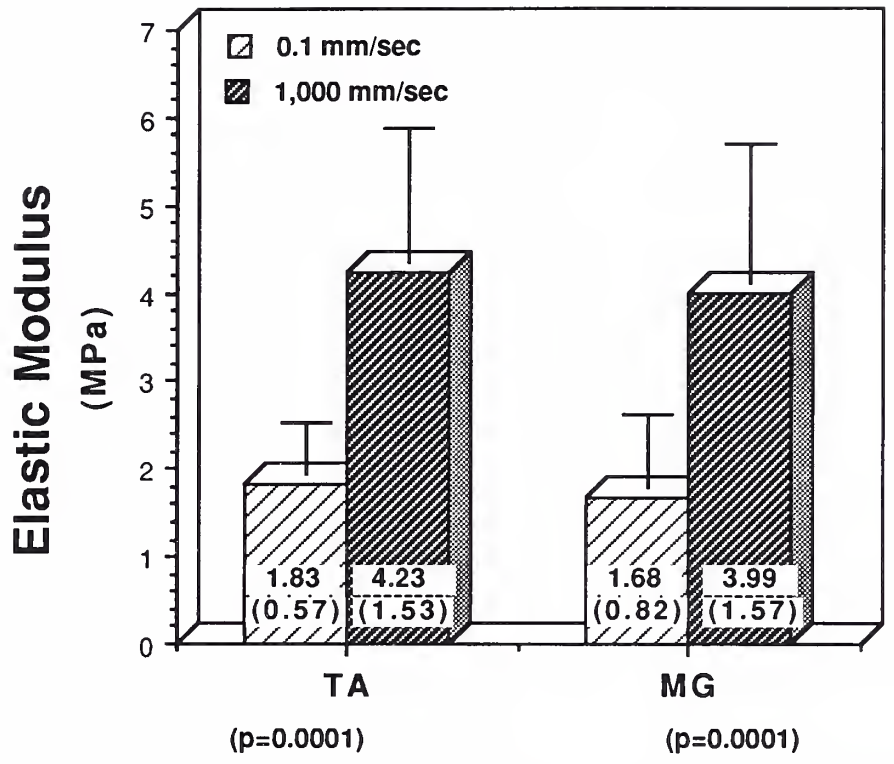

Elastic Modulus: Low stretch rates on the left have significantly lower EM than high stretch rates on right. Means, STDs and p values are given.

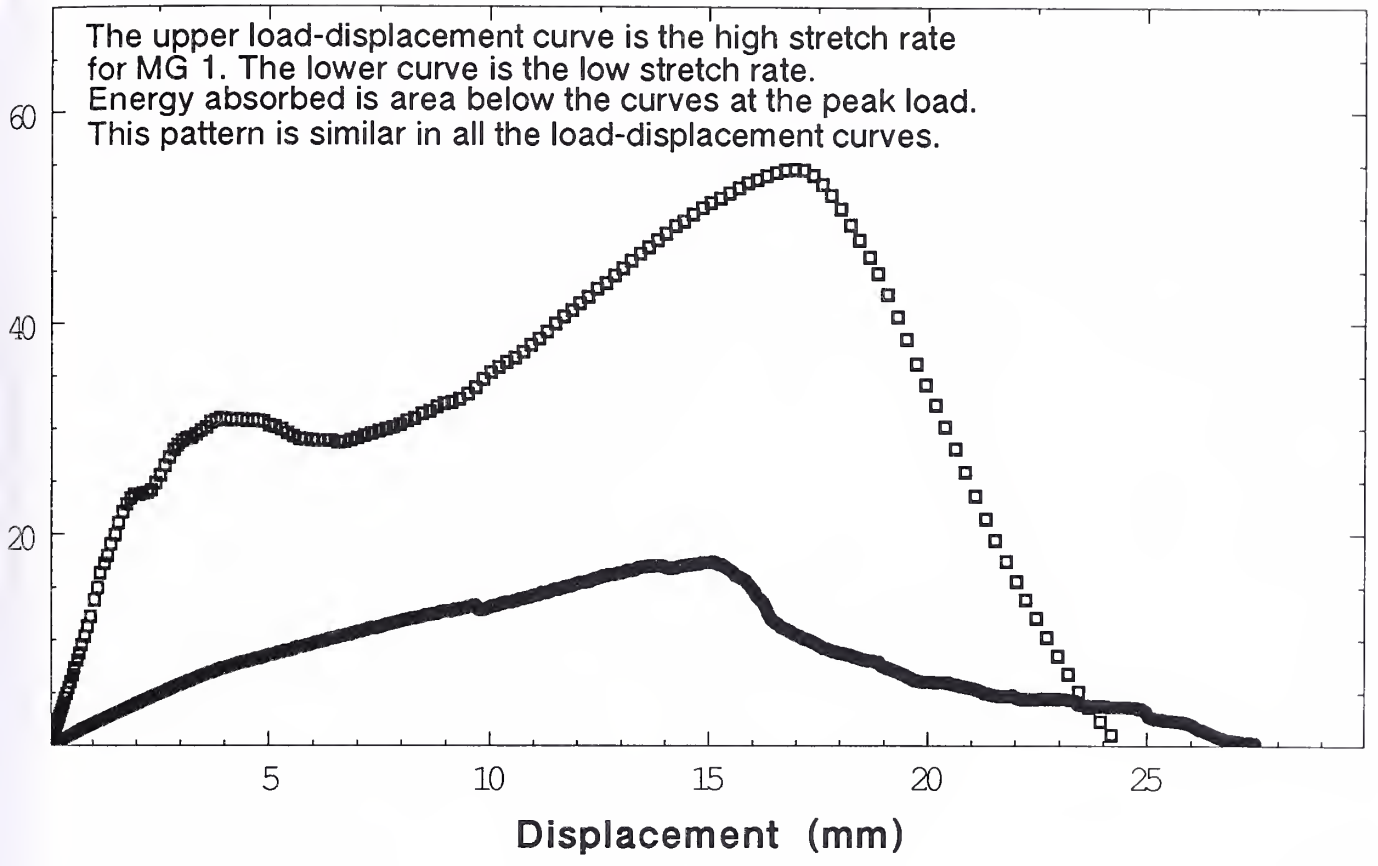

TA 1 Load-Displacement Curve

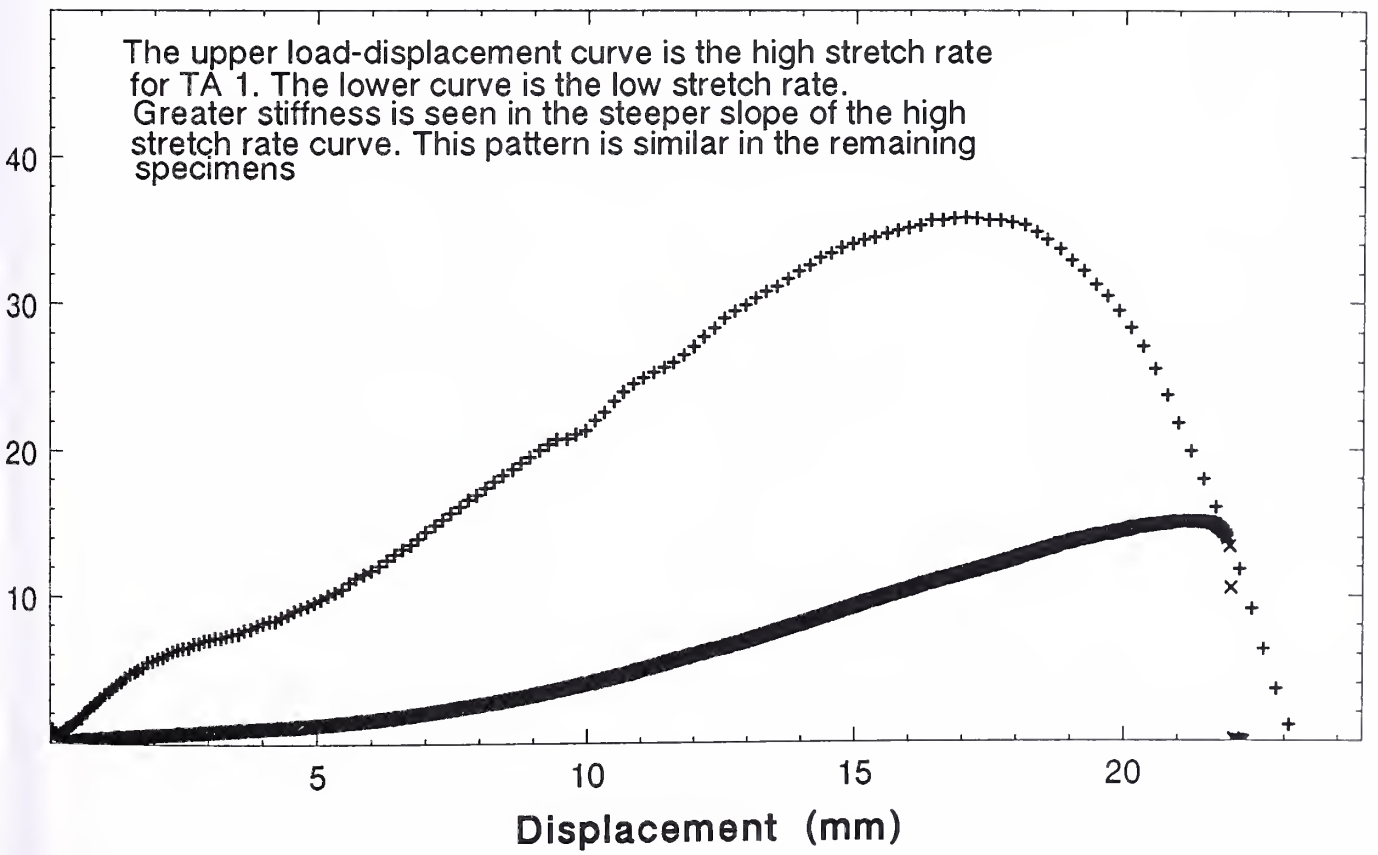

Table 1- TA Values

HIGH SPEED							
TA	Load	Displacement	Stiffness	Energy	Stress	Strain	E
	(N)	(mm)	(N/mm)	(N*mm)	(MPa)	%	stress/strain
1	35.89	17.03	2.2	322.55	0.80	22	3.60
2	28.43	12.58	2.31	191.54	0.69	19	3.71
3	32.53	13.76	2.45	248.12	0.84	20	4.29
4	33.8	17.92	1.88	313.87	0.79	26	3.08
5	22.26	11.3	2.08	138.12	0.57	16	3.65
6	26.24	14.06	1.9	191.03	0.67	20	3.36
7	38.12	10.3	3.58	182.79	1.26	16	8.06
8	24.49	11.35	2.1	143.82	0.90	16	5.56
9	20.24	8.98	2.28	91.92	0.53	13	4.01
10	22.24	14.05	1.65	177.35	0.57	19	3.01
Average	28.42	13.13	2.24	200.11	0.76	19	4.23
STD	6.32	2.83	0.53	74.48	0.22	4	1.53
Count	10	10	10	10	10	10	10
LOW SPEED							
TA	Load	Displacement	Stiffness	Energy	Stress	Strain	E
	(N)	(mm)	(N/mm)	(N*mm)	(MPa)	%	stress/strain
1	15.10	19.95	0.82	128.98	0.36	28	1.30
2	14.20	11.58	1.28	87.70	0.34	16	2.13
3	9.74	10.79	0.93	49.89	0.26	16	1.66
4	14.89	14.60	1.08	109.55	0.43	21	2.09
5	13.19	14.39	0.98	95.13	0.38	20	1.94
6	11.34	13.91	0.87	81.30	0.30	21	1.45
7	14.70	11.26	1.42	71.16	0.52	17	3.11
8	10.08	12.71	0.81	58.53	0.36	19	1.93
9	10.28	13.32	0.83	71.00	0.32	19	1.65
10	9.49	15.77	0.61	79.85	0.21	20	1.06
Average	12.30	13.83	0.96	83.31	0.35	19	1.83
STD	2.34	2.68	0.24	23.52	0.09	3	0.57
Count	10	10	10	10	10	10	10

Table 1- MG Values

HIGH SPEED							
MG	Load	Displacement	Stiffness	Energy	Stress	Strain	E
	(N)	(mm)	(N/mm)	(N*mm)	(MPa)	%	stress/strain
1	54.55	16.94	2.6	585.27	0.56	28	1.99
2	41.27	13.85	2.5	378.22	0.64	22	2.84
3	37.16	5.37	7.56	119.69	0.58	10	6.03
4	30.63	10.14	2.69	229.73	0.46	17	2.78
5	43.57	8.24	5.3	196.49	0.70	14	5.12
6	49.76	10.33	4.76	285.96	0.73	17	4.28
7	63.94	12.14	4.95	368.84	1.27	18	6.89
8	33.56	10.93	2.89	280.37	0.59	18	3.25
9	38.94	9.35	4.17	232.46	0.55	15	3.56
10	36.48	10.19	3.12	239.28	0.54	17	3.16
Average	42.99	10.75	4.05	291.63	0.66	18	3.99
STD	10.31	3.13	1.63	128.47	0.23	5	1.57
Count	10	10	10	10	10	10	10
LOW SPEED							
MG	Load	Displacement	Stiffness	Energy	Stress	Strain	E
	(N)	(mm)	(N/mm)	(N*mm)	(MPa)	%	stress/strain
1	17.34	14.78	1.08	158.68	0.21	26	0.83
2	19.54	13.81	1.32	122.68	0.31	24	1.33
3	21.70	13.22	1.45	125.81	0.34	23	1.51
4	12.85	11.37	1.05	83.97	0.19	18	1.04
5	17.55	8.75	2.07	66.57	0.38	14	2.68
6	16.44	9.60	1.65	78.14	0.30	14	2.11
7	22.34	8.31	2.85	90.05	0.45	13	3.36
8	20.24	15.98	1.03	129.97	0.42	24	1.74
9	16.35	15.17	0.99	142.07	0.25	24	1.05
10	17.31	12.30	1.30	92.28	0.22	20	1.12
Average	18.17	12.33	1.48	109.02	0.31	20	1.68
STD	2.84	2.74	0.59	30.71	0.09	5	0.82
Count	10	10	10	10	10	10	10

Table 2- TA Measurements

HIGH SPEED TA	Failure Rate (m/sec)	Preload (N)	R Sqr	Volume (ml)	Area (vol/L)	Weight (mg)
1	1.29	0.50	0.99	3.40	44.62	3.50
2	1.00	0.60	1.00	2.80	41.30	2.70
3	1.06	0.60	1.00	2.70	38.57	2.60
4	1.23	0.50	0.99	3.00	42.86	3.10
5	0.98	0.50	1.00	2.80	38.89	3.00
6	1.16	0.50	0.99	2.80	39.44	3.00
7	0.93	0.20	0.99	2.00	30.30	2.20
8	0.92	0.50	1.00	1.90	27.14	2.10
9	0.91	0.40	1.00	2.60	38.24	2.80
10	1.07	0.50	1.00	2.90	39.03	3.30
Average	1.06	0.48	1.00	2.69	38.04	2.83
STD	0.13	0.11	0.00	0.45	5.37	0.45
Count	10	10	10	10	10	10
LOW SPEED TA			R sqr	Volume (ml)	Area (vol/L)	Weight (mg)
1			0.96	3.00	42.21	3.20
2			1.00	3.00	41.78	2.90
3			0.99	2.40	36.92	2.50
4			0.99	2.40	34.78	2.40
5			0.99	2.50	34.72	2.50
6			0.99	2.50	37.88	2.70
7			0.97	1.90	28.36	1.70
8			0.98	1.80	27.69	1.70
9			0.99	2.20	32.35	2.00
10			1.00	3.40	44.49	3.20
Average			0.99	2.51	36.12	2.48
STD			0.01	0.50	5.70	0.55
Count			10	10	10	10

Table 2- TA Measurements

HIGH SPEED TA	MT Unit Length (mm)	Tendon (mm)	Initial length (mm)	Final length (mm)	Width (mm)	Breadth (mm)
1	113.15	37.00	76.15	93.18	18.08	4.84
2	112.52	44.68	67.84	80.42	17.32	4.28
3	113.00	43.00	70.00	83.76	14.85	4.58
4	110.00	40.00	70.00	87.92	14.23	4.12
5	114.00	42.00	72.00	83.30	12.62	4.40
6	113.00	42.00	71.00	85.06	13.85	4.48
7	116.00	50.00	66.00	76.30	12.70	4.00
8	112.00	42.00	70.00	81.35	14.19	3.55
9	113.60	45.60	68.00	76.98	13.72	4.78
10	114.48	40.18	74.30	88.35	13.10	4.62
Average	113.18	42.65	70.53	83.66	14.47	4.37
STD	1.58	3.55	3.04	5.24	1.85	0.39
Count	10	10	10	10	10	10
LOW SPEED TA	MT Unit Length (mm)	Tendon (mm)	Initial length (mm)	Final length (mm)	Width (mm)	Breadth (mm)
1	113.32	40.88	72.44	92.39	17.26	4.40
2	123.02	50.35	72.67	84.25	13.80	4.48
3	115.57	47.60	67.97	78.76	15.42	4.05
4	112.12	41.00	71.12	85.72	13.60	3.68
5	106.37	32.80	73.57	87.96	15.00	3.45
6	114.49	47.00	67.49	81.40	14.32	4.78
7	109.41	41.75	67.66	78.92	13.60	3.70
8	112.47	45.00	67.47	80.18	12.10	3.40
9	111.89	42.65	69.24	82.56	14.20	4.00
10	122.01	43.58	78.43	94.20	14.00	3.87
Average	114.07	43.26	70.81	84.63	14.33	3.98
STD	5.15	4.82	3.57	5.43	1.36	0.46
Count	10	10	10	10	10	10

Table 2- MG Measurements

HIGH SPEED	Failure Rate	Preload	R Sqr	Volume	Area	Weight
MG	(m/sec)	(N)		(ml)	Vol/L	(mg)
1	1.33	0.60	0.86	5.90	97.68	6.50
2	1.14	0.60	0.87	4.00	64.83	4.60
3	0.78	0.70	0.98	3.60	64.29	3.80
4	1.03	0.50	0.85	4.00	65.90	4.40
5	0.91	0.50	1.00	3.80	62.60	3.80
6	0.87	0.50	0.99	4.10	67.88	4.80
7	1.08	0.60	0.99	3.30	50.23	4.00
8	0.94	0.50	0.72	3.40	56.67	3.80
9	0.89	0.50	0.94	4.30	70.96	5.00
10	1.02	0.50	0.92	4.10	68.11	4.90
Average	1.00	0.55	0.91	4.05	66.91	4.56
STD	0.16	0.07	0.09	0.73	12.38	0.83
Count	10	10	10	10	10	10
LOW SPEED			R sqr	Volume	Area	Weight
MG				(ml)	Vol/L	(mg)
1			0.98	4.70	81.74	5.20
2			0.96	3.60	62.07	4.00
3			0.95	3.60	62.96	3.80
4			0.99	4.10	67.21	4.40
5			0.97	2.90	46.77	3.10
6			0.99	3.70	54.94	3.90
7			0.99	3.10	50.00	3.30
8			0.91	3.20	48.48	3.60
9			0.99	4.00	64.52	4.50
10			0.97	4.70	77.05	4.80
Average			0.97	3.76	61.57	4.06
STD			0.03	0.62	11.82	0.66
Count			10	10	10	10

Table 2- MG Measurements

HIGH SPEED MG	MT Unit Length (mm)	Tendon (mm)	Initial length (mm)	Final length (mm)	Width (mm)	Breadth (mm)
1	106.40	46.00	60.40	77.34	22.58	8.08
2	102.30	41.00	61.70	75.55	20.76	5.60
3	104.75	48.75	56.00	61.37	22.48	6.20
4	101.65	41.00	60.65	70.79	23.47	6.62
5	100.65	40.00	60.65	68.89	16.68	5.70
6	104.35	44.00	60.35	70.68	20.00	5.70
7	106.70	41.00	65.70	77.84	15.68	5.40
8	104.40	44.40	60.00	70.93	19.85	4.78
9	104.60	44.00	60.60	69.95	20.52	5.00
10	103.20	43.00	60.20	70.39	20.55	5.45
Average	103.90	43.32	60.63	71.37	20.26	5.85
STD	1.96	2.71	2.33	4.77	2.47	0.94
Count	10	10	10	10	10	10
LOW SPEED MG	MT Unit Length (mm)	Tendon (mm)	Initial length (mm)	Final length (mm)	Width (mm)	Breadth (mm)
1	105.33	47.50	57.83	72.61	20.15	6.00
2	100.25	42.00	58.25	72.06	19.42	5.50
3	101.87	44.00	57.87	71.09	20.48	4.82
4	100.82	39.00	61.82	73.19	20.25	5.00
5	106.49	44.00	62.49	71.24	17.60	5.28
6	100.20	32.65	67.55	77.15	18.28	5.70
7	102.91	40.40	62.51	70.82	14.32	5.32
8	100.48	34.00	66.48	82.46	11.94	6.20
9	103.74	41.00	62.74	77.91	20.65	3.42
10	105.55	44.00	61.55	73.85	20.00	6.50
Average	102.76	40.86	61.91	74.24	18.31	5.37
STD	2.40	4.63	3.34	3.78	2.95	0.87
Count	10	10	10	10	10	10

Site of Failure

The majority of ruptures involved the myotendinous junction (MTJ). **Figure 22** diagrams the site of failure for the 40 specimens. Tears at the MTJ were divided into specimens separating with less then 1 mm of muscle on the surface of the tendon and those leaving 1-3 mm of muscle on the tendon. Any tears leaving greater than 3 mm of muscle attached to tendon were defined as distal muscle tears.

For the TA specimens, the most common failure site was the distal MTJ. Eight of the 10 low speed TA tears involved the distal MTJ. Four within 1 mm and four between 1-3 mm of the tendon. Two tore in the distal muscle. In the high speed group, 9 of the 10 tears involved the distal MTJ; 7 failing within 1 mm and two 1-3 mm from the tendon. One tore in the distal muscle.

The MG specimens were not as consistent in site of failure, although all tore at a muscle-tendon junction. Among the 10 low speed specimens, there were seven proximal tears occurring 1-3 mm from the proximal tendinous insertion, and three distal MTJ tears within 1 mm of the tendon. In high speed MG specimens, there were five proximal tears 1-3 mm from the proximal insertion, four distal MTJ tears within 1 mm of the tendon and one distal tear 1-3 mm from the tendon.

DISTRIBUTION OF FAILURE SITES

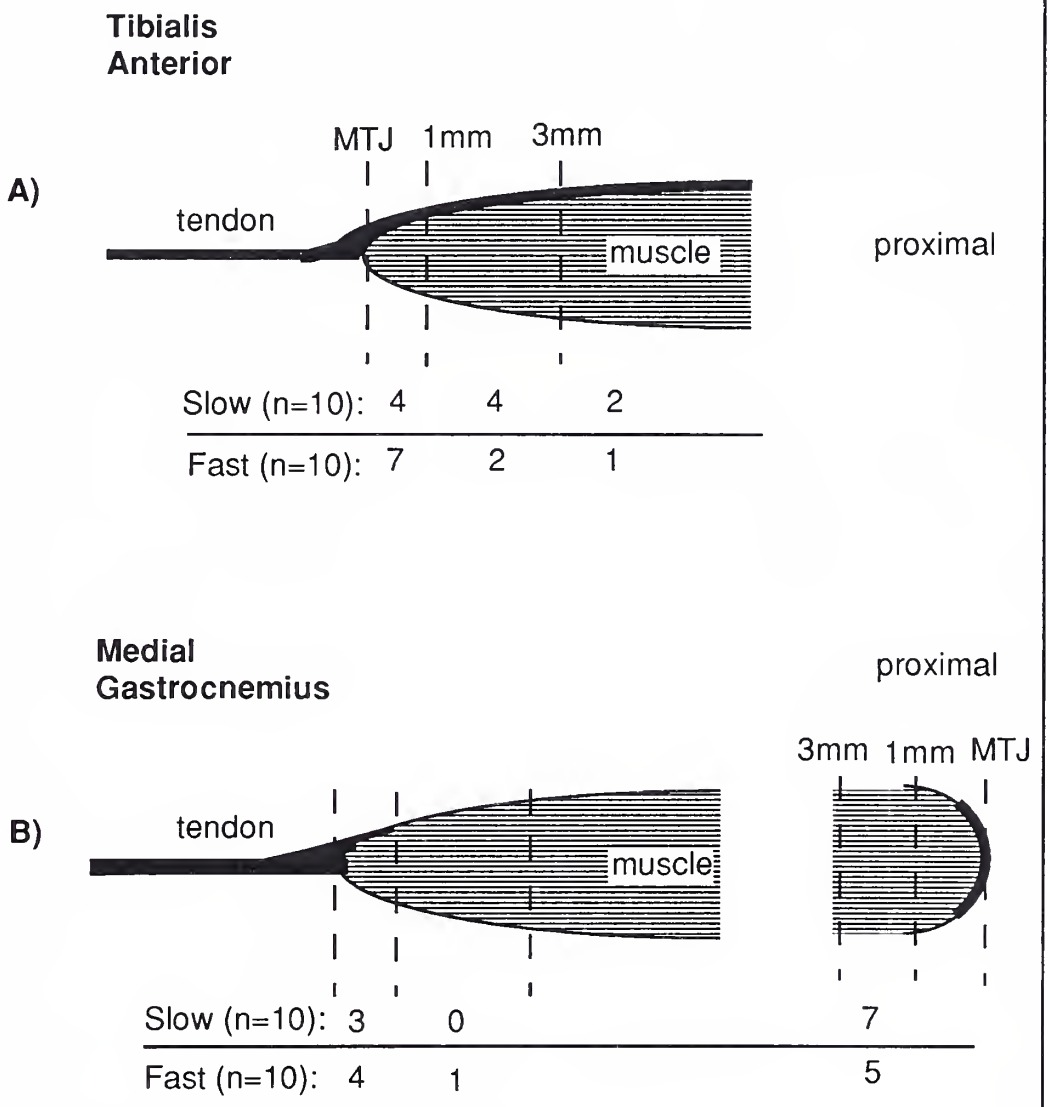

Figure 22

Site of Failure: A) Tibialis anterior tore distally for all 20 specimens with 18 of 20 at the MTJ. B) Gastrocnemius tore at both proximal and distal MTJs.

Histology and SEM

Histology was used to examine the morphology of a normal muscle-tendon junction. Trichrome staining separates the blue collagen against the purple muscle fibers. The specimen in **Figures 23-25** is a longitudinal section of gastrocnemius muscle

Figures 26-28 are SEM photographs of a TA specimen after rupture, which shows the myotendinous junction and terminal muscle fibers in greater detail. (SEM photographs courtesy of Bruce Wolanin.)

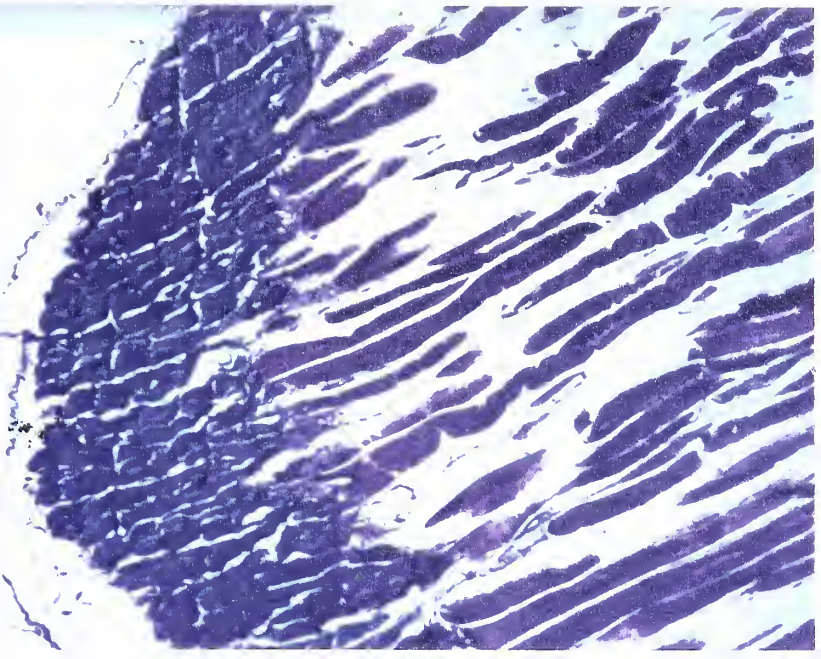

Figure 23: Myotendinous junction of gastrocnemius muscle. Blue collagen bundles are seen on the left, purple cylindrical muscle fibers on right. (Magnification 40X)

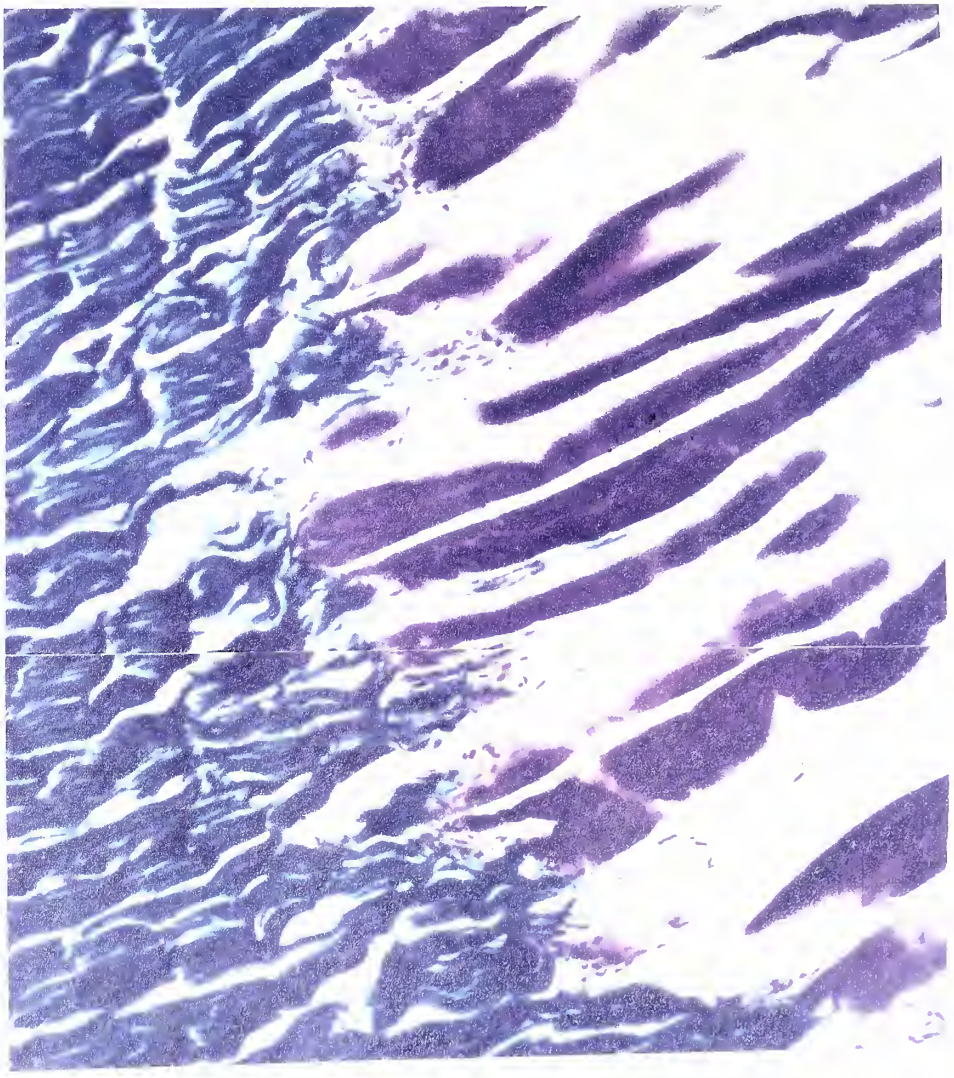

Figure 24: Higher magnification reveals overlapping of muscle and tendinous components. (Magnification 100X)

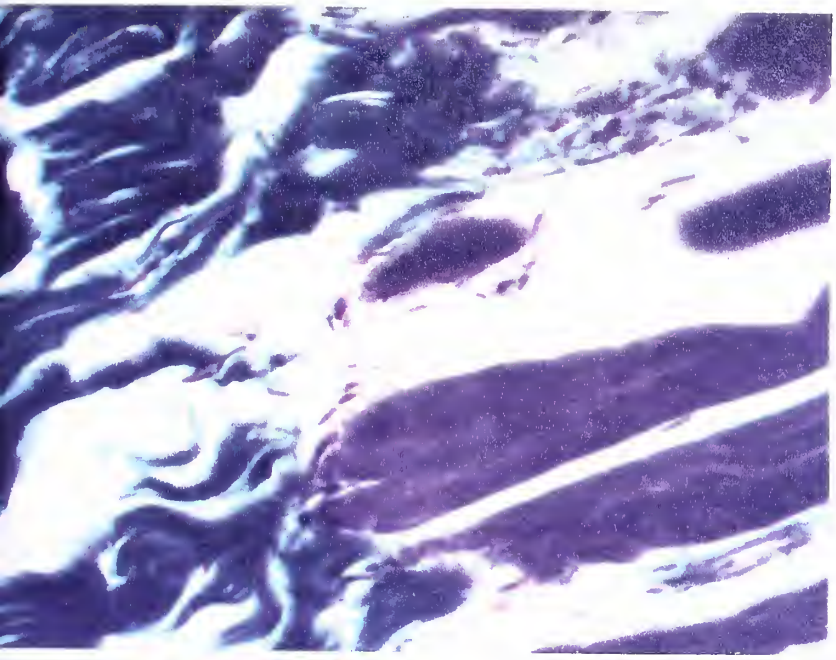

Figure 25: Lower center begins to detail the tapering of an individual muscle fiber at the MTJ. (Magnification 200X)

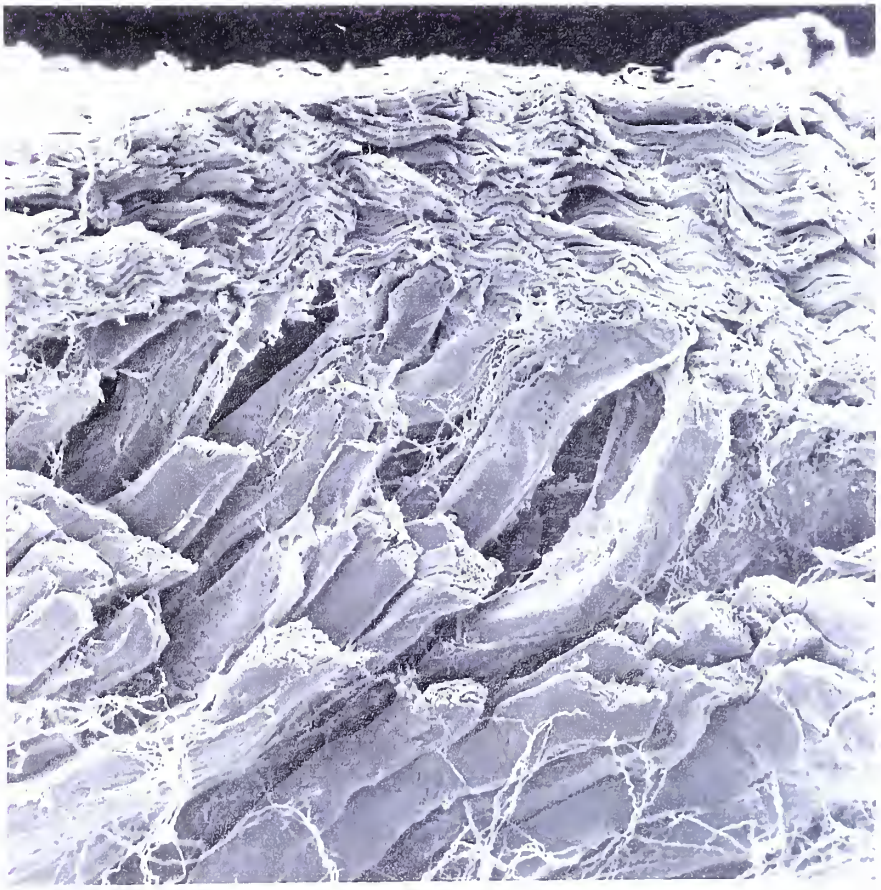

Figure 26: SEM of myotendinous junction. The transition from the larger cylindrical muscle fibers to the layered collagen bundles in the tendon is seen. (Magnification 120X)

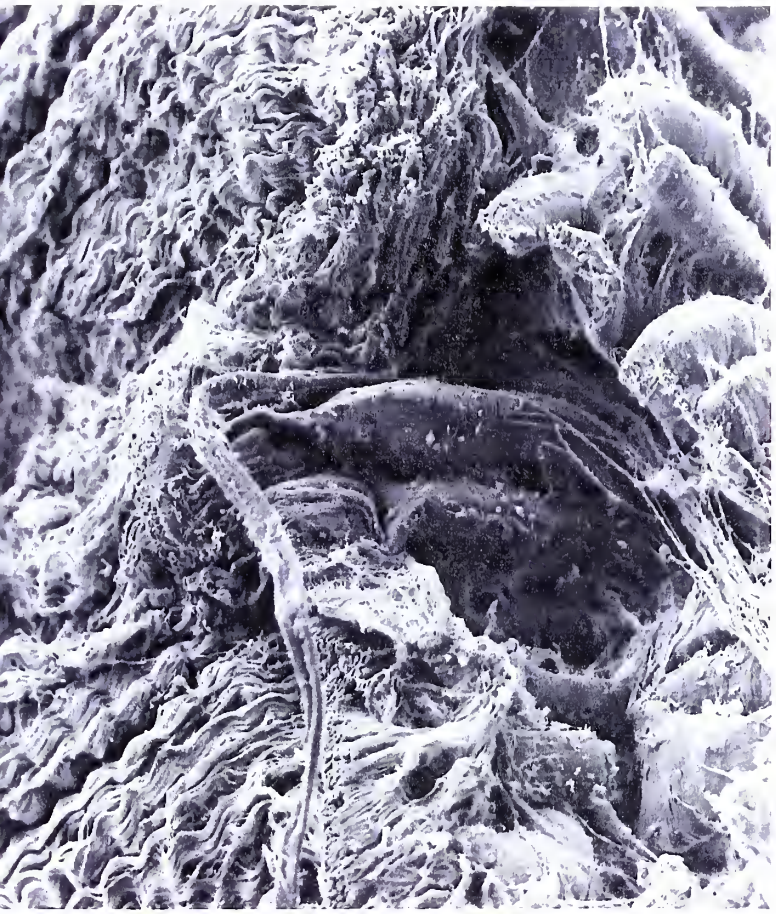

Figure 27: The center of this photo shows the tapered end of a muscle fiber as it blends into the wavy collagen of tendon. (Magnification 150X)

Figure 28: Higher magnification of muscle fiber ends near the MTJ. (Magnification 1500X)

Discussion

Limitations

Several factors must be noted when extrapolating these results to the *in vivo* setting. Muscle strain injuries represent a range of muscle fiber disruption from minimal, without clinical symptoms to complete muscle rupture, with severe disability. Our system was designed to quantitate only complete tears.

In vivo systems better correlate physiologic behavior because there is an intact neurovascular supply, temperature is closely regulated and the muscle-tendon units are stressed within their supporting structures of skin and connective tissue.

Our specimens were harvested and stored frozen for a minimum of one week prior to testing. The most extensive passive failure tests to date are by Katake who reported that muscle becomes "mechanically stabilized" 48 hours after death [56]. A 50% decrease in strength and a 30-40% decrease in elongation at 48 hours after death compared to strength and elongation immediately postmortem was also reported. This included specimens that were stored frozen.

Safran, in studying the effects of warmup on muscle *in vivo*, demonstrated small but statistically significant increases in elasticity of muscle-tendon units after isometric preconditioning prior to pulling muscles to failure [78]. He also reported failure loads of 38 N for nonstimulated TA at a stretch rate of 1.67 mm/sec. Our average failure load was 12.3 N at 0.1 mm/sec and 28.4 N at 1 meter/sec. This difference can be explained by two of the limitations. First, muscle has decreased strength postmortem.

Second, in our experiments, the surrounding soft tissue was dissected away prior to fixation in plaster. Johns reported in 1963 on the rheological properties of tissues in joint stiffness [51]. During passive joint motion in the normal range, the capsule contributed 47%, passive muscle 41%, tendon 10% and skin 2% to the resistance of movement. Toward the extremes of motion the restraining effect of tendons became more important. To what extent the method of dissection altered the biomechanical data cannot be determined at this time.

Complex innervation of muscle and tendon plays an important protective role in strain injuries as well as forming the basis for methods of flexibility training. [2, 12, 17, 21, 40, 51, 77, 78, 87]

Taylor compared innervated and denervated rabbit muscles *in vivo*. [86] He found that peak tensile force and energy absorbed to failure were the same in each group. This supports the assumption made in our experiments that viscoelastic properties can be considered independently of innervation. It should be pointed out that the *in vivo* systems reported in the literature are performed under general anesthesia, which inhibits nervous activity. The degree of inhibition is not known at this time.

When bone-muscle-bone mounts are passively elongated to failure, deformation takes place in the bone, tendon and muscle. The deformation of bone and tendon, however, is negligible compared to muscle. Compare values of strain for bone, tendon and muscle. Bone has an elastic modulus of 10,000 MPa. The greatest stress in our experiment was 0.75 MPa. Since strain is stress divided by the modulus, the bone experiences a strain of 7.5×10^{-5} or 0.0075%. In our experiments, muscle had a strain of approximately 20%. Thus, at the loads used in these experiments, the deformation of bone is insignificant. Tendon is comprised almost exclusively of collagen, which has

a modulus close to that of bone, making its contribution to the displacement negligible as well.

By pulling all muscles continuously to failure, other viscoelastic properties such as creep, hysteresis and relaxation were not recorded. Finally, we report stretch rates instead of strain rates, which permits the report of elongation in more clinically applicable units (meters per second instead of % per second).

Viscoelasticity

Our data shows that muscle and muscle-tendon units respond viscoelastically when passively elongated to failure at high and low speeds. Stretch rate dependence describes the statistically significant increase in failure load, stiffness, energy absorbed to failure, stress, and elastic modulus between the two groups. Failure strains and displacements were not significantly different.

Failure loads for both TA and MG showed a mean increase of 230%, while energy absorbed to failure increased approximately 250%. As mentioned in the literature review, only one other study has addressed the viscoelastic behavior of muscle failure. Welsh determined rate dependence in rabbit tendon (plantaris, flexor digitorum longus, gastrocnemius and soleus) pulled to failure at stretch rates from 0.2 to 20 mm/sec, but contrary to our findings, he found *no* difference in the failure loads of the same muscles pulled to failure [93].

Taylor stretched 20 TA and 20 extensor digitorum longus (EDL) muscles using an *in vivo* rabbit model at rates of 0.01, 0.1, 1.0 and 10 cm/sec [86]. He stretched each muscle to 10% beyond its resting length, keeping elongation in the (pre failure) linear elastic range. Direct comparison to this

study is thus limited, however, he also found statistically significant differences in peak load and energy between each rate (p=.0001). The peak tensile force at 0.01 cm/sec (the same as our low rate) had a mean of 8.35N, while the 10 cm/sec group (our high speed was 100 cm/sec) was 13.8N, which is an increase of 165%. Energy absorbed between the two stretch rates increased by 175%. The conclusions that Taylor reached concerning rate dependence in muscle are similar to ours.

Viscoelastic failure tests of other soft tissues have been conducted in ligaments [72, 97, 98]. Each of these studies reported that failure stress, elastic modulus, and strain increased with increasing stretch rate, except for Yoganandan, who reported that the failure strain was not dependent upon on the rate of stretch (8.9 mm/sec to 2.5 m/sec) in human cervical spine ligaments [98].

Other investigators of failure mechanics in muscle have *not* compared failure loads at different stretch rates. Nikolaou, in his study of the effect of architecture on anatomic failure site, "found no difference in force or elongation to failure at speeds of 10 to 100 cm/min" [70, 71]. This statement can not be substantiated because he did not report failure loads. Also, the difference may have too small to detect given the sensitivity of his recording apparatus and the stretch rtaes, which differed by only a factor of 10. Instead of strain rate, Garrett compared tetanically stimulated and nonstimulated EDLs pulled to failure at 1.67 cm/sec and found statistically significant differences in failure loads and energy absorbed to failure [32].

As noted earlier, higher strain rates allow less time for the viscous components in the muscle-tendon unit to dissipate energy. As a result, the muscle and tendons are exposed to higher tensile forces. Clinical observations reveal that more strain injuries occur during high loading rate actions such as

jumping or sprinting. "Kinesiologic examination of hamstring injuries from a front snap kick similar to hurdler's leading leg give maximum velocity estimates of 70 cm/sec" [30]. Our study was the first to utilize a stretch rate comparable to a clinical injury (1 meter/sec).

Failure stress is the best determinant for maximum strength in muscle, because cross-sectional area allows comparison of different specimens. In our study, the highest mean stress was 76 N/cm^2 for high speed TA and the lowest was 31 N/cm^2 for low speed MG. These values correspond to the range of several *in vitro* and *in vivo* studies. McMahon reported maximum stress of 19.62 N/cm^2 in isolated mammalian muscle [64]. Close gives a value of 30 N/cm^2 for vertebrate striated muscle as isometric stress; Reid showed the strength of erector spinae muscle to be 48 N/cm^2; and Ikai determined average maximum stress of human biceps to be 63 N/cm^2 [20]. Thus, our data correlates with previous values for failure stresses but is the first to define the importance of loading rate on these values.

The increase in the stiffness and elastic modulus between the high and low speed groups reflect two phenomena. The first, already mentioned, is the increase in failure load and stress described by rate dependence. The second is that failure displacement and strain remained unchanged between the two groups.

Why did ultimate strains remain approximately the same for the two stretch rates? These findings are consistent with reports in the literature. Garrett compared stimulated and nonstimulated EDL muscles pulled to failure and found statistically significant differences in failure load and energy absorbed to failure but no difference in length increase. In this study, he reports strains of 26-28%, which are quite close to our values of 20% [32]. In another study, Garrett pulled five different muscles to failure at 1, 10 and 100

cm/min, but did not list the stretch rates when reporting elongation. He inferred that stretch rate does not influence failure strain [30]. As mentioned above, Nikolaou reported no difference in elongation to failure [71].

Safran compared muscles that were preconditioned by isometric stimulation to unconditioned muscles pulled to failure and found statistically significant differences in failure loads ($p=0.001$) *and* length to failure ($p=0.05$), however, the real difference was only $1.5\% \pm 0.6\%$ for the increase in length to tear [78]. The preconditioned muscles were stimulated for 15 seconds at a maximum wave-summated tension, which lengthens collagen fibers in the muscle-tendon unit. Thus, the increase in length in this group may have been present prior to pulling the muscles to failure.

There was a slight trend for the strains to be lower in the high speed groups. The reason loading rate did not cause a statistically significant difference in strain may reflect the relative inelasticity of the collagenous tissues. There simply was not enough time for the dashpot (viscous) components to elongate.

In vitro studies of strain are few. Fung reports isolated muscle fibers have strains on the order of 140%, but fiber studies are of limited value as covered in the literature review [26]. Kabo stretched one pair of human cadaveric sternocleidomastoid, five canine gastrocnemius, a human extensor carpi radialis, and a baboon biceps brachii [54]. Such an assortment precludes any conclusions, but he observed that most muscles failed in the range of 8-10% with a maximum of 36%. The stretch rate was 0.0084 mm/sec. In the sternocleidomastoid pair, he reported loads of 29 and 30N (cross-sectional areas were not given). For two gastrocnemi (unpaired) the strain at failure was 12% in both cases and the failure stress was 0.8 MPa and 1.6 MPa. Strict comparisons are difficult but these results are similar to ours. As mentioned,

lower strain rates compared to fiber studies reflect the increased collagen content of whole muscle. Also, in vitro conditions are conducted at lower temperatures, which can decrease strains.

Another confounding factor is measurement of initial length for the muscle specimens. For example, *in vivo* initial lengths reported by Garrett for TA were 41 mm (strain=73%) compared to 71 mm (strain=19%) for our TA specimens [30]. Both protocols utilized the same breed and age of rabbit. From this evidence, we can conclude that independent of *in vitro* or *in vivo* conditions, many factors affect strain values in muscle, such as preload, temperature, and initial length.

Failure strain was not statistically different between the TA and MG groups, even though these muscles are quite different architecturally. Elongation to failure has been shown to vary with muscle architecture and collagen content of the muscle-tendon unit [30, 64]. Garrett reports that muscles with more pennate architecture, such as the medial head of the gastrocnemius, elongate more to failure than a fusiform muscle like TA [30]. It seems likely that *in vivo* conditions are necessary for muscle fiber architecture to make a large difference in elongation. In an *in vitro* study such as ours, the sarcomeres are locked by fixed actin-myosin bridges that are not freely extensible. Failure stress and elastic modulus were not statistically different between the two muscle types due to the normalizing factor of the cross-sectional area.

In summary, these results demonstrate stretch rate dependence in muscle during passive elongation to failure. Increasing stiffness (elastic modulus), peak loads and energy absorbed at higher stretch rates is adaptative to preventing strain injury, because it increases the strength or maximum stress absorbed by the material before it fails. The fact that muscle is stronger

at higher stretch rates, however, does *not* support the clinical observation that most muscle strain injuries occur at higher stretch rates.

Similar values for ultimate strains at the different stretch rates indicate that muscle as a material can become stronger without rupturing at lower strains. The ability to remain a highly extensible material while resisting the higher tensile forces of faster stretch rates could allow muscle to maintain its dynamic function, since it can keep the range of joint motions similar under conditions of slow or rapid elongation.

Site of Failure

Results of the site of failure in TA specimens shows consistent rupture at the distal MTJ. GC specimens tore at both proximal and distal MTJs. None of the specimens failed in the midbelly of the muscle, within the tendon or at the insertion of tendon into bone.

Similar findings have been reported on rabbit *in vivo* models [30, 32, 71, 78]. Stretch rate in these studies varied from 1 to 100 cm/min and all point to the distal MTJ as the weakest point in the muscle-tendon unit (TA and EDL muscles). Garrett reports that 100% of his TA (n=40) specimens failed at the distal MTJ compared to 17 of our 20 specimens failing at the distal MTJ [30]. More consistent results from *in vivo* models may reflect supporting connective tissue that was dissected in our *in vitro* study.

Our tears did not involve a clean separation of the muscle from tendon. In most cases, there was 0.5-1 mm of muscle fiber attached to the tendon. Garrett found that 0.1-1 mm of muscle remained attached to the tendon at the site of rupture [30]. The site of failure in actively stretched TA and EDL occurs at the distal muscle-tendon junction as well [32]. Increased

collagen content at the distal MTJ compared to the proximal MTJ has been implicated as a factor in the greater incidence of ruptures distally [62].

We found 40% (8 of 20) of the medial head of gastrocnemius failed at the distal MTJ compared to 55.5% found by Garrett for entire gastrocnemius [30]. The multipennate architecture of the gastrocnemius creates a complicated arrangement at the MTJ. As in previous studies, although the distal MTJ was not the consistent site of failure for MG, all tears involved a muscle-tendon junction.

The myotendinous junction is an the area of intense research in understanding muscle strain injuries. [12, 24, 28, 29, 30, 86, 89, 90] Early work by McMaster showed ruptures can occur at any point in the muscle, but that healthy tendon is rarely involved [65]. Clinical studies of tennis leg, a separation of the medial head of the gastrocnemius muscle from its tendon, and hamstring muscle ruptures support the muscle-tendon junction as the site of injury. [24, 68, 80] CT and MR imaging studies have added further evidence to support the MTJ as the site of soft tissue injury [10, 22, 25, 31, 63].

Biomechanically, the MTJ is quite complex. It serves the important role of transmitting contractile forces of muscle cells to the extracellular matrix of tendon. It experiences very high stresses generated by the large area of the muscle as it is concentrated in the smaller area of the tendon.

Myotendinous junctions occur at the end of long, cylindrical skeletal muscle cells as they terminate in connections with the tendons at either origin or insertion [33]. Microscopy shows that the muscle cell membrane is a continuous interface between the extracellular and intracellular compartments. The surface of this membrane is extensively folded creating a highly interdigitated surface composed of four distinct domains: an intracellular domain, the internal lamina; a domain connecting the internal

lamina with the lamina densa of the external domain, the connecting domain; the lamina densa; and a domain which attaches the lamina densa to the collagen fibers, the matrix [90].

Interdigitation at the MTJ increases the area of contact, which is mostly parallel to the direction of force. Adhesive strength from this geometry is increased by converting the tensile stress of the muscle cell to shear stress. Joints loaded in shear, where the force is parallel to the joint interface, are generally stronger than those loaded under tension where force is perpendicular to the joint interface [89]. Calculations in frog semimembranous muscle indicate that loading at healthy junctional membranes is seen almost entirely as shear stress. In atrophied cells, the tensile component doubled, but remained small. Finally, there were no examples of failure at the myotendinous junction in healthy cells [89]. This evidence supports the gross and histological observations of our study and others that failure occurs near but not within the myotendinous junction.

Muscle near the myotendinous junction exhibits lower strains [49]. Huxley and Peachy found that striation spacing was substantially lower near the ends of stretched muscle fibers than in most of their length [42]. Thus, extensibility at the terminal sarcomeres is decreased relative to other regions in the muscle. Studies in mice support a dynamic role of the terminal sarcomeres in response to tensile stress or immobilization in their ability to increase in number and longitudinal growth [95].

Given the mechanisms of repair in muscle, tendon and bone, it may be adaptative for failure to occur near the muscle-tendon junction. First, it has been shown that lacerated muscle (analogous to a muscle rupture) which includes disruption of the nervous supply, causes the muscle to repair by scar formation and a loss of contractile ability [34]. In essence, the muscle then

functions as a tendon. If the site of rupture occurs near the muscle-tendon junction, there is little risk of losing a significant amount of contractile function. Second, muscle can heal more quickly than tendon or bone. It has been shown in rats that early immobilization for proper scar formation followed by progressive activity within 5 days is optimal for healing of muscle ruptures [44]. Bone and tendon require much longer periods of immobilization.

The ability of muscle to change at the terminal sarcomeres and the observation that muscle-tendon units commonly fail in this region suggest that the area of the myotendinous junction is important both structurally and functionally.

Conclusion

In summary, a viscoelastic response of muscle passively pulled to failure was demonstrated by stretch rate dependence in tibialis anterior and medial gastrocnemius muscle. Significantly higher values for failure stress, elastic modulus and energy absorbed to failure were found in the fast stretch rate group. Failure strains were not significantly different between the fast and slow stretch groups, although there was a slight trend for greater strains at the lower rate. There was no difference in the material properties of the two muscle types. The site of failure was consistently at the distal myotendinous junction in TA and at either the proximal or distal myotendinous junction in the MG specimens. Morphology at the site of failure was studied using histology and scanning electron microscopy.

Our results suggest that muscle exhibits stretch rate dependence when continuously elongated to failure and that the site of injury is most likely to occur at the myotendinous junction.

References

1. Abbott, B. C. and J. Lowy. Stress Relaxation in muscle. Proc. Roy. Soc. of Lon. B. **146**: 281-290, 1956.

2. Almekinders, L. C. and W. E. Garrett. Pathophysiologic response to muscle tears in stretching injuries. 30th Annual Meeting of the Orthopaedic Research Society. 307, 1984.

3. Almekinders, L. C. and J. A. Gilbert. Healing of experimental muscle strains and the effects of nonsteroidal antiinflammatory medication. Am J Sports Med. **14**(4): 303-308, 1986.

4. Appenzeller, O. Sports Medicine. 1988.

5. Armstrong, R. B. Initial events in exercise-induced muscular injury. Med. Sci. Sports Exerc. **22**(4): 429-435, 1990.

6. Aronen, J. G., R. Chronister and P. N. Ove. Thigh contusions: minimizing the effects by early immobilization at 120 degrees of flexion. Instructors Course of the American Orthopaedics Society for Sports Medicine. 1990.

7. Bancroft, J. D. and A. Stevens. Theory and Practice of Histological Techniques. 1982.

8. Banthus, M. G. and A. M. Zetlin. The relation of isometric tension to length in skeletal muscle. J. Cell. Comp. Physiol. **12**(403-420): 1938.

9. Bass, A. L. and I. Robertson. Injuries of the leg in football and ballet. Proc. R. Soc. Med. **60**: 527-532, 1967.

10. Belkin, M., R. D. Brown and R. W. Hobson. A new quantitative spectrophotometric assay of ischemia-reperfusion injury in skeletal muscle. Am. J. of Surg. **156**: 83-86, 1988.

11. Bosco, C., J. T. Viitasalo, P. V. Komi and P. Luhtanen. Combined effect of elastic energy and myoelectrical potentiation during stretch-shortening cycle exercise. Acta Physiol Scand. **114**: 557-565, 1982.

12. Brewer, B. J. Mechanism of injury to the musculotendinous unit. Instr. Course Lect. in Orthop. **17**: 354-358, 1960.

13. Byrnes, W. C. and P. M. Clarkson. Delayed onset muscle soreness and training. Clin. Sports Med. 5(3): 605-614, 1986.

14. Canale, S. T. and E. D. Cantler. A chronicle of injuries of an american intercollegiate football team. Am. J. Sports Med. 9(6): 384-389, 1981.

15. Casella, C. Tensile force in total striated muscle, isolated fibre and sarcolemma. Acta phys. Scandinav. **21**: 380-401, 1950.

16. Chammout, M. O. and H. B. Skinner. The clinical anatomy of commonly injured muscle bellies. J. of Trauma. **26**(6): 549-552, 1986.

17. Ciullo, J. V. and B. Zarins. Biomechanics of the Musculotendinous Unit: Relation to Athletic Performance and Injury. Clin. in Sports Med. **2**(1): 71-86, 1983.

18. Clarkson, P. M., W. C. Byrnes, E. Gillisson and E. Harper. Adaptation to exercise-induced muscle damage. Clin. Science. **73**: 383-386, 1987.

19. Craigie, E. H. "A Laboratory Guide to the Anatomy Of The Rabbit." 1966 University of Toronto Press. Toronto.

20. Crisco, J. J. Biomechanics of Cervical Spine. PhD thesis. Yale University School of Medicine. 1989.

21. Dalton, J. D., A. V. Seaber and W. E. Garrett. The effects of passive stretch on muscle pulled to failure. 16th Annual Meeting American Orthopaedic Society for Sports Medicine. 15, 1990.

22. Damron, C. F., E. F. Hoerner and J. S. Shaw. "Monitoring Sports Injuries." Sports Injuries. Vinger and Hoerner ed. 1986 PSG Publishing Company, Inc. Littleton, Massachusets.

23. DeVires, H. A. Evaluation of static stretching procedures for improvement of flexibility. Res. Quart. **33**: 222-229, 1962.

24. Durig, M., J. P. Schuppisser, E. F. Gauer and W. Muller. Spontaneous rupture of the gastrocnemius muscle. Injury. **9**: 143-145, 1977-78.

25. Fleckenstein, J. L. and R. M. Peshock. Sports-related muscle injuries: Evaluation with MR imaging. Radiology. **172**: 793-798, 1989.

26. Fung, Y. C. Elasticity of soft tissues in simple elongation. Am. J. Physio. **213**: 1532-1544, 1967.

27. Fung, Y. C. "Biomechanics." 1981 Springer-Verlag. New York.

28. Garrett, W. E. Muscle strain injuries: clinical and basic aspects. Med. Sci. Sports Exerc. **22**(4): 436-443, 1990.

29. Garrett, W. E., J. C. Califf and F. H. Bassett. Histochemical correlates of hamstring injuries. Am. J. Sports Med. **12**(2): 948-103, 1984.

30. Garrett, W. E., P. K. Nikolaou, B. M. Ribbeck, R. R. Glisson and A. V. Seaber. The effect of muscle architecture on the biomechanical failure properties of skeletal muscle under passive extension. Am J Sports Med. **16**(1): 7-12, 1988.

31. Garrett, W. E., P. K. Nikolaou and J. B. Vogler. Computed tomography of hamstring muscle strains. Med. Sci. Sports Exer. **21**(5): 506-514, 1989.

32. Garrett, W. E., M. R. Safran and A. V. Seaber. Biomechanical comparison of stimulated and nonstimulated skeletal muscle pulled to failure. Am. J. Sports Med. **15**(5): 448-454, 1987.

33. Garrett, W. E. and J. G. Tidball. "Myotendinous Junction: Structure, Function, and Failure." Injury and Repair of the Musculoskeltal Tissues. Woo and Buckwalter ed. 1988 American Academy of Orthopaedic Surgeons. Park Ridge, Illinois.

34. Garrett, W. E., J. R. Urbaniak and J. L. Goldner. Recovery of skeletal muscle after laceration and repair. J. Hand Surg. **9A**(5): 683-692, 1984.

35. Guyton, A. C. "Textbook of Medical Physiology." 1986 W.B. Saunders. Philadelphia.

36. Herring, S. A. Rehabilitation of muscle injuries. Med. Sci. Sports Exerc. **22**(4): 453-456, 1990.

37. Hill, A. V. The series elastic component of muscle. Proc. Roy. Soc. B. **137**: 273-280, 1950.

38. Hill, A. V. "First and Last Experiments in Muscle Mechanics." 1970 Cambridge University Press. Cambridge, Great Britain.

39. Hill, D. K. Tension due to interaction between the sliding filaments in resting striated muscle. The effect of stimulation. J. Physiol. **199**: 637-684, 1968.

40. Holt, L. E. "Scientific Stretching for Sport." 1973 Sport Research, Ltd.

41. Huxley, A. F. Review lecture Muscular Contraction. J. Physiol. **243**: 1-43, 1974.

42. Huxley, A. F. and L. D. Peachey. The maximum length for contraction in vertebrate striated muscle. J. of Physiology. **156**: 150-65, 1961.

43. Huxley, H. E. The Mechanism of Muscular Contraction. Science. **164**: 1356-66, 1969.

44. Jarvinen, M. Healing of a crush injury in rat striated muscle, #2. Acta. Path. Microbiol. Scand. **Sect A, 83**: 269-282, 1975.

45. Jarvinen, M. Healing of a crush injury in rat striated muscle, #4. Acta. Chir. Scand. **142**: 47-56, 1975.

46. Jarvinen, M. Healing of a crush injury in rat striated muscle, #3. Acta. path. microbiol. scand. **Sect. A, 84**: 85-94, 1976.

47. Jarvinen, M., A. J. Aho, M. Lehto and H. Toivonen. Age dependent repair of muscle rupture. Acta orthop. scand. **54**: 64-74, 1983.

48. Jarvinen, M. and T. Sorvari. Healing of a crush injury in rat striated muscle, #1. Acta path microbiol. scand., Sect. A. **83**: 259-265, 1975.

49. Jewell, B. R. and D. R. Wilkie. An analysis of the mechanical components in frog's striated muscle. J. Physiol. **143**: 515-540, 1958.

50. Jewell, B. R. and D. R. Wilkie. The mechanical properties of relaxing muscle. J. Physiol. **152**: 30-47, 1960.

51. Johns, R. J. and V. Wright. Relative importance of various tissues in joint stiffness. J. Appl. Physiol. **17**(5): 824-828, 1963.

52. Jones, D. A., D. J. Newham, J. M. Round and S. E. J. Tolfree. Experimental human muscle damage: morphological changes in relation to other indices of damage. J. Physiol. **375**: 435-448, 1986.

53. Kabat, H. Studies of neuromuscular dysfunction- The role of central facilitation in restoration of motor function paralysis. Arch. Phys Med. **33**(523): 1952.

54. Kabo, J. M., W. Goldsmith and M. Nystrom. Stretch characteristics of whole muscle. J. of Biomech. Engin. **104**: 253-255, 1982.

55. Kamen, G. Serial isometric contraction under imposed myotactic stretch conditions in high and low strength men. European J Applied Physiology. **41**: 73-82, 1979.

56. Katake, K. and I. Asami. Studies on the strength of human skeletal muscles. J. Kyoto Pref. Med. Univ. **69**: 444-448, 1961.

57. Kibler, W. B. Clinical aspects of muscle injury. Med. Sci. Sports Exerc. **22**(4): 450-452, 1990.

58. Kime, R. C., III, A. V. Seaber and W. E. Garrett. Changes in muscle biomechanical properties following immobilization in various degrees of passive tension. 16th Annual Meeting American Orhtopaedic Society for Sports Medicine. 14, 1990.

59. Kirkendall, D. T. Mechanisms of periheral fatigue. Med. Sci. Sports. **22**(4): 444-449, 1990.

60. Lehto, M., V. C. Duance and D. Restall. Collagen and fibronectin in a healing skeletal muscle injury. J. Bone Joint Surg. **67-B**(5): 820-828, 1985.

61. Lehto, M., M. Jarvinen and O. Nelimarkka. Scar formation after skeletal muscle injury. Arch Orthop Trauma Surg. **104**: 366-370, 1986.

62. MacDonald, B. L. Hydroxyproline quantitation in normal muscle and denervated muscle after immediate and delayed nerve repair. Transactions of the Orthopaedic Research Society. **11**: 186, 1986.

63. McCully, K. K. Detection of muscle injury in humans with 31-P magnetic resonance spectroscopy. Muscle and Nerve. **II**: 212-216, 1988.

64. McMahon, T. A. "Muscles, Reflexes, and Locomotion." 1984 Princeton University Press. Princeton, New Jersey.

65. McMaster, P. E. Tendon and Muscle Ruptures. J Bone Joint Surg. **15**: 705-722, 1933.

66. McMaster, W. C. A literary review on ice therapy in injuries. Am. J. Sports Med. **5**(3): 124-126, 1977.

67. Medeiros, J. M. and G. L. Smidt. The influence of isometric exercise and passive stretch on hip joint motion. Phys. Ther. **57**(5): 518-523, 1977.

68. Miller, W. A. Rupture of the musculotendinous juncture of the medial head of the gastrocnemius muscle. Am. J. of Sports Med. **5**(5): 191-193, 1977.

69. Newbury, D. E. "Advanced Scanning Electron Microscopy and X-ray Microanalysis." 1986 Plenum Press. New York.

70. Nikolaou, P. and W. E. Garrett. The effect of architecture on the anatomic failure site of skeletal muscle. 32nd Annual Meeting of the Orthopaedic Research Society. 228, 1986.

71. Nikolaou, P. K. and W. E. Garrett. Biomechancal and histological evaluation of muscle after controlled strain injury. Am J Sports Med. **15**(1): 9-14, 1987.

72. Noyes, F. R. Functional properties of knee ligaments and alterations induced by immobilzation. Clin. Orthop. **123**: 210, 1977.

73. Panjabi, M. M. and A. A. White III. "Biomechanics A to Z." Clinical Biomechanics of the Spine. 1990 J.B. Lippincott Company. Philadelphia, Pennsylvania.

74. Phillips, C. A. and J. S. Petrofsky. Mechanics of Skeletal and Cardiac Muscle. 1983.

75. Pinto, J. G. and Y. C. Fung. Mechanical properties of the heart muscle in the passive state. J. Biomech. **6**: 597-616, 1973.

76. Pitman, M. I. and L. Peterson. "Biomechanics of skeletal muscle." Basic Biomechanics of the Musculoskeletal System. Nordin and Frankel ed. 1989 Lea & Febiger. Malvern, Pennsylvania.

77. Sady, S. P. Flexibility training: ballistic, static or proprioceptive neuromuscular facilitation? Arch Phys Med Rehab. **63**: 261-263, 1981.

78. Safran, M. R. and W. E. Garrett. The role of warm-up in muscular injury prevention. Am. J. Sports Med. **16**(2): 123-129, 1988.

79. Schwane, J. A., S. R. Johnson and R. B. Armstrong. Delayed-onset muscular soreness and plasma CPK and LDH activities after downhill running. Med. Sci. Sports. **15**(1): 51-56, 1983.

80. Shields, C., L. Redix and C. Brewster. Acute tears of the medial head of the gastrocnemius. Foot & Ankle. **5**(4): 186-190, 1985.

81. Standish, W. D. "Neurophysiology of Stretching." Prevention and Treatment of Running Injuries. D'Ambrosia and Drez ed. 1982 Charles B. Slack, Inc. Thorofare, New Jersey.

82. Stephens, R. E. "The neuroanatomical and biomechanical basis of flexibility exercises in dance." Preventing Dance Injuries: an interdisciplinary perspective. Solomon ed. 1990 American alliance for health, physical education, recreation, and dance. Reston, Virginia.

83. Stone, M. H. Muscle Conditioning and muscle injuries. Med. Sci. Sports Exerc. **22**(4): 457-462, 1990.

84. Stromberg, D. D. and C. A. Wiederhielm. Viscoelastic description of collagenous tissue in simple elongation. J. of Appl. Phys. **26**(6): 857-862, 1969.

85. Subotnick, S. I., DPM. Sports Medicine of the Lower Extremity. 1989.

86. Taylor, D. C., J. D. Dalton, A. V. Seaber and W. E. Garrett. Viscoelastic properties of muscle-tendon units. Am. J. Sports Med. **18**(3): 300-309, 1990.

87. Taylor, D. C., A. V. Seaber and W. E. Garrett. Cyclic repetitive stretching of muscle-tendon units. Surg. Forum. **36**: 539-541, 1985.

88. Thorstensson, A. and J. Karlsson. Fatiguability and fibre composition of human skeletal muscle. Acta physiol scand. **98**: 318-322, 1976.

89. Tidball, J. G. The geometry of actin filament-membrane associations can modify adhesive strength of the myotendinous junction. Cell Motil. **3**: 439-447, 1983.

90. Trotter, J. A., S. Eberhard and A. Samora. Structural Connections of the Muscle-Tendon Junction. Cell Motil. **3**: 431-438, 1983.

91. Viidik, A. A rheological model for uncalcified parallel-fibered collagenous tissue. J. of Biomechanics. **1**: 3-11, 1968.

92. Watkins, A. and P. M. Clarkson. "Dancing Longer dancing stronger." 1990 Princeton Book Company, Publishers. Pennington, N.J.

93. Welsh, R. P., I. Macnab and V. Riley. Biomechanical studies of rabbit tendon. Clin. Orthop. Rel. Res. **81**(Nov-Dec): 171-177, 1971.

94. Wilkie, D. R. "Muscle." 1968 Edward Arnold. London.

95. Williams, P. E. and G. Goldspink. Longitudinal Growth of Striated muscle Fibers. J. Cell. Sci. **9**: 751-767, 1971.

96. Williford, H. N., J. B. East and F. H. Smith. Evaluation of warm-up for improvement in flexibility. Am. J. of Sports Med. **14**(4): 316-319, 1986.

97. Woo, S. L.-Y., M. A. Gomez and T. J. Sites. The biomechanical and morphological changes in the medial colllateral ligament of the rabbit after immobilization and remobilization. Journ. Bone Joint Surg. **69A**: 1200-1211, 1987.

98. Yoganandan, N. Dynamic response of human cervical spine ligaments. Spine. **14**(10): 1102-1110, 1989.

99. Zarins, B. and J. V. Ciullo. Acute Muscle and Tendon Injuries in Athletes. Clin. Sports Med. **2**(1): 167-182, 1983.

Appendix

Load-displacement Curves

for

Specimens 2-10

Figure 29 MG 2 Load-Displacement Curve 76

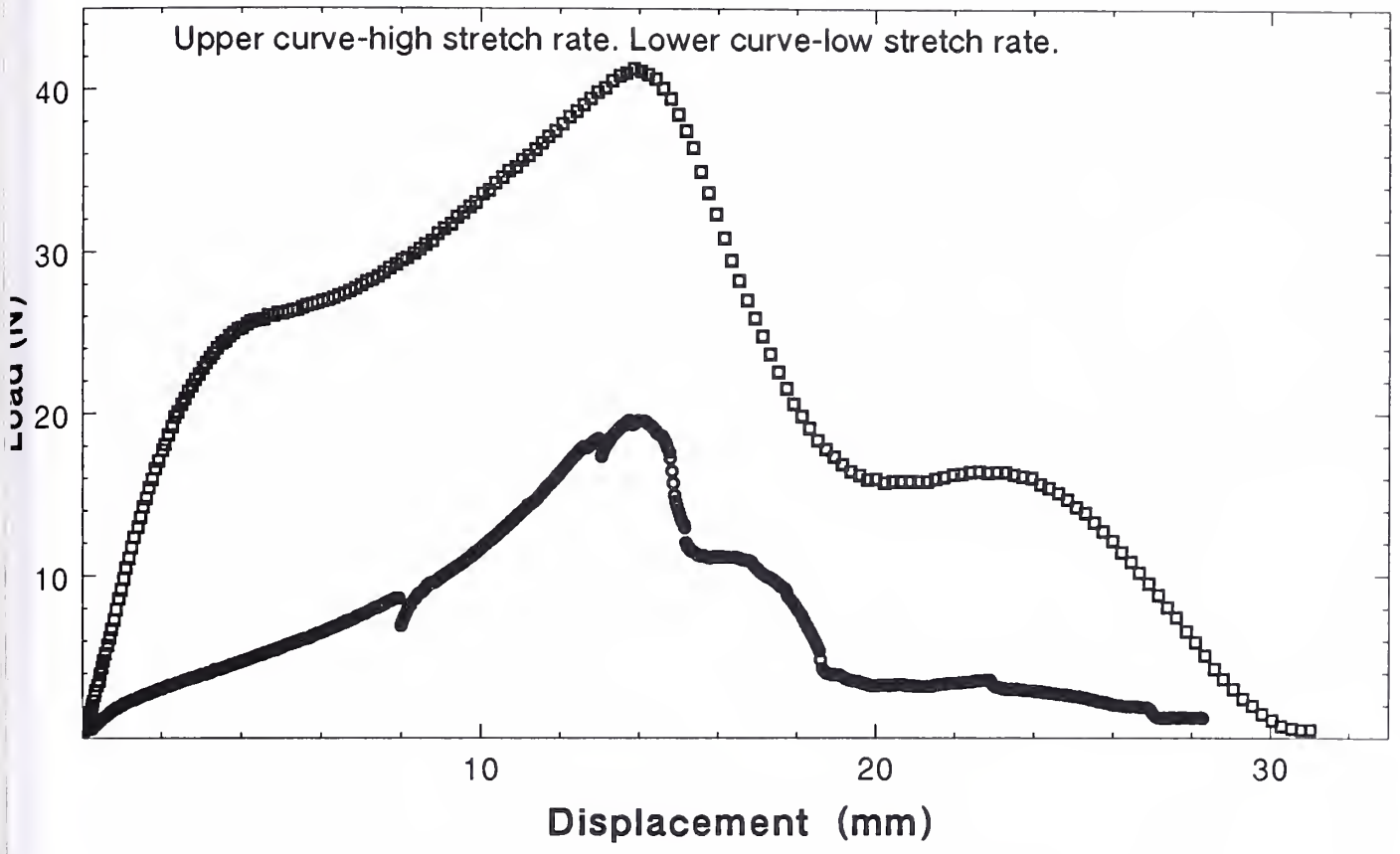

TA 2 Load-Displacement Curve

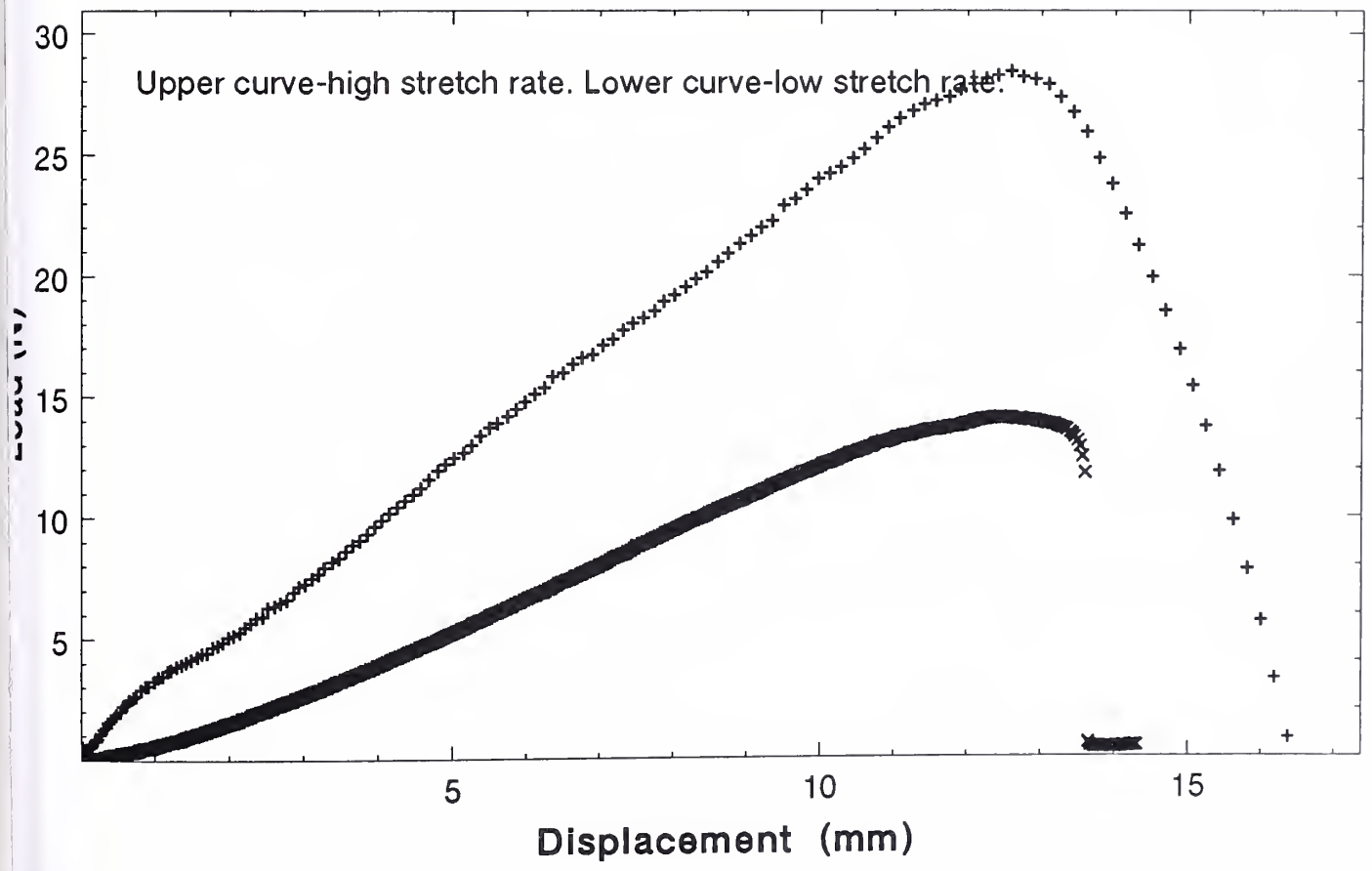

Figure 30 MG 3 Load-Displacement Curve 77

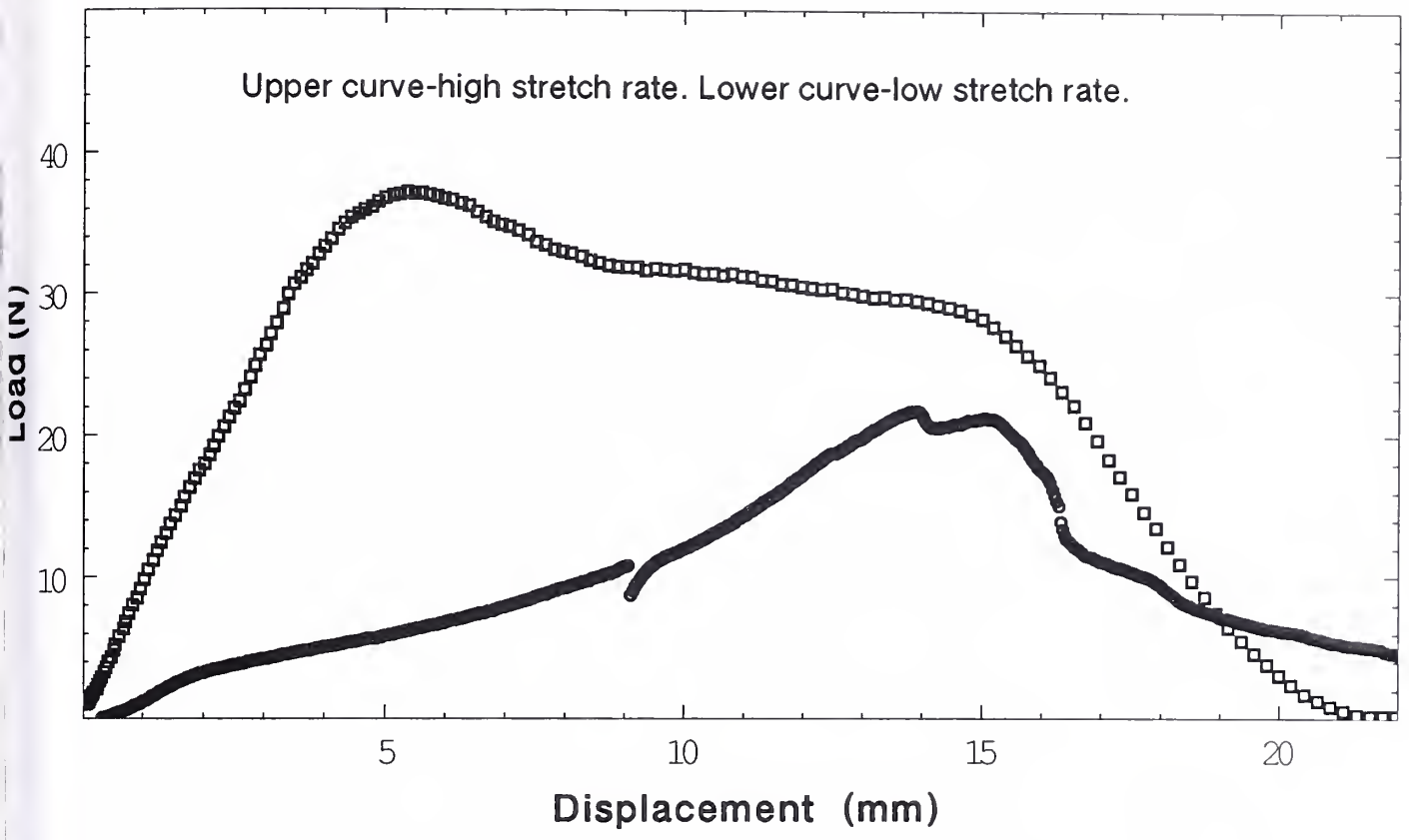

TA 3 Load-Displacement Curve

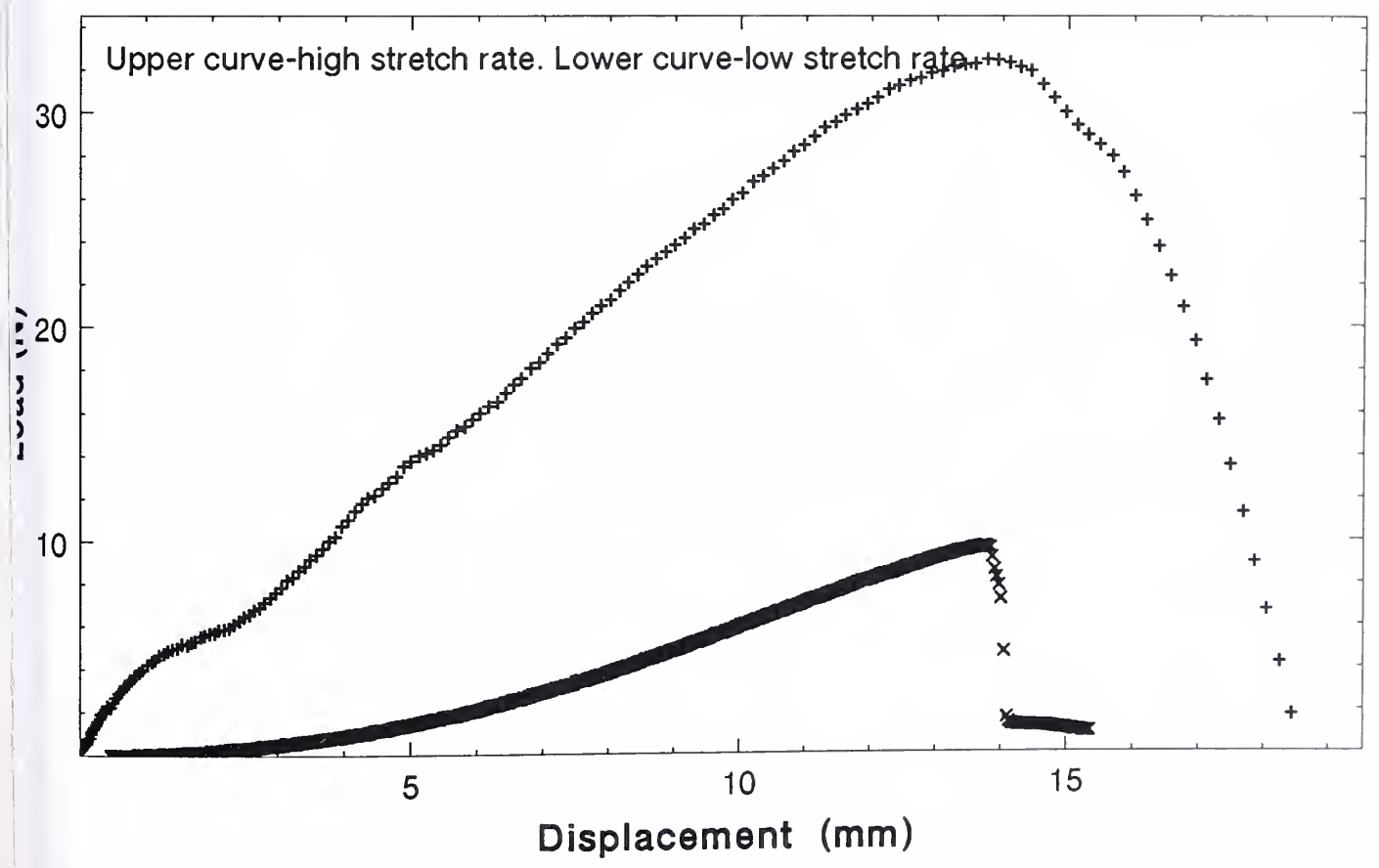

Figure 31 MG 4 Load-Displacement Curve 78

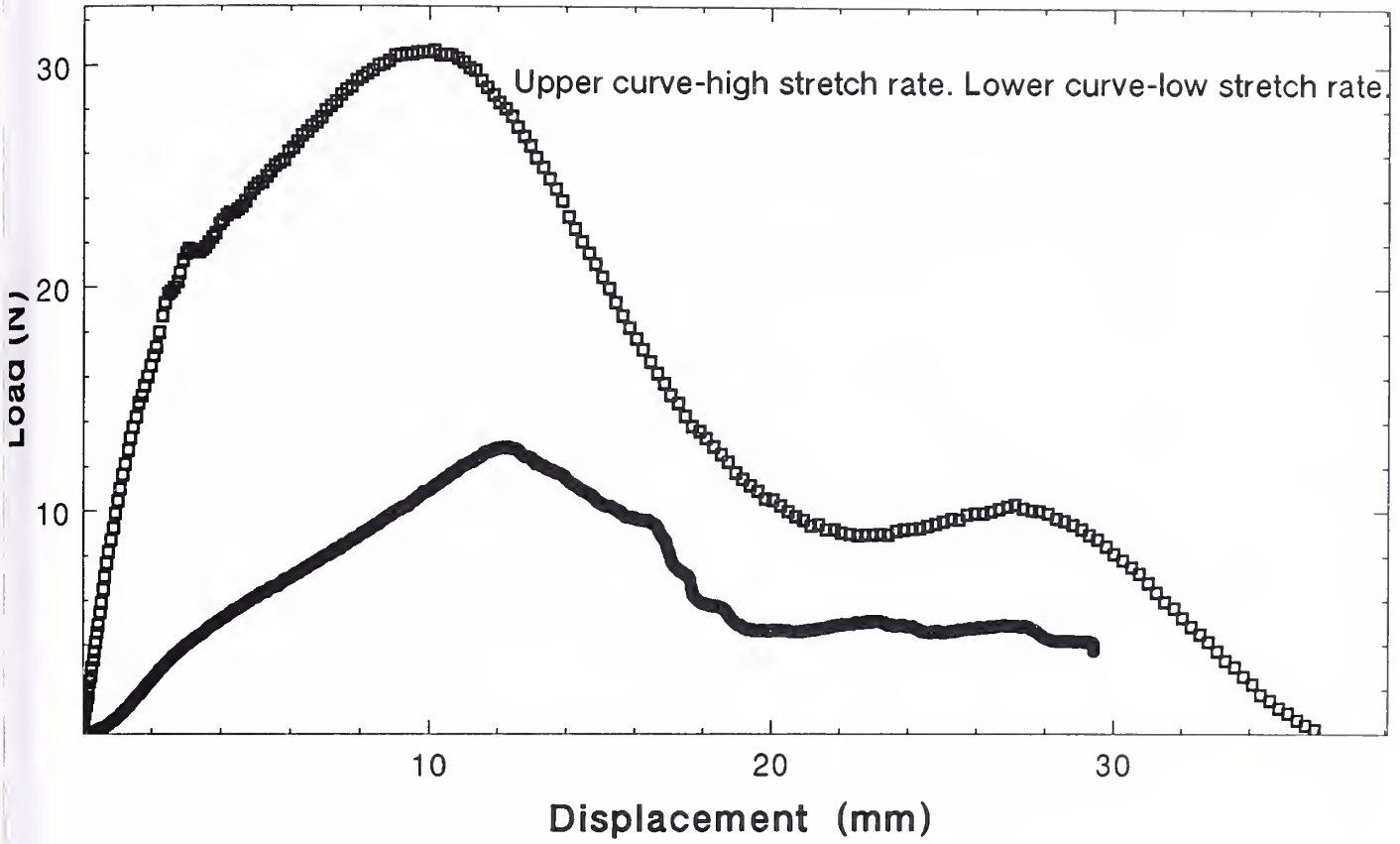

TA 4 Load-Displacement Curve

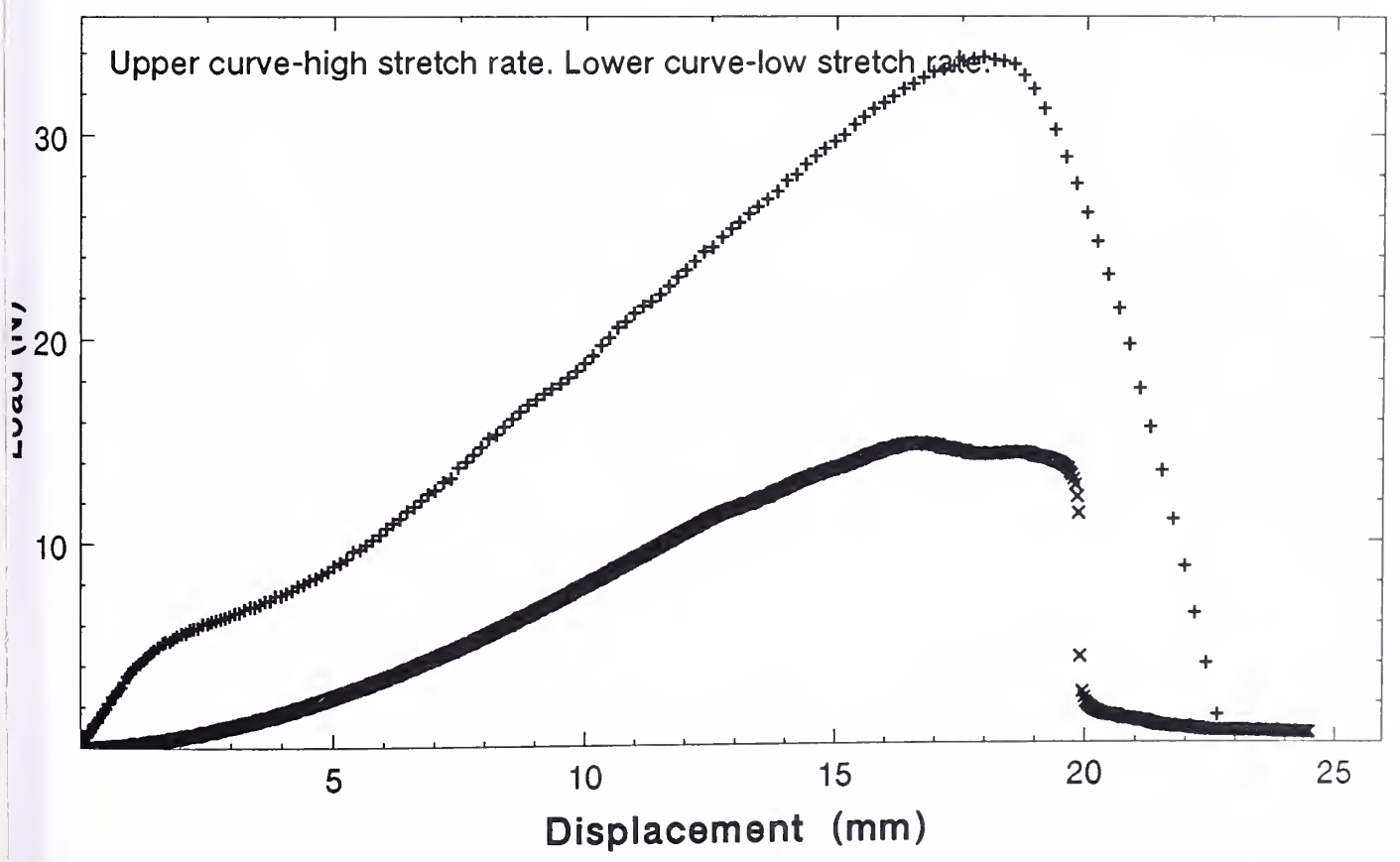

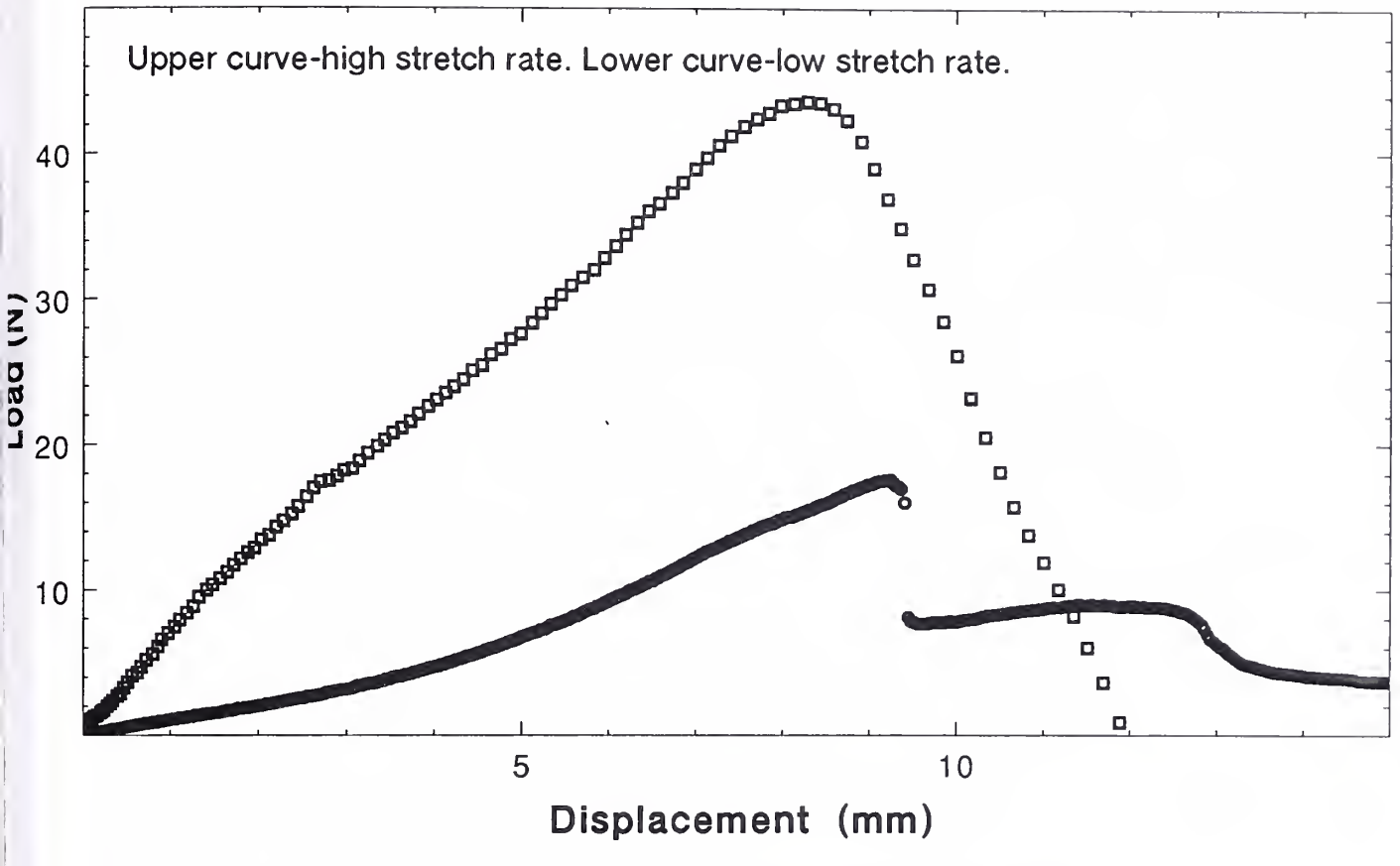

TA 5 Load-Displacement Curve

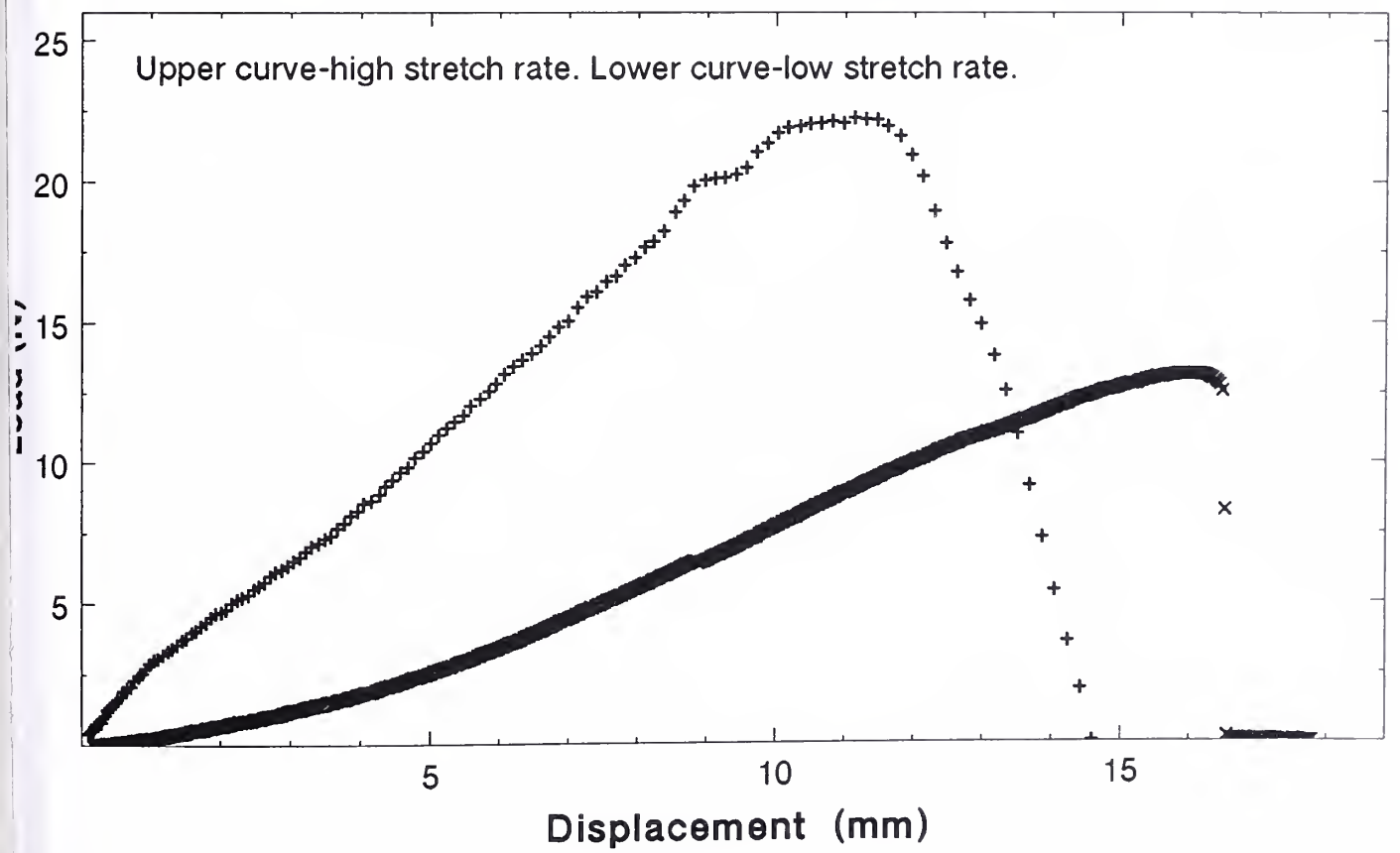

Figure 33 MG 6 Load-Displacement Curve 80

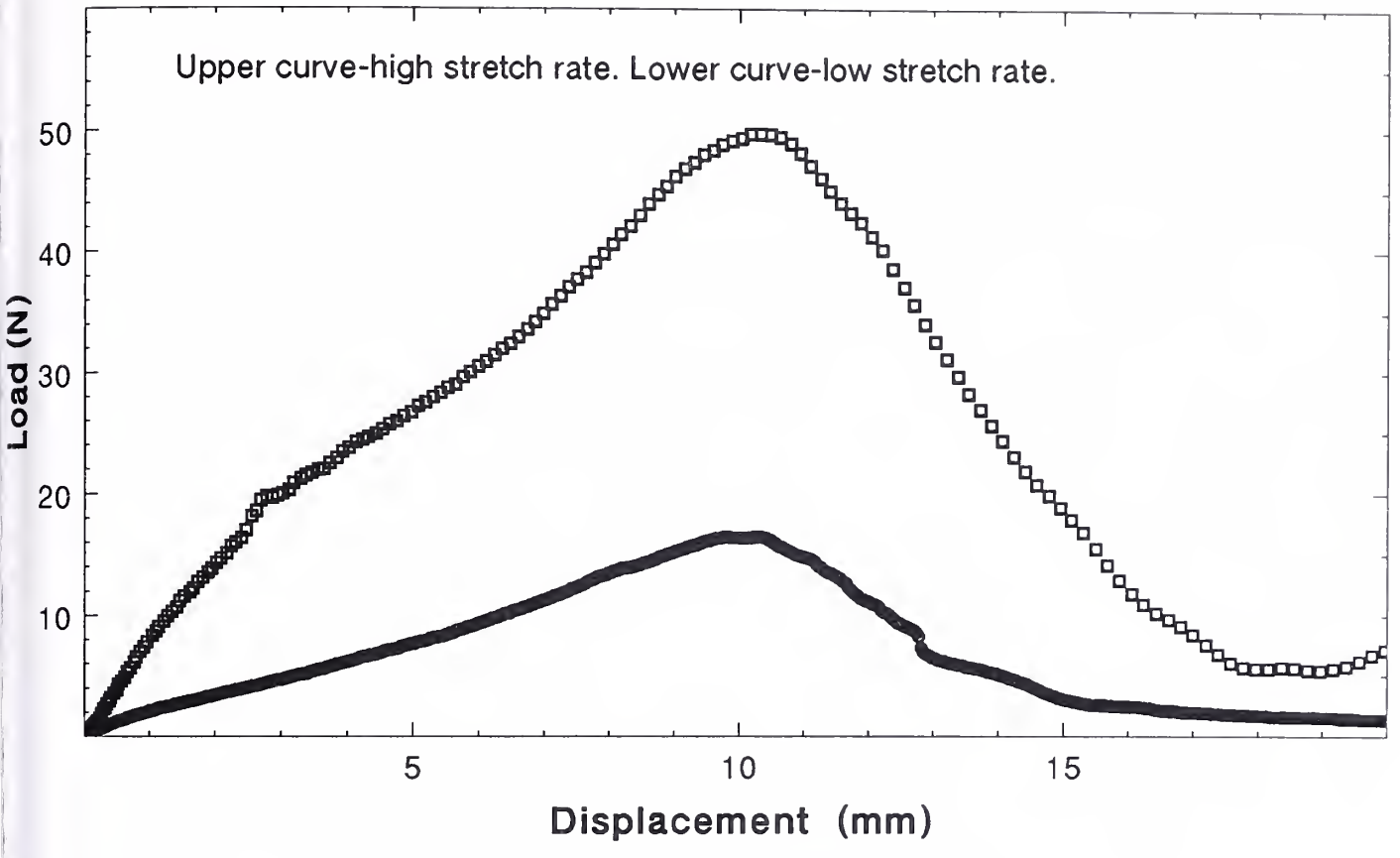

TA 6 Load-Displacement Curve

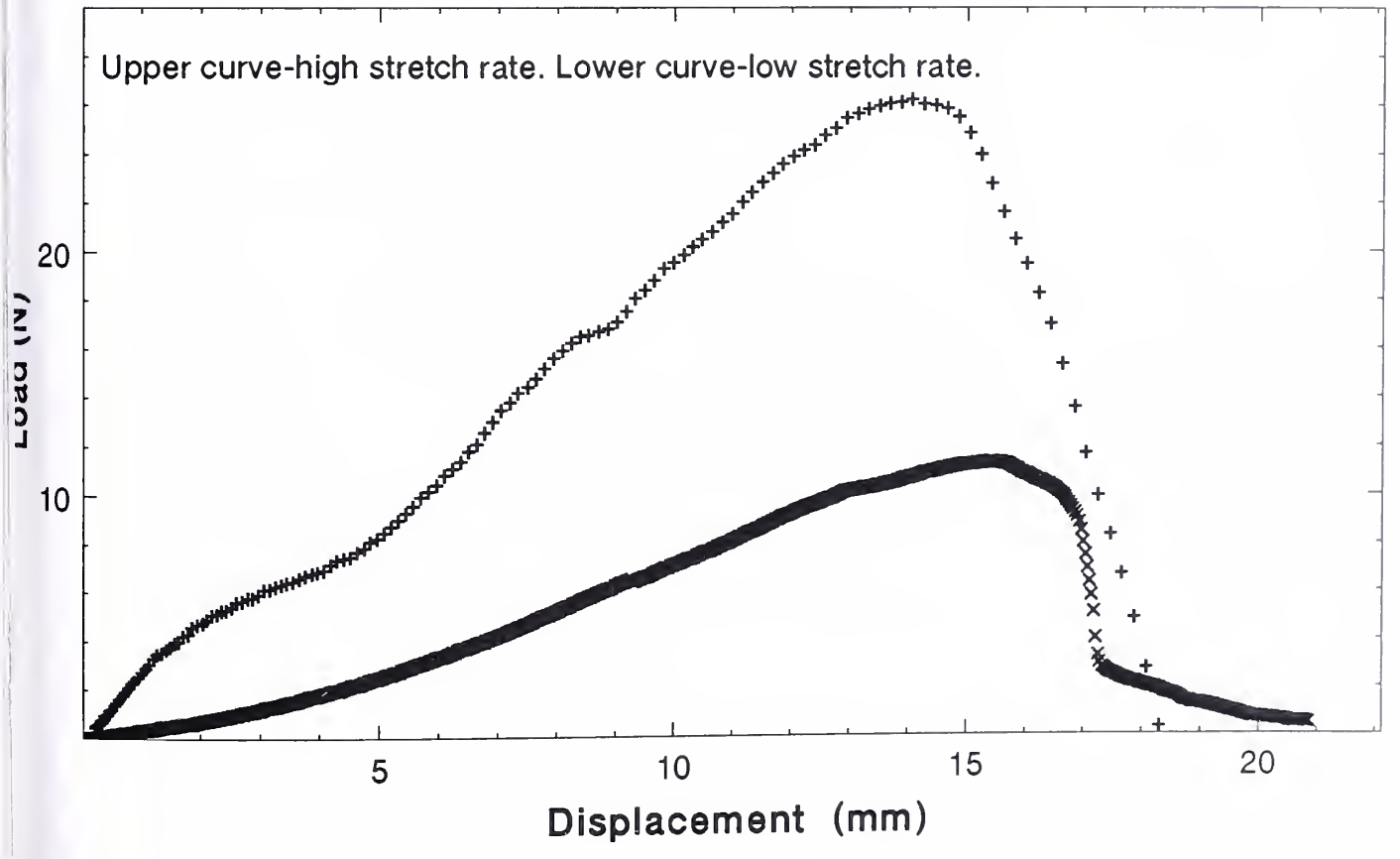

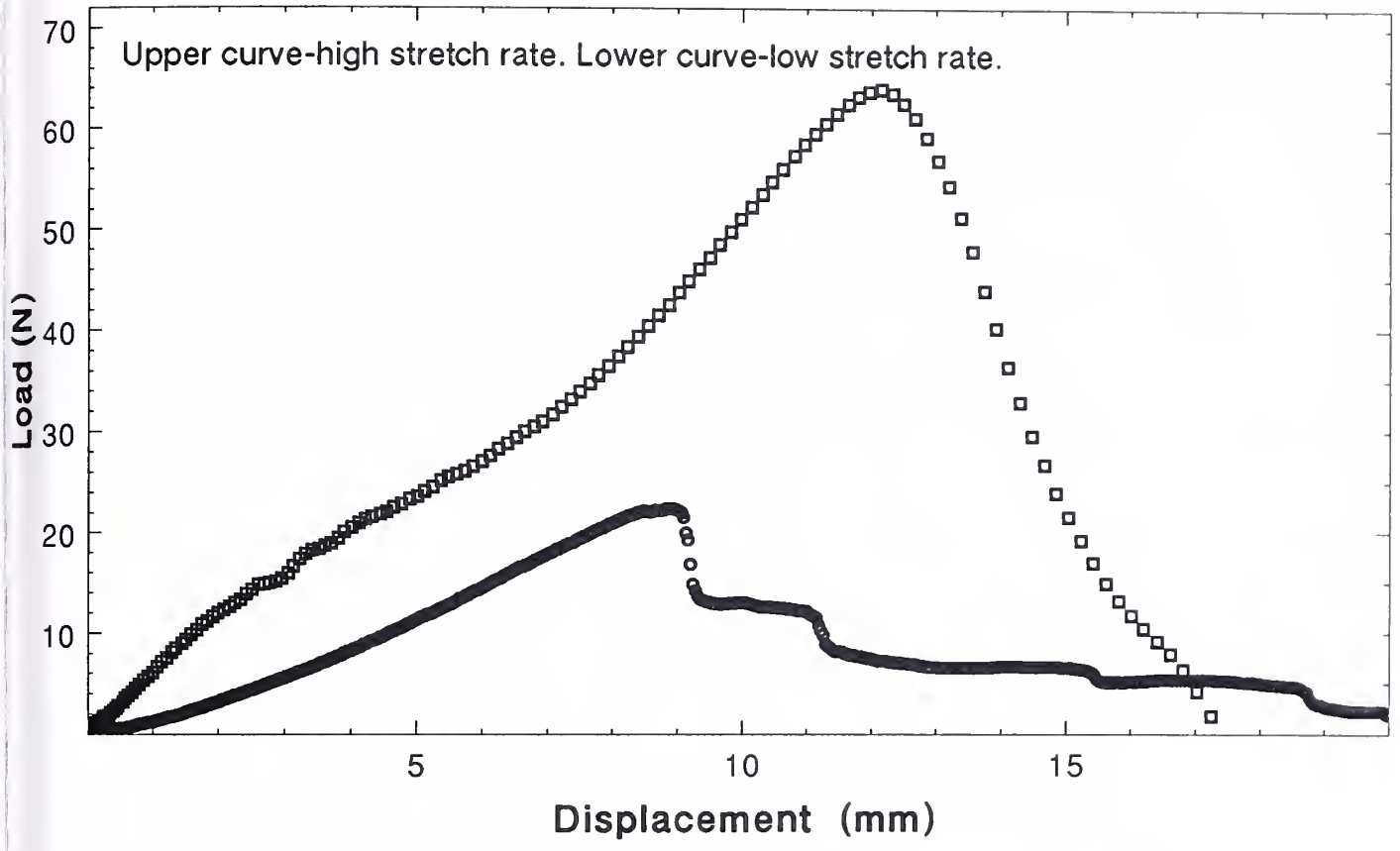

TA 7 Load-Displacement Curve

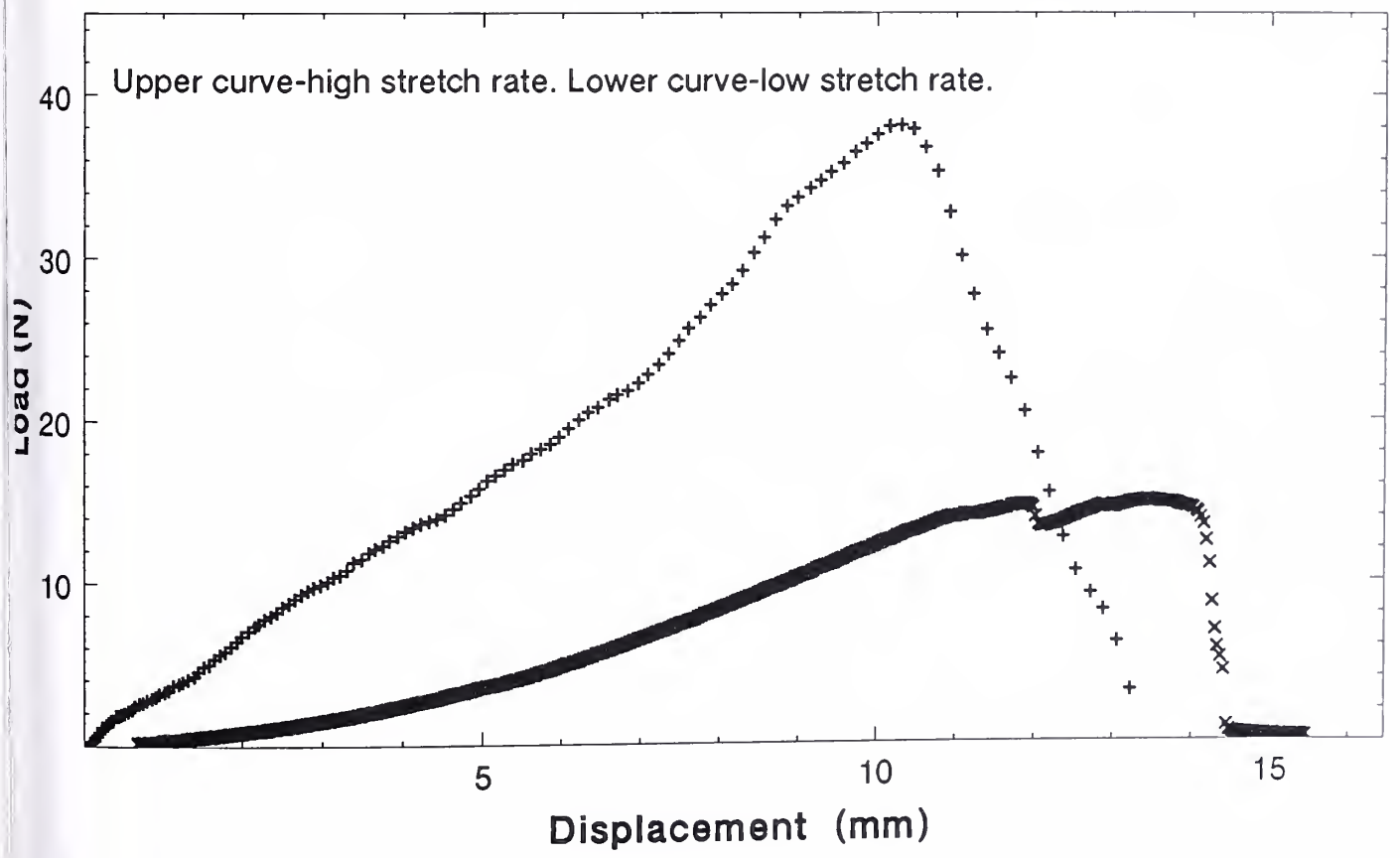

Figure 35 MG 8 Load-Displacement Curve

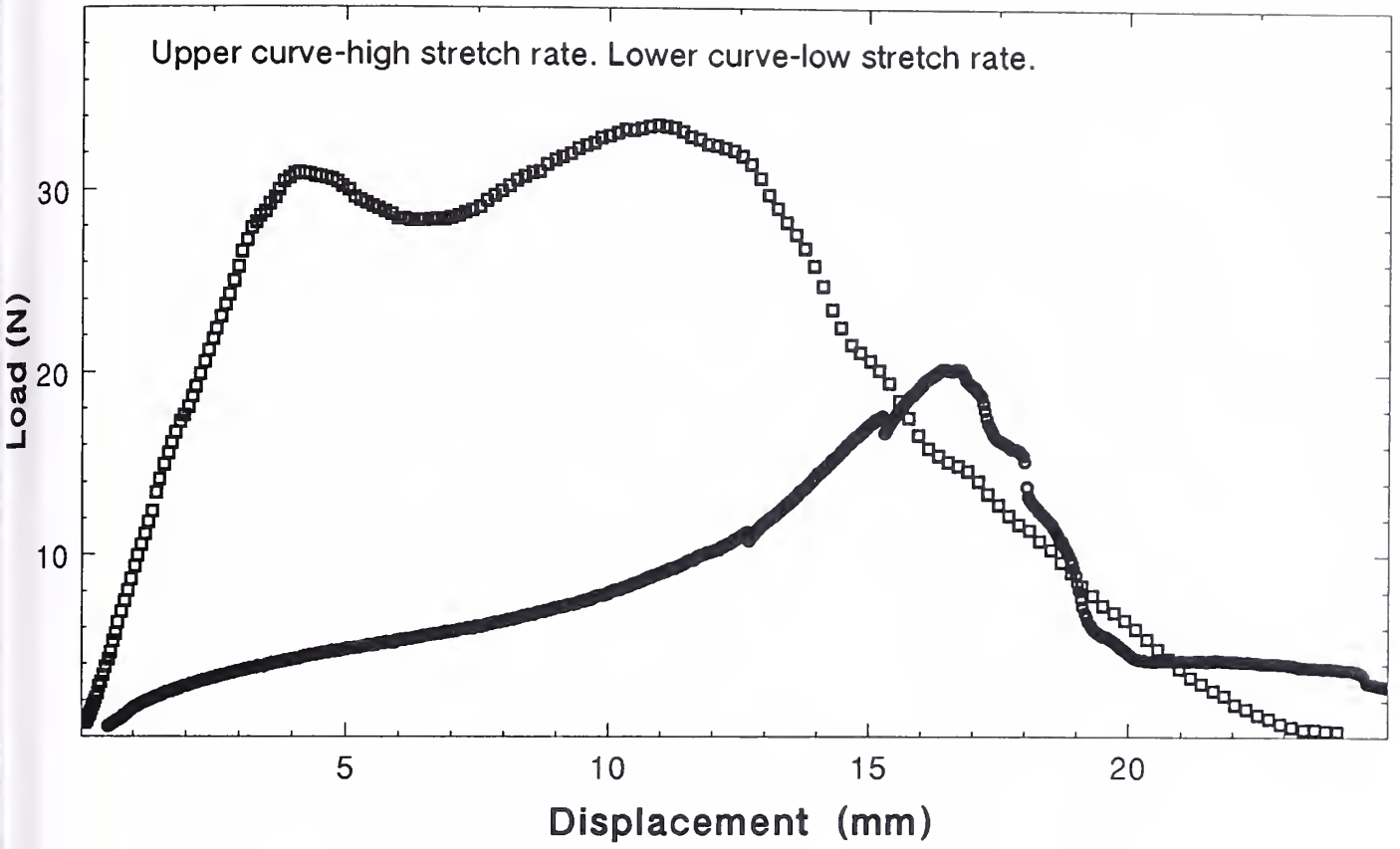

TA 8 Load-Displacement Curve

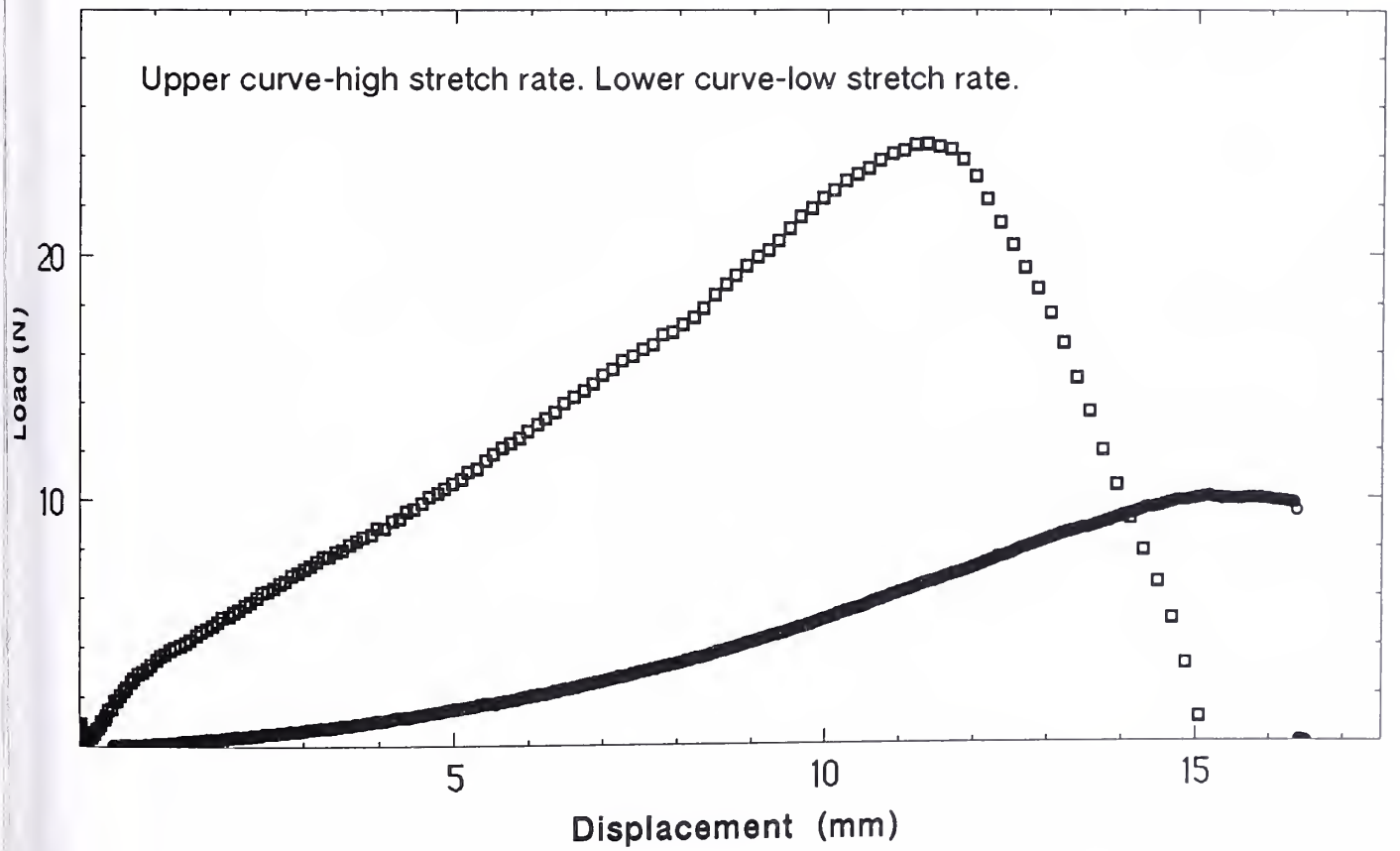

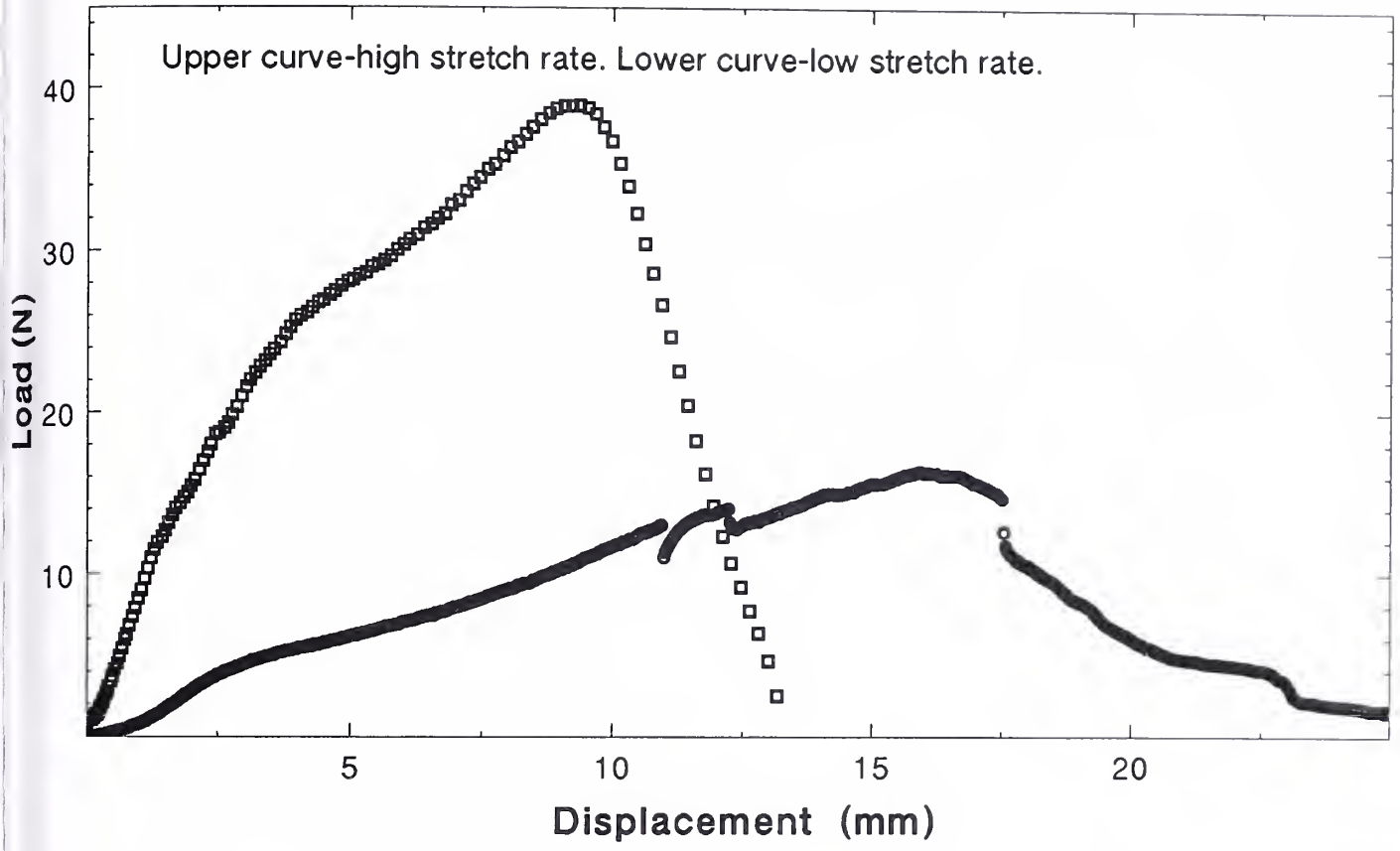

TA 9 Load-Displacement Curve

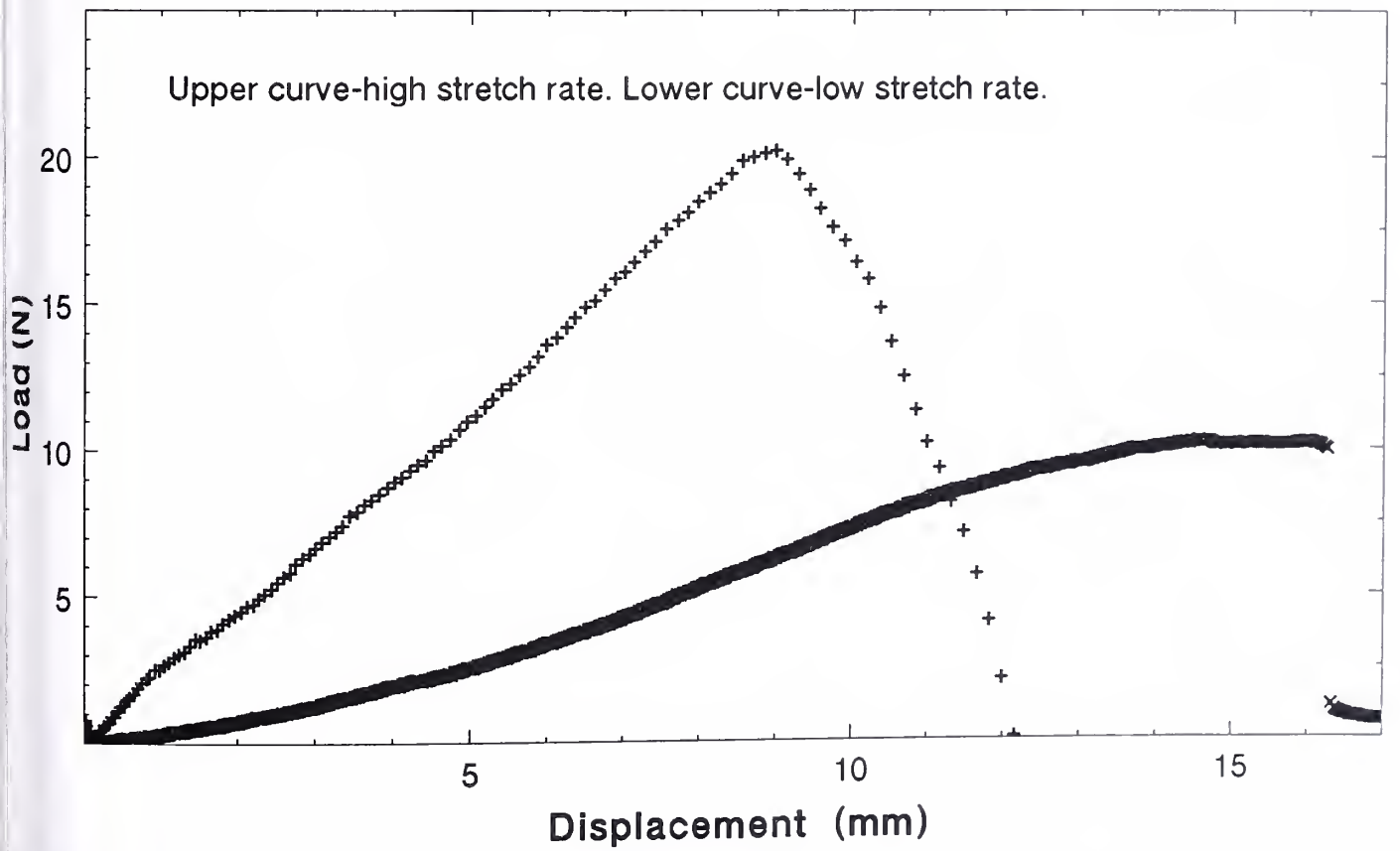

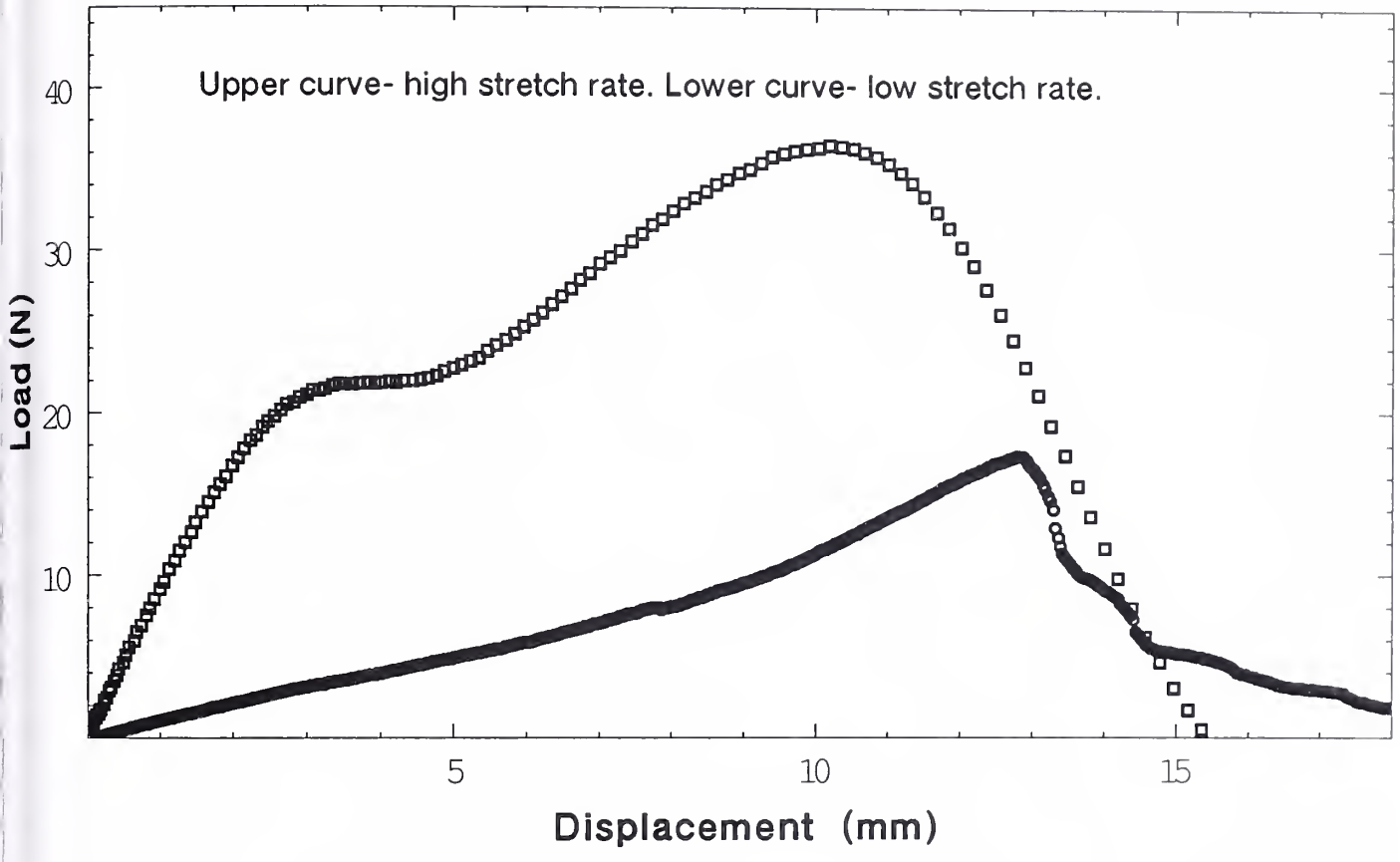

TA 10 Load-Displacement Curve

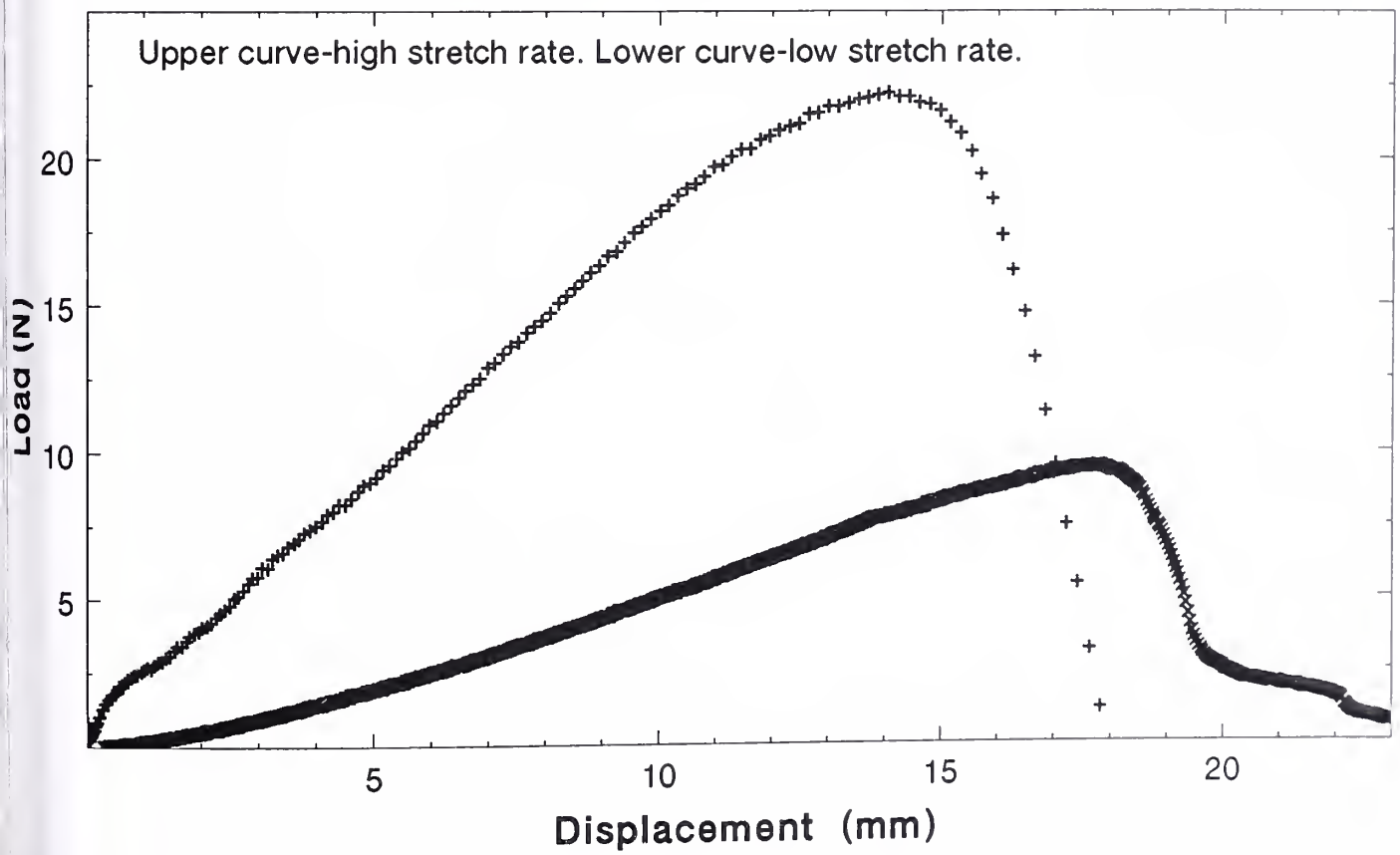

HARVEY CUSHING / JOHN HAY WHITNEY
MEDICAL LIBRARY

MANUSCRIPT THESES

Unpublished theses submitted for the Master's and Doctor's degrees and deposited in the Medical Library are to be used only with due regard to the rights of the authors. Bibliographical references may be noted, but passages must not be copied without permission of the authors, and without proper credit being given in subsequent written or published work.

This thesis by has been used by the following persons, whose signatures attest their acceptance of the above restrictions.

NAME AND ADDRESS DATE

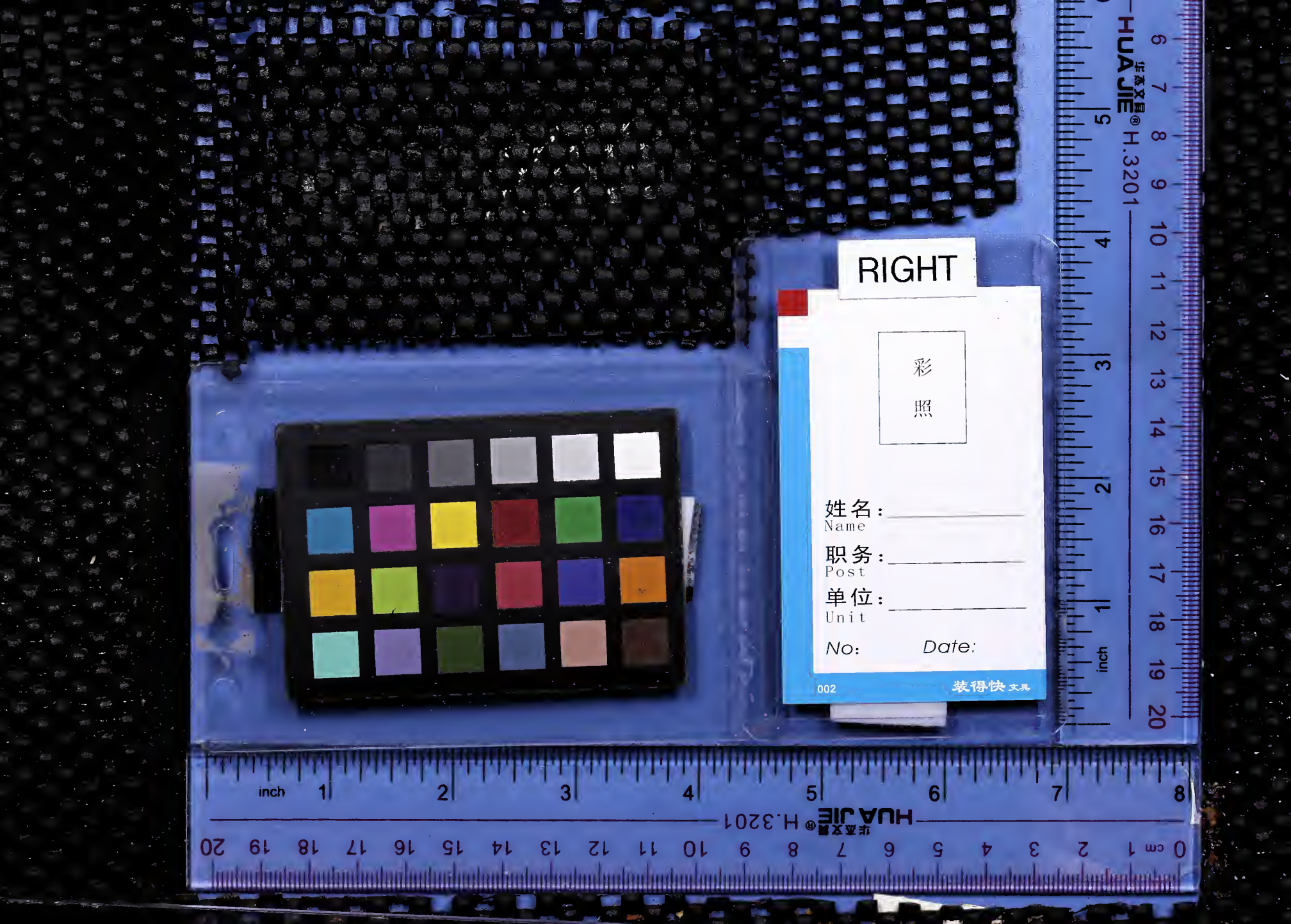
RIGHT
彩
照
姓名：
Name
职务：
Post
单位：
Unit
No:
Date:
002
装得快 文具
HUA JIE 华杰文具 H.3201
inch
cm

HARVEY CUSHING / JOHN HAY WHITNEY
MEDICAL LIBRARY

MANUSCRIPT THESES

Unpublished theses submitted for the Master's and Doctor's degrees and deposited in the Medical Library are to be used only with due regard to the rights of the authors. Bibliographical references may be noted, but passages must not be copied without permission of the authors, and without proper credit being given in subsequent written or published work.

This thesis by has been used by the following persons, whose signatures attest their acceptance of the above restrictions.

NAME AND ADDRESS DATE